Age-Related Changes in Depth Perception through Shape-from-Shading

Hannah. E. Broadbent, BSc, MSc.

A thesis submitted to the University of Nottingham

for the degree of Doctor of Philosophy.

Acknowledgements

Foremost, I extend my deepest gratitude to Harriet Allen, whose relentless encouragement and support, academically and at times emotionally, have been a cornerstone of my progress. My thesis has only seen the light of day with your guidance and support. I am equally thankful to Andrew Schofield, whose enthusiasm and fervour for research have motivated me. His depth and breadth of knowledge have been invaluable throughout this journey.

Thank you to my colleagues at Nottingham University and Birmingham University, both within the vision group and beyond, for the stimulating dialogues we shared over coffee or a pint.

Also, a special note of thanks to Cristiana Cavina-Pratesi, who kindled my passion for research. Thank you for instilling in me the confidence to embark on a PhD. Your deep love for research has left an indelible mark on me.

I am indebted to the Economic and Social Research Council for their financial support. My research, in the absence of their generosity, would have remained a dream.

Thank you to Sheila, Steve and Katharine Broadbent, who have been my pillars of strength throughout this journey, from being test subjects to counsellors and proofreaders.

A heartfelt thanks to Harriet Craig, a constant presence by my side for what seems an eternity. You have been an incredible friend, standing by me through all the ups and downs.

Lastly, I want to acknowledge Tom Hart. Thank you for enduring my nonsensical monologues about vision and always being there on the tough days. Your support has made all the difference.

I dedicate my thesis to my dear friend, Xing Ding. I cherish the years we spent together, and I'm grateful for the friendship we shared.

Your legacy lives on through my academic pursuits and the achievements of countless others fortunate enough to have known your friendship.

Table of Contents

1 General Introduction

The primary objective of this thesis was to explore the sensitivity of perception of shape-from-shading. Concurrently, age-related perceptual and cognitive function were also investigated to determine how these changes contribute to the sensitivity to shape-from-shading cues. The human visual system operates through different mechanisms capable of perceiving and interpreting information from the surrounding environment. This chapter reviews the literature on first- and second-order vision, emphasising studies investigating shape-from-shading. First, the origins of shape-from-shading observed in natural scenes are discussed alongside our understanding of the interaction between first- and second-order vision in depth perception. First- and second-order vision principles are then discussed, and models of processing that seek to further our understanding of this association are presented. Lastly, the impact of ageing on visual sensitivity of first- and second-order processing is discussed, along with research corroborating both visual and neural contributions to age-related alterations in the visual system.

1.1 Cues in Depth Perception

The ability to perceive depth is fundamental to interacting with objects and navigating surfaces. This interaction involves the ability to perceive and estimate depth accurately, manipulate objects around us, or adjust our body movements to interact with them. For example, we can normally ascend and descend staircases without experiencing any difficulty or colliding with nearby objects. When viewing a scene, each retinal image is two-dimensional. However, using cues that convey depth, the visual system can accurately represent depth and shape depth from these cues. Despite the brain's ability to efficiently perceive depth with few errors, the absence or ambiguity of these cues can lead to inaccurate depth judgements and even illusions of depth, as depicted in the following examples.

Figure 1-1. Various examples of illusions simulating depth in artificial scenes. a) presents an example of ambiguous monocular depth cues in natural settings. In this image, a man is skydiving at approximately 15,000 ft. The significant distance to the ground below creates an illusion of him appearing unusually large. This image is reprinted with permission, © Tom Shorten. In image b), a woman sits on an oversized chair at a great distance, with another woman in the foreground. The difference in their relative positions and the proportion of the chair to the seated woman creates the illusion that the woman in the background is much smaller than she is. Image c) presents another depth illusion where two women stand on a bridge while a third woman appears to be swept away by the water below. The geometry of the bridge and scene and the arrangement of the women and the

painted bridge enable us to perceive the scenario. d) demonstrates an illusion of depth created partly through shading. The floor appears to drop away behind the woman on a magic carpet.

The visual system interprets depth through various visual cues. Two broad categories of cues allow us to perceive depth: monocular and binocular cues. Binocular depth perception arises from the slight positional differences between our two eyes, whereas monocular depth cues interpret depth based on the information obtained from a single retinal image. Although this thesis examines the impact of monocular cues on depth perception, it is important to note the various cues that contribute to depth perception, as listed in Table 1-1.

Table 1-1.

Monocular and binocular static cues in depth perception.

Depth Cue	Cue Type	Function	Authors
Occlusion	Monocular - Pictoral	When one object obstructs the line of sight towards a portion of another object	(Braunstein et al., 1982).
Relative Cues (Size & Height)	Monocular – Pictoral	Objects appear smaller in size when placed further away due to size constancy. Additionally, objects farther away are perceived to have a higher position in the observer's field of view.	(Gillam, 1995; Ooi et al., 2001)
Familiar Size	Monocular – Pictoral	Prior knowledge about the size of an object can influence how we perceive its distance, dependent on how much field of view it occupies	(McIntosh & Lashley, 2008)
Texture compression	Monocular – Pictoral	The orientation of a surface can be determined by observing how the texture elements on that surface appear to decrease in size as they get further away from the observer.	(Anobile et al., 2014)
Linear perspective	Monocular – Pictoral	Parallel lines in a three-dimensional world converge to a vanishing point in a two-dimensional image.	(Muller et al., 2009)

Texture anisotropy	Monocular – Pictoral	Texture elements often appear compressed along the direction of the surface's slant or tilt, reflecting the orientation of the surface.	(Warren & Mamassian, 2010)
Texture gradient	Monocular – Pictoral	A gradual shift in texture from defined, coarse texture, to fine and less distinct when further away.	(Stevens, 1981; Stevens & Brookes, 1988)
Shading	Monocular – Pictoral	The reflections and shadows created by light interacting with an object enable the brain to determine its shape.	(Horn, 1970, 1989; Ikeuchi & Horn, 1981; Pentland, 1984, 1988)
Aerial perspective	Monocular – Pictoral	When observing distant objects, the atmosphere can impede and scatter light. The presence of dust and water particles in the atmosphere hinders the transmission of high-frequency light to our eyes, resulting in a blurred, low contrast appearance of distant objects.	(Held et al., 2012; O'Shea et al., 1997)

Defocus blur	Monocular – Physiological	Objects situated on different depth planes tend to appear less sharp or more blurred.	(S. Chaudhuri & Rajagopalan, 1999; Krotkov, 1988)
Accommodation	Monocular - Physiological	The process through which the eyes adjust their focal length depending on the viewing distance provides a cue to interpret the relative distance of an object.	(Wallach & Norris, 1963)
Horizontal disparity	Binocular - Stereopsis	The slight difference in the visual field of each eye due to their separate positions. This disparity in the retinal images is compared to deduce depth and distance, i.e. stereopsis.	(Blakemore, 1970; Kaufman et al., 1973)
Vergence angle	Binocular - Triangulation	The angle of convergence between the eyes, which adjusts depending on the object's proximity, offers another cue for depth perception where greater convergence is required for objects that are closer to the observer.	(Morgan, 1944)

In some situations, binocular cues may not be present in a scene. For instance, individuals with visual impairments like strabismus or amblyopia are unable to use binocular cues effectively. Binocular cues, such as paintings or photographs, also lack disparity cues. Figure 1-2 illustrates the significance of depth cues by contrasting their application in pre-Renaissance and Renaissance art. The comparison underscores that consistent use of monocular cues can yield a convincingly realistic depiction of depth even without binocular cues. This thesis primarily focuses on shading depth cues, which enable the perception of depth through variations in light and shadow across an object or scene, which will now be discussed.

Figure 1-2. Evolution of Depth Perception in Art from Pre-Renaissance to Renaissance. (a) A pre-Renaissance painting “The Peasants' Revolt” from The Chronicles of Jean Froissart is dated between 1385 and 1400. In this artwork, depth is interpreted primarily through occlusion cues, but without a consistent perspective, leading to less convincing depth depiction. Distributed under Public Domain from the British Library's collections, 2013. (b) “The School of Athens” by Raffaello Sanzio da Urbino dated between 1508 and 1511 depicts a Renaissance painting. The painting demonstrates a consistent linear perspective, shading from a uniform light source direction, and other monocular depth cues like occlusion and relative size. These elements contribute to a significantly enhanced and more realistic representation of depth. Public Domain.

1.2 Shape-from-Shading

When light illuminates a surface, depending on the properties of the surface, such as surface material and shape, it will reflect the light in different patterns. This reflectance is essential for interpreting depth when other cues, such as boundaries and binocular disparity, are absent. This process of interpreting shading patterns on surfaces in natural and artificial scenes has been termed shape-from-shading (Brooks & Horn, 1985; Horn, 1970; Pentland, 1984, 1988; Ramachandran, 1988). These variations in illumination can be used to identify the surface's orientation relative to the light source. As demonstrated in Figure 1-3, surfaces oriented towards the light source are brighter, while areas facing away from the light source appear darker. Therefore, the perception of shape-from-shading is a process that allows the interpretation of the three-dimensional properties of an object or scene from its two-dimensional image based on the distribution and intensity of illumination (Adelson & Pentland, 1996). The process relies on the assumption that the shading of an object is directly related to its surface orientation and shape, which therefore is utilised to infer depth information (Ramachandran, 1988).

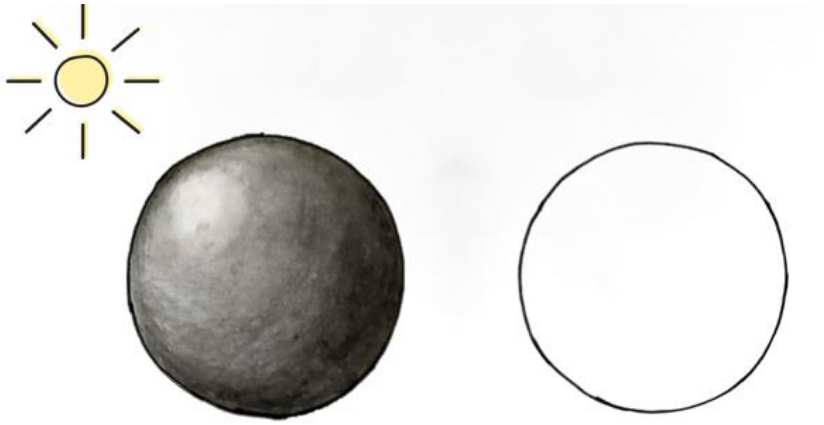

Figure 1-3. A comparative Illustration of two circles, the right circle has no shading, while the left circle features shading consistent with a light source positioned upper left, giving perception of depth through shape-from-shading.

Shape-from-shading is conveyed through the perception of first- and second-order luminance cues. First-order vision refers to the ability of the visual system to detect luminance variations in a scene, thus serving as a response to light intensity. However, vision is not just limited to detecting linear variations in brightness. Second-order visual processing allows us to discern variation in properties ascertained by comparing two points in space, such as contrast, orientation and spatial frequency (Baker & Mareschal, 2001; Schofield, 2000; Schofield et al., 2010; Schofield & Georgeson, 2003; Sutter et al., 1995). In terms of perceiving shape-from-shading, first-order modulations refer to changes in brightness, while second-order modulations refer to changes in contrast. Therefore, first-order modulations are defined as changes in local luminance, where the local luminance is divided by the mean luminance of an image. Second-order modulations encompass the systematic variations in attributes of an image that go beyond mere luminance, capturing intricate details such as contrast, texture, and local changes in orientation or frequency.

Therefore, while changes in first-order luminance alter the mean local luminance, they do not change the range of pixel values. Conversely, second-order contrast does not alter the mean local luminance but modulates the range of luminance values. In this thesis,

the term amplitude modulation (AM) refers to second-order modulations in local contrast, whereas luminance modulations (LM) refer to changes in local mean luminance in first-order vision. The channel responsible for processing first-order visual information provides the basis for detecting shape and depth. Whereas the second-order processing stream not only contributes to depth perception but, in synergy with first-order cues, a lso conveys changes in material properties(Dakin & Bex, 2003).

1.2.1 Image changes supporting the perception of shape-from-shading.

Therefore, relationship between first- and second-order information in natural images influences the observer's interpretation of texture versus illumination changes (Barbot et al., 2012; Johnson & Baker, 2004; Schofield et al., 2010). Figure 1-4 illustrates differences in local mean luminance between the zebras and the surrounding background (Barbot et al., 2012). In this image, a change in local mean luminance conveys a texture boundary between the foreground zebra and the background grass. However, if the local mean luminance remains the same, the visual system can detect changes in texture through contrast-defined modulations based on orientation. The boundary cues between the two zebras on the right appear to have the same mean luminance, but their horizontal and vertical stripes create a visible boundary. This highlights the importance of accurately perceiving both the first- and second-order information in a scene to represent changes in texture accurately.

Figure 1-4. An example of a natural scene's first- and second-order properties conveying boundary cues and different textures. Replicated from (Barbot et al., 2012). Reprinted from " Differential effects of exogenous and endogenous attention on second-order texture contrast sensitivity" by Barbot A., Landy M. S., Carrasco M., 2012, Journal of Vision, 12(8), p.2.

Boundaries that occur due to natural contours have different first- and second-order properties to boundaries that form due to material changes (Johnson & Baker, 2004). The statistical relationship between first- and second-order properties is presented in figure 1-5, where the plots reflect the average and range of pixel value in grayscale luminance. The yellow line shows the luminance values for each pixel, while the purple line displays local contrast values. The box marked by a solid line shows a change in reflectance due to a change in material properties, where the corresponding plot shows that a spike or drop in luminance results, which is spatially coincident with an inverse shift in local contrast. Within the dashed box, the material properties remain consistent but the orientation of the wall changes as it extends outward. This causes a spike/drop in local luminance, which is positively correlated to local contrast values, resulting in areas of both illumination and shade.

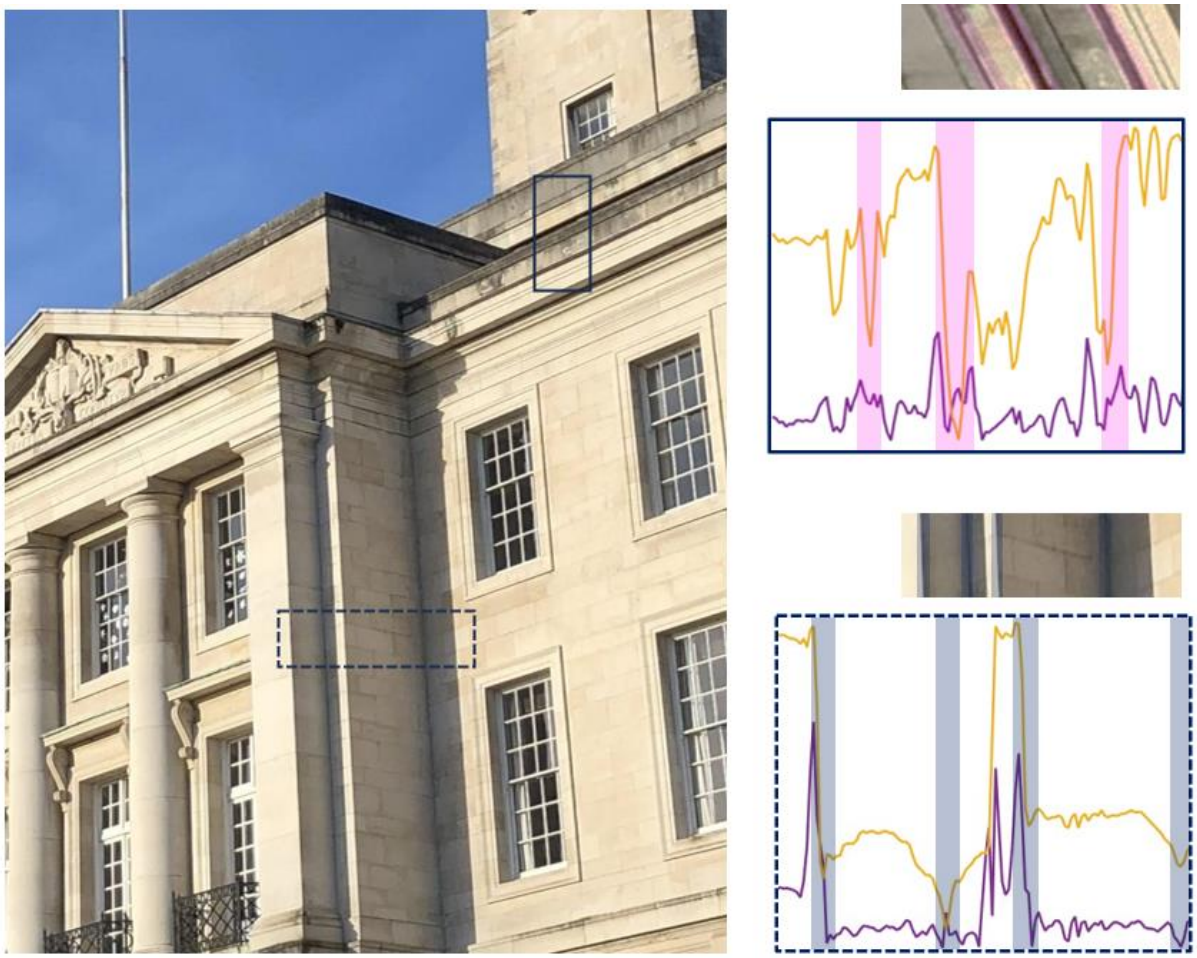

Figure 1-5. An image of Trent Building at Nottingham University. The upper sample, enclosed by a solid line in the main image, provides a cross-sectional view of a surface alternating between two materials. For clarity, this segment, presented to the right above the plots, has been rotated counterclockwise by 90°. The corresponding plots detail the average pixel values for luminance (depicted in yellow) and contrast (shown in purple) where the horizontal spatial extent of this image segment aligns with the plots below. The lower sample, enclosed by a dashed line in the main image, illustrates the variations in lighting due to the wall's orientation in relation to the light source. Within the plots, the pink band in the upper graph signifies a change in material, while the grey band in the lower graph indicates a shift in depth.

When both first- and second-order details are combined, it can therefore affect how we perceive the depth and structure of a visual scene. When these first- and second-order modulations occur in the same location, a positive correlation between local luminance and

local contrast indicates changes in depth or orientation, whilst a negative correlation indicates a change in material (Johnson & Baker, 2004; Kingdom, 2003; Schofield, 2000).

Shape-from-shading in natural images suggests that the visual system maintains separate representations of illumination and reflectance, enabling it to deduce lightness properties and shading in variable natural lighting settings (Pentland, 1984; Schofield et al., 2011). This is achieved through layer decomposition, suggested to be a necessary precursor to shape-from-shading (Barrow & Tanenbaum, 1978; Schofield et al., 2011; Sun & Schofield, 2011). The process of layer decomposition in the visual system involves distinguishing changes in surface material properties from changes caused by shape (Dövencioğlu et al., 2013; Sun & Schofield, 2011). This highlights that for depth perception, first- and second-order cues must be detected and represented accurately (Baker & Mareschal, 2001; Dakin & Mareschal, 2000; Langley et al., 1996; Schofield & Georgeson, 1999). Therefore, it is suggested that second-order signals are detected independently from first-order cues.

1.3 First-Order Luminance Modulations

Chapter 3 explores how depth perception is conveyed through first-order luminance modulations (LM) in first-order vision. The following section will introduce first-order vision, its characteristics, and how they change with age.

1.3.1 Properties of first-order vision

First-order vision is described as the modulation of local luminance, which is detectable through changes in energy in the Fourier domain (Campbell & Robson, 1968). Research on early-stage visual processing has shown that first-order vision is sensitive to orientation, as demonstrated by receptive fields in the visual cortex of cats that respond to specific orientation, (De Valois et al., 1982; Hubel & Wiesel, 1962). These first-stage filters are a result of linear summation of response energy from filters in the visual system that are narrowly tuned for orientation (Prins & Kingdom, 2006). Research has mapped the sensitivity of the visual system to changes in visible contrast by spatial frequency, resulting in what is

known as the contrast sensitivity function (CSF) (Campbell & Robson, 1968; Robson, 1966). Figure 1 illustrates early findings on contrast sensitivity functions, which suggest that the visual system is limited to a specific range of spatial frequencies. The figure indicates that the human visual system is most sensitive at approximately 3-5 cycles per degree (cpd).

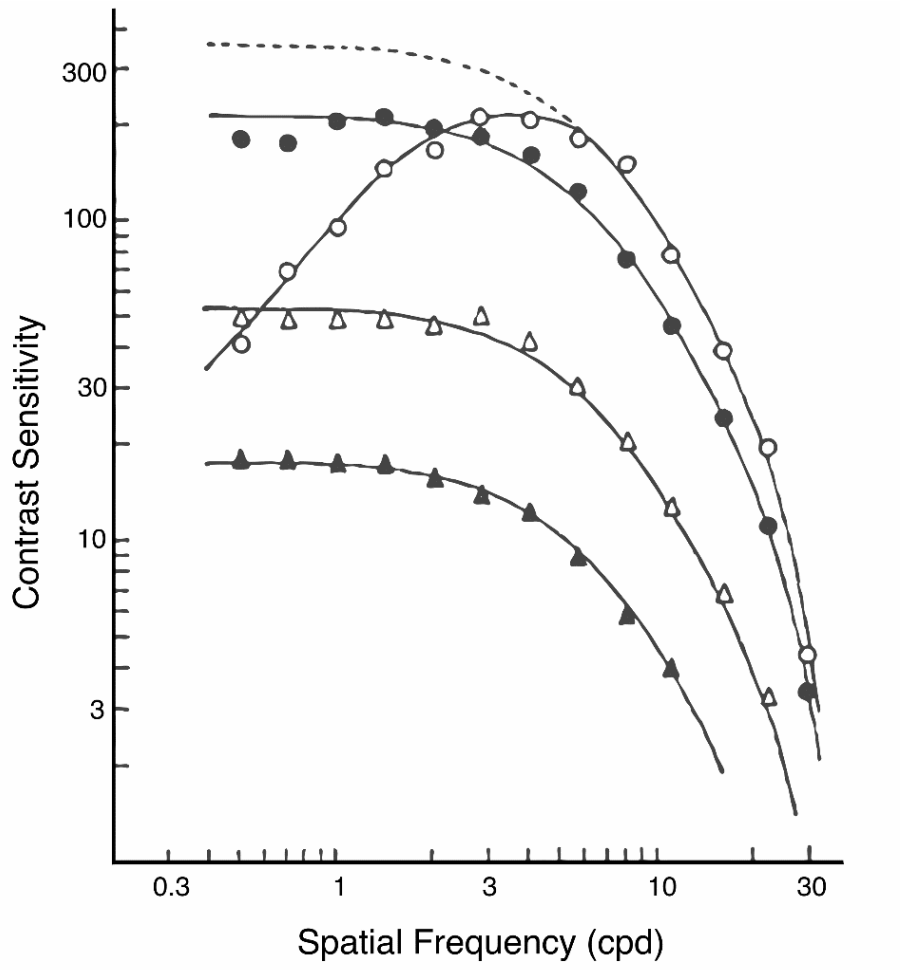

Figure 1. The contrast sensitivity function for adults, with each point representing the mean sensitivity for different temporal frequencies. The lines indicate the conditions for each temporal frequency, O 1, ● 6, Δ 16, and ▲ 22 cycles per second. Note. Reprinted from "Spatial and temporal contrast-sensitivity functions of the visual system" by Robson, J. G., 1966, Journal of the Optical Society of America, 56(8), p.1141.

Campbell and Robson (1968) introduced the concept of spatial frequency channels. Figure shows how temporal and spatial frequency relate to each other. At higher spatial

frequencies, sensitivity decreases regardless of the temporal frequency. This could be due to limitations in eye physiology or neural functions. However, when spatial and temporal frequencies are low, a decrease in sensitivity is likely to be due to opposing interactions between the receptive fields in the centre and surroundings. As a result, it was concluded that first-order channels are sensitive to both temporal and spatial frequency, but the interaction between these parameters depends on the signal strength.

Although the CSF serves as a measure for sensitivity of spatial and temporal frequencies, it doesn't explain how the visual system handles multiple frequency bands simultaneously. Studies have found that the human visual system processes information from different spatial frequencies separately, as orientation and spatial features can be selectively adapted to or masked, indicating that they are handled by different channels in the visual system (Blakemore & Campbell, 1969; Movshon & Lennie, 1979). Research on cats' visual systems has also shown that various retinal ganglion cells are sensitive to different spatial frequencies, based on their receptive field size (Hubel & Wiesel, 1962). These findings therefore suggest that the human visual system may be controlled by multiple individual linear channels, each with a narrow-band filter, optimised for a specific spatial frequency to process first-order luminance modulations.

The concept of multiple independent channels, each detecting contrast within a restricted spatial frequency range, has been validated through adaptation experiments where exposure to high contrast gratings resulted in increased thresholds for similar spatial frequency gratings (Blakemore & Campbell, 1969; Pantle & Sekuler, 1968). This adaptation effect is usually represented by the function's half-maximum width when plotted against spatial frequency (Braddick et al., 1978). The width is approximately 1.2 octaves of spatial frequency, which is equivalent to 0.6 octaves on either side of the adaptation frequency using the relative threshold elevation metric (Blakemore & Campbell, 1969). In contrast, using an alternate metric, the equivalent contrast transform, a full width at half-height of 0.75 octaves was identified (Blakemore et al., 1973). While there is some variation in channel

bandwidths, there's no detectable threshold elevation approximately 1.5 octaves from the adaptation frequency on either side. Masking studies have also shown a similar trend. When a test frequency is roughly 0.6 octaves outside the noise band, the relative threshold elevation is halved (Blakemore & Campbell, 1969). Optimal masking is therefore understood to be achieved within a 1-2 octave noise bandwidth, particularly when the noise band is centred on the test frequency and its width is expanded and noise outside this bandwidth appears ineffective for masking (Carter & Henning, 1971). Therefore, if each spatial frequency is detected by its corresponding most sensitive channel, research into adaptation and masking illustrates the bandwidth of these channels based on their distance in spatial frequency.

1.3.1 First-order processing

To effectively process first-order information, the visual system must be sensitive to luminance, orientation, temporal frequency, and spatial frequency. Therefore, it is essential to detect and process each characteristic independently within the first-order channel. Photoreceptor cells play a crucial role in detecting first-order visual cues by responding to shifts in light intensity (Enroth-Cugell & Robson, 1966). This information is subsequently relayed to the brain through the optic nerve where the primary visual cortex (V1) further refines this information. Each V1 cell receptive field is narrowly tuned to detect visual stimuli based on its orientation, spatial frequency, and luminance intensity. To determine the cell response, the luminance intensities from all points within the receptive field are summed linearly (Graham & Sutter, 1998; Sutter & Graham, 1995; Wilson et al., 1992). First-order vision is critical for many basic visual tasks, such as object recognition, scene segmentation, and motion perception (Levi & Carney, 2011). It is also a key component in many higher-level visual processes require integrating first-order information with other visual cues, such as shape-from-shading and texture perception (Doerschner et al., 2016).

1.3.2 Age-related changes in sensitivity of first-order luminance modulations

As people get older, their vision tends to deteriorate, which in turn could affect their overall well-being. This decline is typically caused by changes in the eye's physiology, such as the crystalline lens becoming denser and less flexible, resulting in lower retinal illumination. (Glasser et al., 2001; Owsley, 2011; Xu et al., 1997). Studies indicate that this decline can start as early as 45 years old, but more significant decreases are typically observed around 60 years old(Adrian Glasser & Campbell, 1998). Increased lens density also results in intraocular light scattering, which can lead to visual disturbances such as halos, glare, and reduced contrast sensitivity (Hennelly et al., 1998). Age-related changes in lens and cornea shape could also result in more optical aberrations (Artal et al., 2002). In addition, the eye is susceptible to the formation of cataracts. These occur when the proteins in the lens bond and create a cloudy appearance, potentially causing vision impairment or blindness if left untreated. Cataracts can slowly develop as early as 40 years old but become more problematic when they start affecting daily tasks due to reduced vision (Seddon et al., 1995). As we get older, our eyes also experience a gradual loss of lens elasticity (Charman, 2008; Glasser et al., 2001; Glasser & Campbell, 1998). This is known as presbyopia, which causes difficulty in focusing on nearby objects often resulting in the use of reading glasses to compensate for reduced flexibility in the lens.

Physiological changes in the eye consequently lead to reduced sensitivities in first-order vision. However, internal neural noise arises, such as random neuron firing or photoreceptor response fluctuations, which also increases with age (Pardhan, 2004). This has been observed in studies that have used a spatial contrast sensitivity function to explore the effects of age on spatial frequency (Owsley, 2011; Robson, 1966; Weale, 1982).

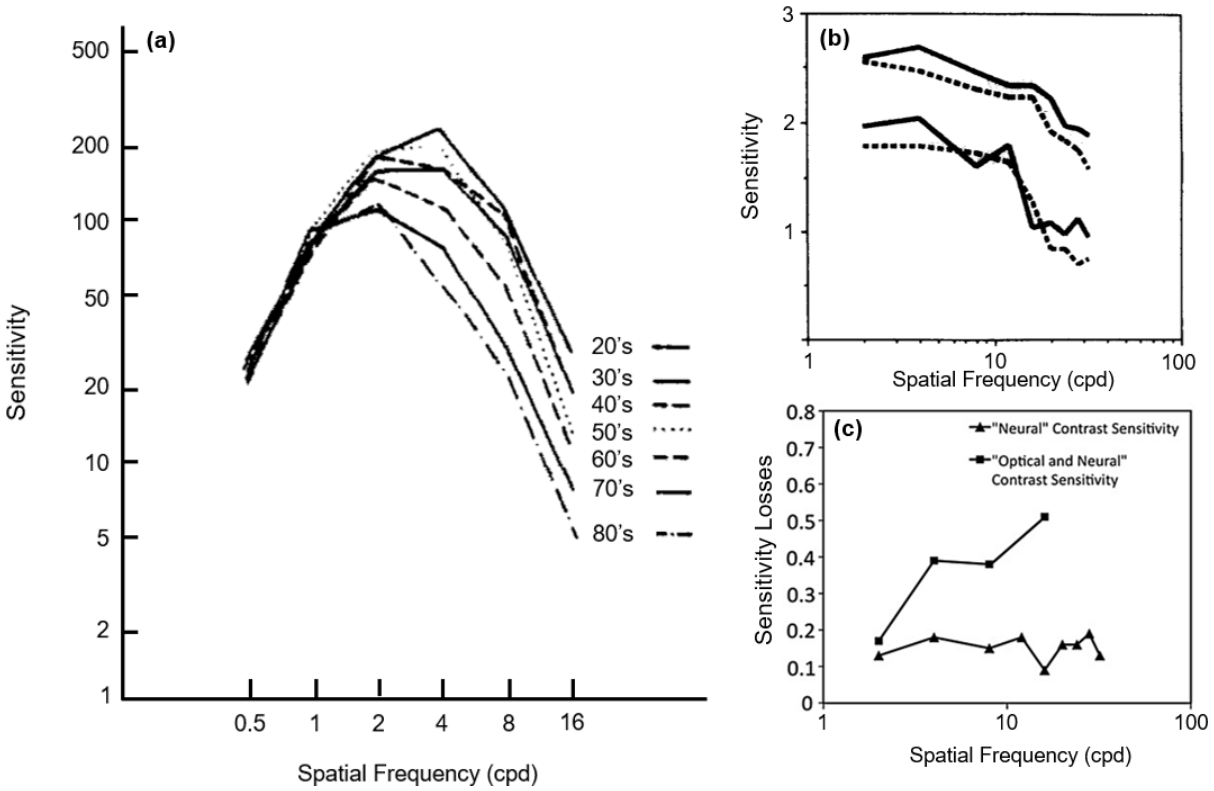

Figure 1-6. A comparison of first-order spatial contrast sensitivity with age. (a) a comparison of sensitivity across adulthood, segmented into age groups ranging from 20-80, demonstrating variation with age (Owsley et al., 1983). (b) the range of sensitivity across spatial frequency within each age group was mapped with a solid line representing younger adults (age range: 17-29) and the dashed line representing older adults (age range: 60-80) (Burton et al., 1993). (c) the loss of spatial contrast sensitivity in terms of neural and optical losses in adulthood, comparing sensitivity losses from two studies: the neural contributions to losses for older adults aged 60-80 (Burton et al., 1993) and a dataset that accounts for optical and neural changes in older adults aged 60-87 (Owsley et al., 1983). Note. (a) Reprinted from " Contrast Sensitivity Throughout Adulthood" by Owsley, C., Sekuler, R., & Siemsen, D., 1983, Vision Research, 23(7), p.694. (b) Reprinted from "Aging and neural spatial contrast sensitivity: photopic vision" by Burton, K. B., Owsley, C., & Sloane, M. E., 1993, Vision Research, 33(7), p.942. (c) Reprinted from " Aging and vision" by Owsley, C., 1993, Vision Research, 51(13), p.1612.

As illustrated in Figure 1-6(a), the ability to perceive high spatial frequencies diminishes due to age-related decline whereas sensitivity of low spatial frequencies was

relatively preserved (Owsley et al., 1983). From this figure, it is evident that sensitivity decreases continuously with age, however, the most substantial losses appear to be from the age of 60. In Figure 1-6(c), the observed losses at low spatial frequencies are predominantly influenced by neural changes. To exclude the influence of optical factors, targets were created using interference fringes from laser interferometry. The beam was split into two and directed onto the pupil, by-passing the optics of the eye. The spatial frequency of the interference fringes could then be adjusted by changing the distance between the two beams. Using this technique, the decline in contrast sensitivity at higher frequencies is unlikely to be due to neural factors alone, which accounted for less than half of the total loss, as shown in Figure 1-6(c) (Burton et al., 1993). Instead, optical factors, including reduced retinal illuminance, increased intraocular light scatter, and increased aberrations were primary reasons for the decline in spatial contrast sensitivity in older individuals. It is suggested that the slight reduction in sensitivity at low spatial frequencies is due to changes in their visual processing, while the declines in sensitivity of higher frequencies is likely due to optical factors. It's worth noting that there is significant overlap between the two age groups as illustrated in Figure 1-6(b) which could also account for the observed results in the "Optical and Neural" contrast sensitivity data set. Neural image processing, which could involve a drop in photoreceptor efficiency or neuron loss that can influence visual perception and contrast sensitivity, and internal noise, which pertains to the inherent variability within the visual system that can affect signal processing could all be factors here. These findings are supported by later work that also suggests older individuals have reduced perception of lower spatial frequencies due to neural decline, and experience deficits at higher frequencies due to optical impairments (Pardhan, 2004). Thus, both neural and optical factors uniquely contribute to the decline in visual acuity and contrast sensitivity.

1.4 Second-Order Amplitude Modulations

In Chapters 5 and 6, the role of texture modulated by first- and second-order shape-from-shading cues was explored, and how sensitivity of these change with age. First-order

stimuli are characterised by simple variations in luminance across space, whereas second-order stimuli are characterised by variations in the contrast of a carrier signal. Therefore, the characteristics of second-order vision, how it is processed, and how it changes with age will now be presented.

1.4.1 Properties of second-order vision

Second-order vision refers to visual stimuli that can be detected without a peak in Fourier energy (i.e. luminance intensity) (Chubb & Sperling, 1988; Graham & Sutter, 1998; Schofield, 2000; Sutter et al., 1995; Zhou & Baker, 1993). This means that it includes information beyond just changes in local luminance, such as contrast, texture, and motion (Johnson et al., 2007; Ledgeway & Smith, 1994; Nishida et al., 1997; Schofield & Georgeson, 1999, 2000). The focus of this thesis is specifically on changes in contrast, which are also known as amplitude modulations or AM. The term second-order amplitude modulations refer to modulating the local contrast of a visual texture on a larger scale than its individual components, without altering the local mean luminance (Baker & Mareschal, 2001).

A first-order carrier signal is required to convey these modulations, which in turn interacts with AM signals (Schofield & Georgeson, 2003). A noise carrier refers to a random visual pattern that is modulated to convey a signal. Narrowband carriers concentrate their energy within a limited range of spatial frequencies, whereas broadband carriers contain energy across a wide range of spatial frequencies offer rich information about an object's surface and depth (Schofield et al., 2017). In second-order stimuli, the signal is not expressed through changes in luminance. As a result, the higher-level properties of the noise carrier (e.g. local contrast) are varied across space (and/or time), and this modulation pattern is the second-order signal.

The spatial sensitivity of AM in adults is characterised by the relationship between the first-order carrier and second-order signal frequencies (Dakin & Mareschal, 2000; Schofield & Georgeson, 2003; Sun & Schofield, 2011). This is because of the first-order

carrier signal being required to convey second-order modulations. As illustrated in Figure 1-7, second-order vision shows marked sensitivity to carriers that contain high frequencies, such as white noise and high-pass noise. However, 1/f noise is characterised by a power spectrum in which the power diminishes proportionally with the frequency. This type of noise includes a broad range of spatial frequencies where density at higher frequencies is lower. As depicted in Figure 1-7, this characteristic of low-frequency 1/f noise renders it less effective as a carrier, indicating a greater sensitivity to second-order stimuli when conveyed through higher frequency carriers. The sensitivity function for second-order modulations exhibits similarities to that of the first-order, but with a peak in sensitivity that appears to be closer to 1 cpd. Furthermore, sensitivity to AM is much lower compared to first-order modulation sensitivity.

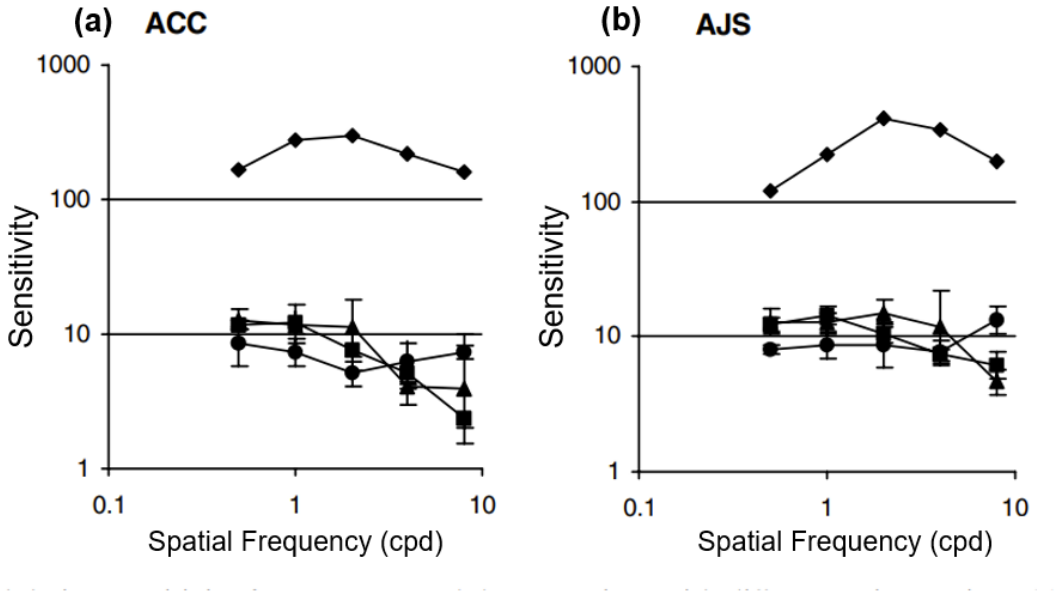

Figure 1-7. The effect of different noise carriers on AM sensitivity. The accompanying graph illustrates the results for two individuals and compares the sensitivity of three types of noise (1/f (●), white (■), and high-pass (▲)) to the contrast sensitivity function of first-order luminance gratings (◆). Note. Reprinted from "Sensitivity of contrast modulation: the spatial frequency dependence of second-order vision " by Schofield, A. J., & Georgeson, M. A., 2003, Vision Research, 43(3), p.250.

Orientation of the carrier is also thought to interact with spatial frequency (Dakin & Mareschal, 2000). In this study the orientation of the carrier (isotropic, vertical, and horizontal) was manipulated whilst also examining various spatial frequencies. An increased sensitivity was observed to vertical second-order contrast modulations in cases where the carrier had a higher spatial frequency, irrespective of it being isotropic or vertical. For carriers with a horizontal orientation, sensitivity to vertical contrast modulations at low spatial frequencies surpassed those isotropic carriers at lower spatial frequencies. However, this trend inverts when the carrier-to-envelope spatial frequency ratio reaches approximately 4:1, where performance for conditions with horizontal carriers is consistently worse in comparison to isotropic carriers. Previous research supports the idea that sensitivity of second-order modulations improves as the carrier to modulation frequency increases.

However, this improvement is only observed when the ratio of an isotropic carrier to second-order modulation frequency reaches 16:1 (Sutter et al., 1995). Beyond this point, a significant decline in sensitivity is reported, likely to be due to the poor visibility of the first-order carrier signal.

The findings indicate that there are distinct patterns for spatial frequency and orientation, suggesting filters that detect second-order structure are influenced by the outputs of presumably earlier mechanisms that extract Fourier information from the carrier and are sensitive to both orientation and spatial frequency. Although there are some similarities between the sensitivity functions for first- and second-order modulations, it appears that second-order vision is processed differently to first-order.

1.4.2 Non-linear processing in second-order channels

Second-order vision is believed to involve non-linear processing, whereby Y-cells detect non-Fourier properties of an image in the absence of a change in local energy (Graham & Sutter, 1998; Johnson & Baker, 2004; Rosenberg & Issa, 2011; Schofield, 2000). The summation of receptive fields is split into two distinct categories, where the role of retinal ganglion cells and the response characteristics differ: X-cells and Y-cells (Rosenberg & Issa, 2011). X-cells are responsible for processing high spatial frequency information and respond in a linear summation proportional to luminance. Y-cells process low spatial frequency information and respond non-linearly to luminance, thus introducing non-linearities into the visual system. This distinction in function enables the visual system to process both fine details and broad spatial patterns efficiently by responding to changes in the overall pattern of a stimulus, which is critical in detecting subtle changes in contrast or texture.

1.4.3 A separate channel for processing second-order modulations?

Previous studies have explored the relationship between first- and second-order vision, with models suggesting separate channels for processing. Research has indicated that second-order modulations are processed independently, suggesting that the perception

of second-order modulation is not enhanced by first-order modulations or vice versa (Schofield & Georgeson, 1999). Based on the findings, first- and second-order vision seems likely to be processed through distinct pathways. The following section supports the presence of second-order channels as distinct pathways.

Previous research supports that the visual system has distinct mechanisms that enable the perception of second-order cues (Baker & Mareschal, 2001; Graham & Sutter, 1998; Landy & Oruç, 2002; Mareschal & Baker, 1998). These mechanisms are specialised in detecting texture and contrast variations rather than only changes in average luminance. As a result, the visual system can efficiently detect and interpret image characteristics beyond just luminance, such as texture and contrast. The perception of second-order visual stimuli is suggested to be reliant upon the activation of selective neurons tuned to specific second-order patterns of modulation (Chubb & Sperling, 1988; Dakin & Mareschal, 2000). Studies have found that neurons in the visual cortex of cats and monkeys respond selectively to second-order stimuli, including patterns defined by changes in carrier orientation, spatial frequency, and contrast (Larsson et al., 2006; Leventhal et al., 1998; Mareschal & Baker, 1998; Zhou & Baker, 1993). However, these neurons also responded to first-order patterns that had similar properties to second-order modulations, suggesting they encode a cue-invariant representation of the stimuli (G. Li et al., 2014). This observation aligns with previous findings that area 18 neurons in the visual cortex exhibit phase-dependent responses to combined luminance and contrast modulation patterns where both simple and complex cell types demonstrate these phase-sensitive responses (Hutchinson et al., 2016).

Studies have also shown that the visual system has specific areas that allow for separate processing of second-order stimuli. Human fMRI research identified areas in the visual pathway that respond differently to displays containing texture boundaries specifically in areas V4, and inferior temporal area TEO (Kastner et al., 2000). Studies have also demonstrated that Macaque monkeys with lesions in areas V2 and V4 of the visual cortex exhibited difficulty performing texture discrimination tasks (De Weerd et al., 1996; Merigan et

al., 1993). In these studies, contrast sensitivity remained similar, further supporting the existence of separate cortical regions involved in visual texture processing.

First- and second-order vision channels also exhibit differences in their sensitivities to spatial properties. Typically, the second-order visual channel is less sensitive than the first-order due to the need for more processing, and therefore subject to more additive neural noise (Manahilov et al., 2005). Second-order channels have lower resolution compared to first-order channels, and a low-pass filter optimised for second-order signals (Kingdom et al., 1995; Lu & Sperling, 1995; Smith & Ledgeway, 1998). Therefore, to effectively detect and process an image, early non-linearities serve to demodulate so that both first- and second-order components can be processed independently before integrating (He & MacLeod, 1998). Separate channels for visual processing are supported by the concept that the stimulus can be distorted by early non-linearities when the carrier contrast is high, making it detectable by first-order mechanisms (Derrington & Ukkonen, 1999; He & MacLeod, 1998; Scott-Samuel & Georgeson, 1999). When processing two types of information in the same channel, it is possible for high contrast in the carrier signal to not cause any noticeable distortions detectable by the first-order mechanisms. This is because second-order attributes could potentially overpower or mask these distortions. However, the occurrence of distortions caused by high contrast carrier signals on first-order mechanisms indicates that they operate separately from the second-order mechanisms and are processed in different ways. Hence this supports the idea of independent channels for processing information.

1.4.4 Models of Processing

In Chapters 5 and 6, the role that first- and second-order modulations play in shape-from-shading is explored, and how this sensitivity changes with age. Therefore, the following section will present the characteristics of second-order vision; how it is thought to be processed, and the changes in sensitivity that occur with age.

1.4.4.1 Filter-rectify-filter model

The processing of first-order vision utilises linear filters to detect changes in luminance. However, second-order signals do not combine linearly, suggesting an independent processing mechanism for the second-order channel, which is thought to involve a two-stage filtering process (Wilson, Ferrera, & Yo, 1992). The filter-rectify-filter (FRF) model presented in Figure 1-8 proposed that second-order processing involves filtering the carrier signal by orientation and spatial frequency, a non-linear rectification, and a second low-pass filtering (Cavanagh & Mather, 1989; Chubb & Sperling, 1988; Kingdom et al., 2003; Wilson et al., 1992). This results in a smoothed-out second-order signal to eliminate anomalies in a higher-frequency carrier. This model supports the notions that neurons in the visual cortex are tuned to both spatial frequency and orientation and can distinguish differences in second-order contrast even when mean average luminance remains consistent (Chaudhuri & Albright, 1997; Ledgeway, Zhan, Johnson, Song, & Baker, 2005; Von Der Heydt & Peterhans, 1989).

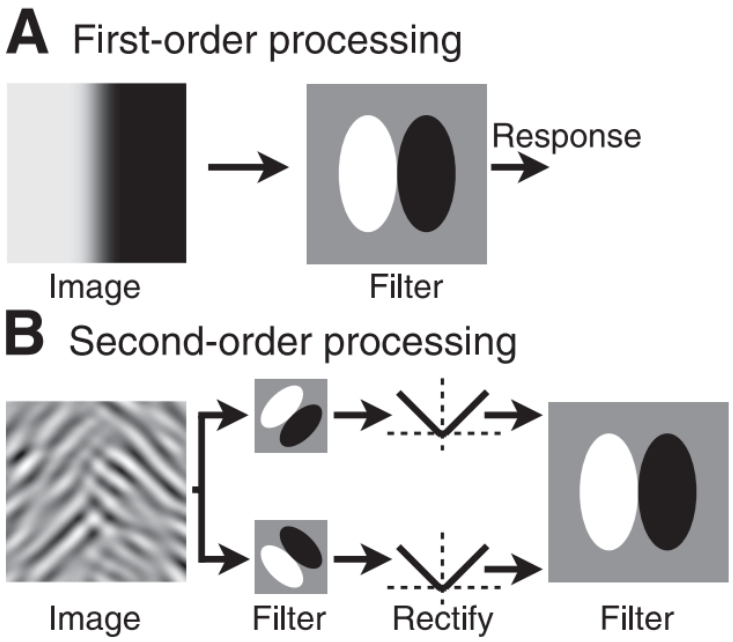

Figure 1-8. An illustration depicting the FRF model's response to (a) first- and (b) second-order stimuli. In second-order processing, the model has two types of filters: first-stage linear and second-stage filters that sum the non-linear outputs from the rectification stage. The process of rectification involves nonlinearity, usually through full-wave rectification.

The characteristics of these two channels shed further light on the relationship. Second-order modulation sensitivity function is characterised by a lower frequency tuning and reduced sensitivity compared to first-order sensitivity functions (Ledgeway & Hutchinson, 2005; Smith, Greenlee, Singh, Kraemer, & Hennig, 1998). Orientation thresholds for second-order modulations demonstrate lower frequency tuning and less overall sensitivity than first-order sensitivity functions (Ledgeway & Hutchinson, 2005; Reynaud et al., 2014). Differences in tuning are also observed where second-order sensitivity reaches its highest point roughly 3-4 octaves lower than the carrier frequency. (Sutter et al., 1995). This could be attributed to the prevalence of multiple second-stage filters tuned to low modulation frequencies and orientation.

1.4.4.2 Is there a relationship between first-order and second-order sensitivity?

When examining the relationship between the two channels, second-order modulations and carrier are perpendicular, and the perception of second-order modulations with a low-frequency carrier increase (Dakin & Mareschal, 2000; Westrick & Landy, 2013). However, as the carrier's spatial frequency increases, this relationship declines. This finding suggests that second-stage filters struggle to differentiate between first- and second-order information at similar frequencies, implying that it relies on inputs from the first-stage filters tuned to identify carrier texture. Therefore, the output of the second-stage filter depends on the carrier sensitivity.

However, greater sensitivity was observed for high-frequency texture modulations than the FRF model predicts (Westrick & Landy, 2013). It was proposed that the visual system pools first-order channels tuned to a range of spatial frequencies before filtering the carrier signal from the second-order modulations to obtain the output signal. By pooling the first-stage filter outputs before the second stage, a single second-stage filter could process the signal (Schofield, 2000). If the signal is not processed with early pooling, multiple second-stage filters would be required to process the signal. Additionally, pooling information across multiple orientation channels could omit important information regarding second-order orientation modulations. Combining orientation channels antagonistically or processing them individually in texture segmentation could mitigate the loss (Landy & Bergen, 1991). Therefore, early pooling models may not be suitable for texture processing. Late pooling models could preserve sensitivities to orientation modulations by not pooling all signals. However, sensitivities to orientation change suggest that pooling models are flexible enough not to pool all signals (Schofield, 2000).

1.4.4.3 How do first- and second-order signals combine to create a shape-from-shading cue?

The shading channel model was introduced to describe the role of AM in layer decomposition. Shading channels are also thought to contribute to the perception of depth

and surface properties by segregating shading patterns from texture variations (Georgeson & Schofield, 2003). The model is structured into three distinct stages. The initial stage suggests that LM and AM are detected by a bank of linear filters tuned to specific spatial frequencies and orientations, akin to the FRF model (Schofield et al., 2010; Y.-X. Zhou & Baker, 1996).. These filters operate under a shared gain control mechanism, adjusting each filter's response. As previously explained in the FRF model, the second stage is rectification, which is responsible for extracting the AM cue. In the third stage, the outputs from linear and FRF channels with similar orientations are combined and then undergo a late gain control. This separation and two-stage gain control is thought to contribute to the perception of depth and surface properties by enabling the segregation of shading information from other visual cues (Georgeson & Schofield, 2003). A model incorporating the spatial frequency and orientation properties of first- and second-order channels could preserve shading profiles for stimuli exhibiting both shading and material changes (Schofield et al., 2011). This could explain how the visual system maintains an accurate representation of depth and texture. By distinguishing shading signals from texture variation and other visual cues, the system can achieve this.

1.5 Age-Related Differences in Sensitivity of First- and Second-Order Stimuli

First- and second-order visual perception changes as the human visual system ages (Tang & Zhou, 2009). A comparison between first- and second-order stimuli found that ageing resulted in a decline in detection for both mechanisms. It was found that second-order sensitivity decreases significantly earlier than first-order sensitivity; however, it also has a slower progression (Owsley et al., 1983; Sutter et al., 1995; Tang & Zhou, 2009). Investigation of how the ageing process affects first-order vision found no change in sensitivity at low spatial frequencies throughout adulthood. The differences are magnified between younger (aged 20-40) and older adults (aged 60-70) at intermediate (2-4 cpd) and high (8-16 cpd) spatial frequencies, which is assumed to be a consequence of reduced retinal luminance in the eye and impairment in cognitive processing in older adults (Derefeldt

et al., 1979; Owsley et al., 1983). When high spatial frequency information is diminished, the first stage filters in the filter-rectify-filter model become less effective in perceiving the finer details in a visual scene. This loss of sensitivity of high spatial frequency information will, in turn, impact on second-order vision, as it receives inputs from the first-stage filters before undergoing rectification and subsequent second-order filtering.

1.6 Introduction to Studies

Despite considerable research on the effects of ageing on the visual system, a comprehensive understanding of the specific contributions of neural and optical deficits still awaits discovery. While studies have demonstrated the impact of ageing on various aspects of visual function such as contrast sensitivity, spatial frequency processing, and depth perception, the precise interaction of the mechanisms underlying these changes still needs to be fully understood.

Investigating the relationship amongst visual factors in the ageing visual system is key for understanding their influence on shape-from-shading sensitivity. This could also explain how age-related factors might interact with the visual system to further amplify age-related visual impairments. To address these gaps in the literature, this thesis aims to explore the themes of ageing and depth perception through shape-from-shading and the relationship between them. The following questions have guided the research included in this thesis:

i. How does ageing affect sensitivity to shape-from-shading?
ii. Does the perception of depth through shape-from-shading rely solely on the perception of its components?

The empirical chapters in this thesis aim to provide a comprehensive understanding of the effects of ageing on sensitivity to shape-from-shading, as well as the potential interactions with cognitive and optical factors. The following summaries briefly outline the research questions in each chapter, highlighting their contributions to the overall

investigation of age-related changes in depth perception using shape-from-shading information.

1.6.1 Chapter 3: Perceptual and cognitive load on shape-from-shading of textured surfaces

This chapter explores the role of cognition in shape-from-shading perception and whether there is an age-related interaction. It aims to determine the influence of cognitive factors on depth perception and their potential relationship to ageing in a series of online experiments, manipulating perceptual and cognitive load.

1.6.2 Chapter 4: Piloting and methodology refinement for psychophysical studies

This chapter details the piloting and refining of the methodology used to investigate first- and second-order contributions to shape-from-shading perception. It outlines the different methods employed in the study, and their respective strengths and weaknesses. It also discusses the challenges faced during the piloting process and how they were addressed. By refining the methodology for investigating first- and second-order contributions, the chapter lays the groundwork for the following empirical chapters.

1.6.3 Chapter 5: Perceived depth magnitude of luminance and contrast-modulated noise textures

This chapter delves into the effects of ageing on sensitivity to shape-from-shading and explores whether visual deficits contribute to the certainty of detecting shape from texture variations. The findings provide further insight into the relationship between age-related visual changes and the ability to perceive depth using shape-from-shading information.

1.6.4 Chapter 6: Contributions to age-related changes in shape-from-shading depth perception

In the final empirical chapter, the research examines the impact of ageing on sensitivity to shape-from-shading and the interactions between these factors. This analysis helps to better understand the complex relationship between age-related changes in the visual system and depth perception using shape-from-shading cues.

2 General Methods

This chapter provides an overview of the methodologies employed in the research detailed in this thesis, encompassing both stimulus presentation and data collection techniques. In subsequent chapters, the specific methodologies and stimulus manipulations employed in the individual studies will be further refined and expanded upon.

2.1 Stimuli

2.1.1 Noise-based Stimuli

First-order stimuli are characterised by simple variations in luminance across space, whereas second-order stimuli are characterised by variations in the contrast of a carrier signal. The experiments presented in chapters 5 and 6 utilised visual noise carriers for the second-order stimuli.

Noise textures are commonly used in shape-from-shading studies to simulate natural variations in luminance that occur in real-world scenes (Johnson et al., 2005). Furthermore, controlling the spatial frequency, contrast, and orientation of a noise texture aids the precise investigation of the role of these factors in form perception. Additionally, the use of noise enables us to represent changes in local contrast within a scene. The following section will present the properties of noise stimuli utilised in the subsequent empirical chapters.

A binary noise texture is commonly used in vision research and consists of a random pattern of pixels, wherein each pixel takes on one of two possible luminance levels, typically presented as black and white as illustrated in Figure 2-1 (Schofield & Georgeson, 2003). This results in a high-contrast, stochastic pattern that lacks any discernible structure or regularity. Binary noise is considered an effective carrier for second-order signals because its spatial properties exhibit equal power across all spatial frequencies. This characteristic

ensures that the binary noise effectively conveys second-order information, enabling the study of shape-from-shading perception (Schofield & Georgeson, 1999).

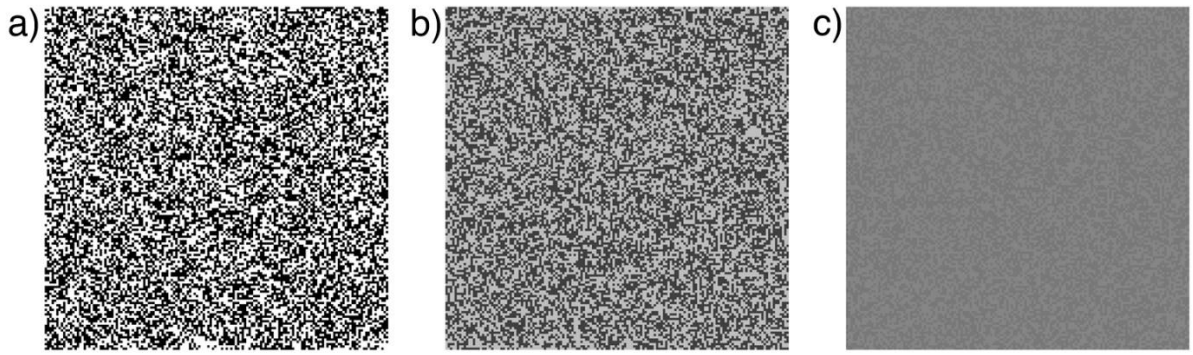

Figure 2-1. Three samples of binary noise with high-, medium-, and low-contrast. The figure displays three different levels of contrast in binary noise patterns generated with a 2x2 pixel component element at a) high contrast, b) mid contrast, and c) low contrast relative to the display. The contrast levels are determined by the difference in intensity between the light and dark pixels in the image.

Given the inherent spatial properties of binary noise, which prohibit manipulation of its spatial properties, it was deemed unsuitable for use in age-related research studies where carrier sensitivity is manipulated. In scenarios where the research objective involves manipulation of spatial frequency narrowband noise was therefore considered.

Isotropic noise textures, on the other hand, contain equal energy in all orientations along their amplitude spectrum (Li & Zaidi, 2003). By utilising isotropic noise, the objective was to examine the impact of shading information on shape perception while eliminating potential interference from non-uniformity in texture or directional cues. In the experiments where the spatial frequency was manipulated, employing an isotropic noise carrier was considered suitable for controlling the visibility of the spatial frequency.

Spatial-frequency narrowband, but orientationally isotropic noise, was produced in the Fourier domain. This involved filtering two-dimensional broadband noise using a non-oriented filter, selectively allowing a specific range of spatial frequencies to pass through. Gaussian filtering was applied to the isotropic noise following the principle of full width half-

height, where ‘full width’ refers to the total extent of the noise distribution, while ‘half-height’ is the point where the peak's value is half of its highest intensity (see Figure 2-2).

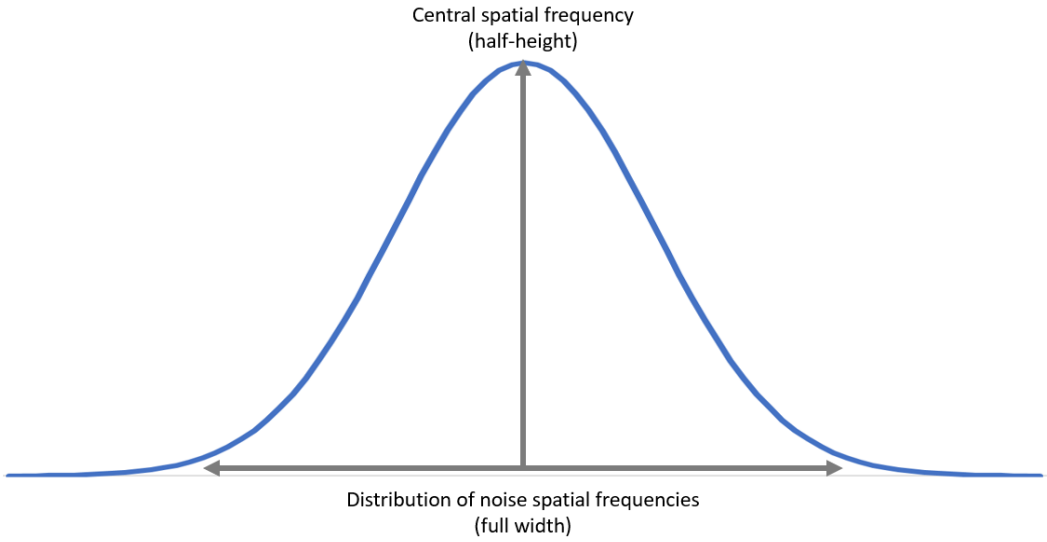

Figure 2-2. Example of the Gaussian filtering process that was applied to the isotropic noise sample, employing a full width half-height distribution of spatial frequencies.

This isotropic noise was then used as the basis for the stimuli and was further manipulated to convey shading information. This methodology, which incorporates isotropic noise carriers in our study, enables focus on the role of spatial frequency and ageing on shading cues in shape perception while minimising interference of noise component orientations.

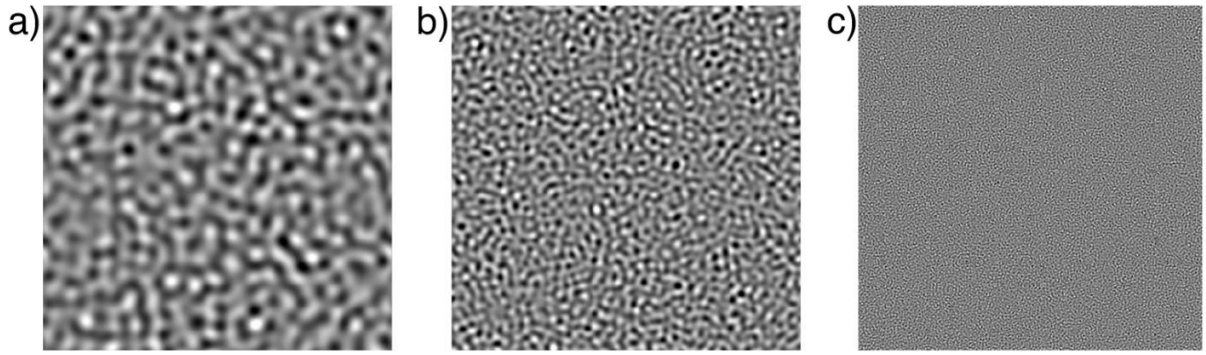

Figure 2-3. Three samples of an isotropic noise texture with varying spatial frequencies. The textures were drawn to specific spatial frequencies of a) 4 cpd, b) 8 cpd, and c) 12 cpd to illustrate examples of low, medium, and high frequencies, respectively. All stimuli were drawn to the specified spatial frequencies and resized for this figure.

In the present studies, isotropy was maintained, and shape information was conveyed through sinusoidal modulations of luminance and AM contrast. The stimulus preparation was similar to that of (Schofield & Georgeson, 1999), where sinusoidal modulations in amplitude and luminance were imposed onto the noise. The frequency bandwidth of the noise was set to 1 octave (full width, half-height), meaning the frequency content of the carrier spanned a range of frequencies that were twice the lowest frequency present. For example, a carrier with a centre frequency of 3 cpd had a frequency bandwidth ranging from 2.12 to 4.24 cpd in a normal distribution (see Figure 2-3). The overall contrast of the stimulus was set to 0.4 root mean square (rms).

For some studies in this thesis, an isotropic noise texture was employed as a carrier and modulated by an envelope. When the noise carrier is modulated by an envelope, the properties of the noise can interact with the properties of the envelope in various ways, such as the noise influencing the perceived intensity of the envelope's signal. These interactions arise due to the communalities in spatial characteristics between the envelope and carrier, which interfere with the envelope signal resulting in masking or distorting the envelope modulations. To minimise the impact of noise-to-envelope interactions, it is recommended to

use a noise carrier with a frequency at least 3-4 times higher than the modulation frequency of the envelope (Dakin & Mareschal, 2000).

The parameters of any noise utilised can be affected by artefacts. Additionally, a high-contrast signal can sometimes lead to side-band detection, where second-order cues within the stimulus are detected as first-order cues (Dakin & Mareschal, 2000; Georgeson & Schofield, 2003; He & MacLeod, 1998).

The presence of noise can introduce non-linearities in the relationship between stimulus contrast and detectability, leading to a phenomenon known as the pedestal or dipper effect. The pedestal effect is observed when small increases, in contrast, are added to a grating presented in noise similar in spatial frequency, orientation, and phase. Under these conditions, the detectability of the grating is significantly improved, even though the added contrast is relatively small (Foley & Legge, 1981; Kontsevich & Tyler, 1999).

The pedestal effect is thought to arise from non-linearities in the transduction process of the visual system. Transduction refers to the conversion of perception of a stimulus into the neural activity that the brain can process, and non-linearities in transduction can arise when the visual system's response to a stimulus is not proportional to the stimulus intensity. These non-linearities can introduce a biological luminance artefact at any point in the visual system that impairs shape-from-shading perception (Derrington & Ukkonen, 1999). In the case of the pedestal effect, adding a small amount of contrast to a grating in noise can cause a disproportionately large change in the neural response, improving detectability.

Using a noise sample with a large component size relative to the second-order modulation frequency can also lead to clumping, which introduces an artefact in the signal (Smith & Ledgeway, 1997). Clumping occurs when the noise components are large and subsequently disrupts the signal of the modulations. Conversely, a component size that is too small can cause other luminance artefacts, such as adjacent pixel non-linearities (Schofield & Georgeson, 1999). This non-linearity occurs when the total luminance values in a row of pixels do not sum linearly, causing a reduction in the average luminance of each

pixel row (Klein et al., 1996). Therefore, an appropriate component size and carrier-to-envelope ratio were employed to mitigate the risk of these potential artefacts.

2.1.2 Luminance and Amplitude Sinusoidal Modulations

As discussed in chapter 1, shape-from-shading is a monocular cue for conveying depth based on the observation that the luminance gradient of a surface varies with its orientation relative to a light source. In previous research, shape-from-shading has been utilised to convey depth in experimental stimuli (Schofield et al., 2006; Schofield & Georgeson, 1999). This thesis employed different combinations of luminance (LM) and amplitude (AM) sinusoidal modulations to create shape-from-shading cues. The following section will outline the method employed to create LM and AM sinusoidal modulation. Following this, the incorporation of these modulations into the experimental design will be explained. Luminance sinusoidal modulations were constructed by multiplying a constant luminance value (I_0) by a sinusoidal function of a specified spatial frequency (see Equation 2-1). In Figure 2-4, a change in local mean luminance varies sinusoidally in the horizontal direction, whereas the local range of pixel values remains constant. The luminance modulation was added to the noise texture by the equation below.

$$I(x,y) = I_0(1 + nN(x,y) + l\sin(\omega x))$$

Equation 2-1

In this equation I_0 is the mean luminance, $N(x,y)$, is the 2-d noise sample, and n, is the noise contrast, where l is the overall luminance contrast, and ω is the sinusoid frequency.

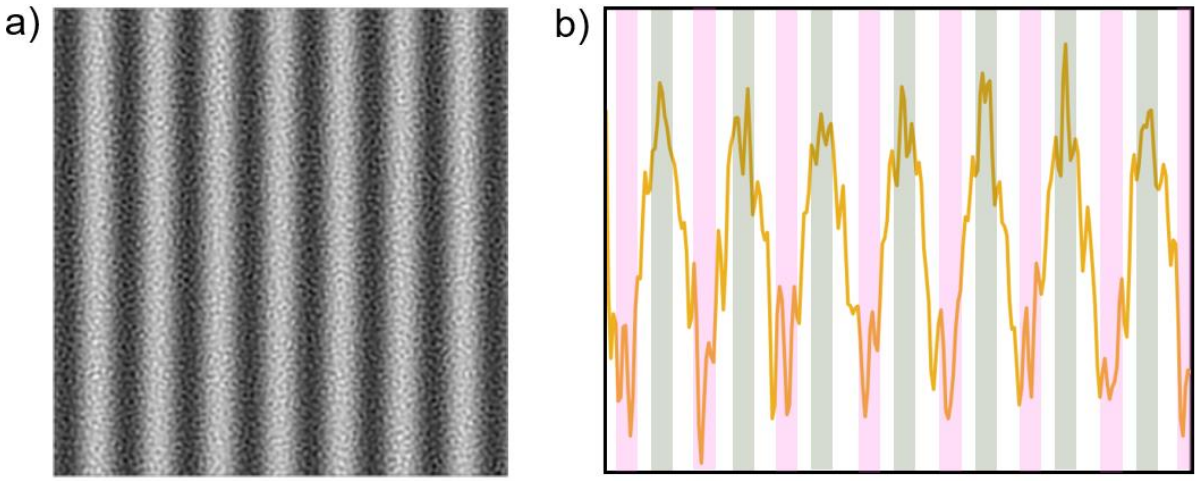

Figure 2-4. An illustration of pixel luminance values in a luminance-modulated stimulus. (a) depicts an isotropic texture modulated by luminance. (b) shows a horizontal slice of the luminance modulations, with the luminance values of each pixel plotted, areas of high luminance are highlighted in green, areas of low luminance in magenta.

The AM contrast-modulated (AM) noise carrier increases or decreases the local contrast in a particular area. AM affects the difference in luminance values between pixels, either increasing in value for a high amplitude or decreasing for a low amplitude. Figure 2-5 demonstrates how the local range of pixel luminance values (i.e., contrast) varies across the image in relation to the constant amplitude of the sinusoidal wave. The AM grating was constructed by modulating the noise texture by multiplying the noise contrast by the specified amplitude modulation. The equation for amplitude-modulated noise is below in Equation 2-2.

$$I(x,y) = I_0\big(1 + (mn(sin(\omega x) + 1)N(x,y)\big)$$

Equation 2-2

In this Equation 2-2 the process of amplitude-modulating noise is defined, where $I(x,y)$ represents the intensity of the noise at any given point, determined by coordinates x and y. I_0 denotes the noise intensity, mn indicates the modulation depth of the noise, and the

function, $sin(\omega x) + 1$, shifts the oscillations between 0 and 2, ensuring that the modulation amplifies the base noise intensity I_0. $N(x, y)$ represents the noise pattern at each point, which is modulated by the combined effect of the sinusoidal wave and the modulation depth.

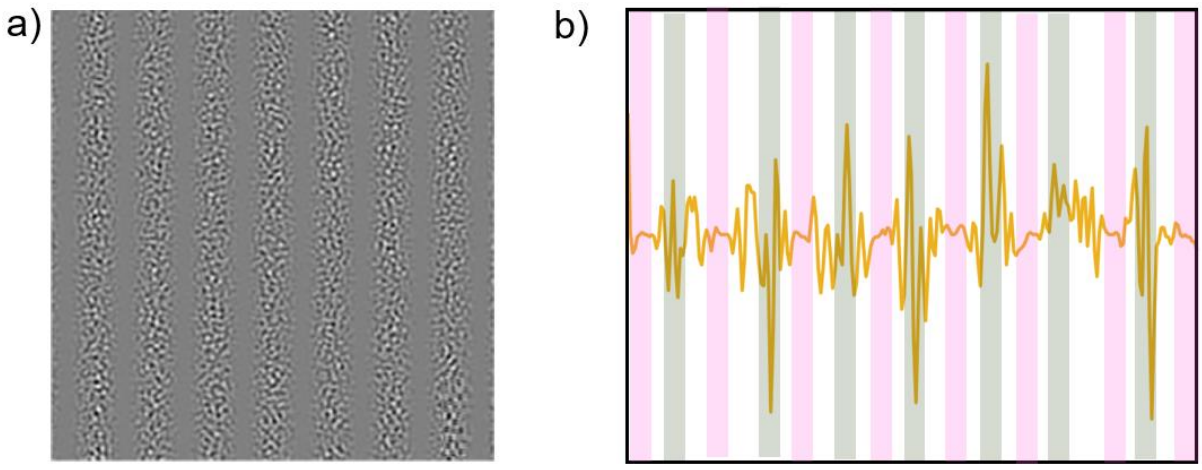

Figure 2-5. A representation of pixel luminance values in an amplitude-modulated texture (a) displays an isotropic texture that is modulated in contrast (amplitude). (b) plots the luminance values of a cross-section for each pixel. Areas of high contrast are highlighted in green, areas of low contrast in magenta.

2.1.3 Compound Gratings

A compound grating combines a noise texture, a luminance-modulated (LM) sine wave, and an amplitude-modulated (AM) sine wave. But the statistical relationship between LM and AM can vary. The 'in-phase' grating presented in Figure 2-6a illustrated a compound grating where LM and AM have a positive correlation with their respective intensities, meaning that when the amplitude is high, the luminance is also high. In contrast, the 'anti-phase' grating presented in Figure 2-6b presents LM and AM with a negative correlation, meaning in a high local region of amplitude, the luminance is low, creating a half-cycle (0.5) difference.

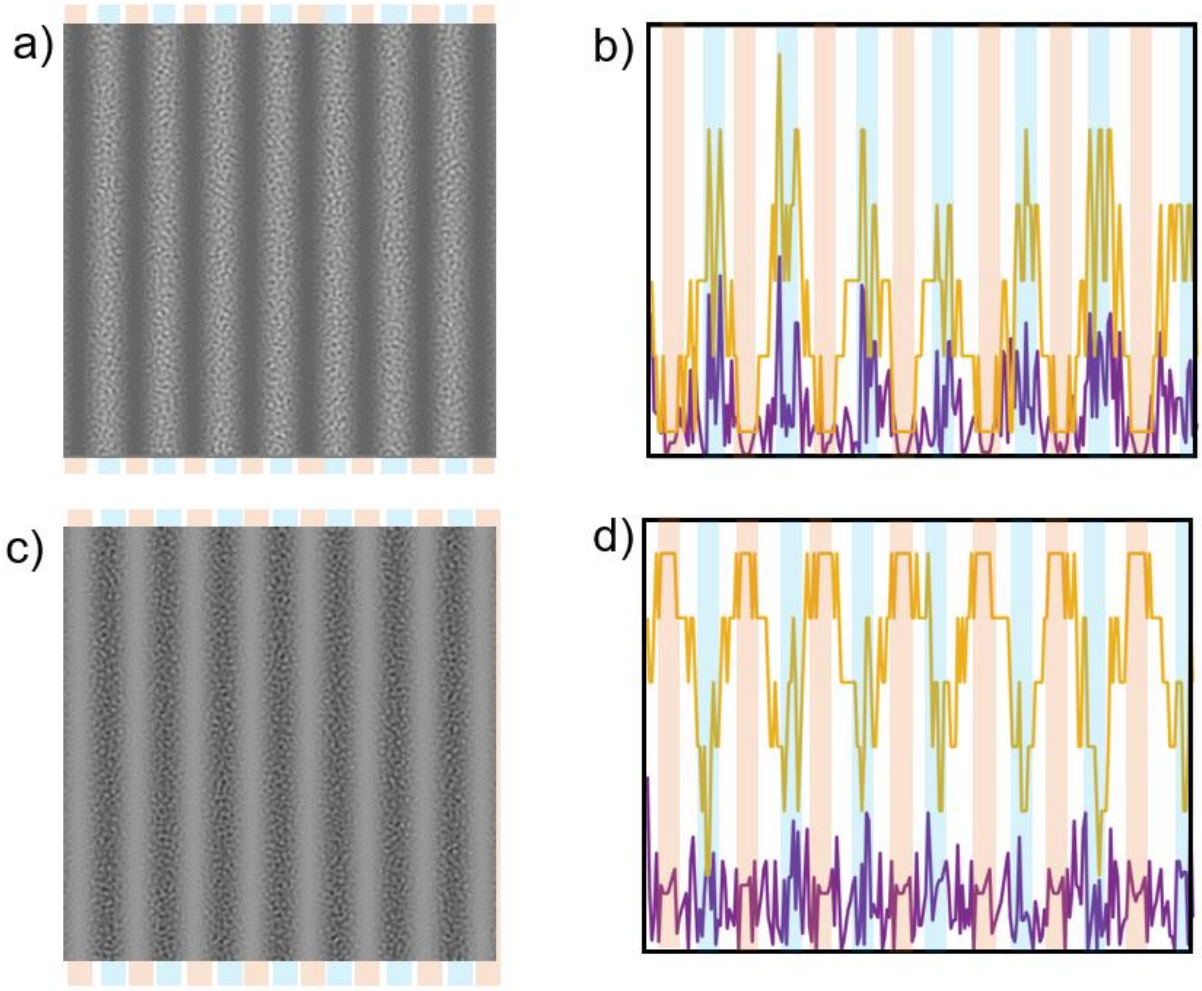

Figure 2-6. The figure includes (a) an LM+AM grating and (b) a plot showing the values of luminance and contrast. In this plot, areas with high AM contrast (resulting in high luminance) are highlighted in blue, while areas with low contrast (and correspondingly low luminance) are marked in orange. The plot demonstrates that an increase in the mean luminance value is accompanied by an increase in the variance (amplitude) of the pixel values. Additionally, figure (c) shows an LM-AM grating, alongside a plot in figure (d), illustrating that as the luminance values decrease, the variance in these pixel values increases. In this plot, areas of high AM contrast (leading to low luminance) are highlighted in blue, and areas of low contrast (resulting in high luminance) are indicated in orange.

2.1.4 Sinusoidal Plaid

A sinusoidal plaid is typically a composition of two luminance sinusoids at different orientations. In chapter 6, two compound gratings (the in-phase and anti-phase components)

were superimposed over the visual texture at two adjacent orientations (45° and 315°), randomly assigned for each trial. The absolute phase of each sinusoidal wave grating was randomised, and gratings were presented within a raised cosine window to prevent detection of the in-phase component by examining the wave's phase at the edge of the window. As found in previous research, the presence of the two obliques in one single configuration (i.e. a plaid) strengthens the signal of both obliques so that it is possible for the viewer to discriminate between changes in shape and shading (Dövencioğlu et al., 2013).

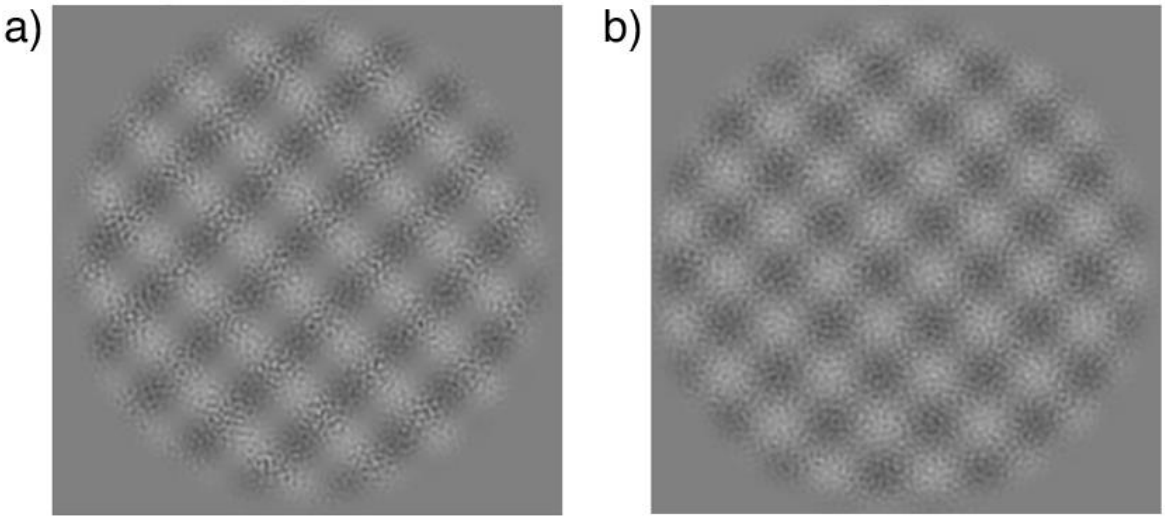

Figure 2-7. A sinusoidal plaid is illustrated with two different amplitude modulation intensities. (a) presents the plaid with a large amplitude modulation, meaning the luminance and contrast of the individual gratings interact more strongly, creating a more distinct interference pattern. (b) displays the same plaid with low amplitude modulation depth, where the modulation is weaker, resulting in a simpler interference pattern resulting in gratings that are difficult to distinguish.

2.2 Design

This chapters 5 and 6 utilised four psychophysical experimental designs to investigate the relationship between age and shape-from-shading perception. These designs included the method of constants, paired comparisons, staircase procedure, and a QUEST staircase method. The method of constants entails presenting a stimulus with a

predetermined set of intensity levels to obtain an estimated proportion of correct responses at each level. Paired comparisons are a method used to assess perceptual differences between stimuli, participants are presented with two stimuli, either simultaneously or sequentially, and are asked to make a judgment about a specific aspect, such as perceived intensity. A staircase method presents the stimuli in a procedure that changes the stimulus intensity depending on the previous response. Lastly, the QUEST method is adaptive and adjusts the stimulus intensity based on accumulating participants' previous responses. The selection of the appropriate experimental design was carefully considered based on each study's objectives, as each design has its strengths and limitations.

2.2.1 Method of Constants

The method of constants involves presenting a stimulus from a series of predetermined intensities and recording participants' responses. The stimuli were presented at predefined levels in a randomised order, which are held constant throughout the experiment, allowing for precise control and measurement of the perception of the stimulus intensity being tested. By repeating each stimulus presentation multiple times and calculating the proportion of correct responses at each level, a psychometric function can be fitted to describe the relationship between stimulus intensity and detection. To accomplish this, each trial has a predefined set of values for the amplitude modulation magnitude to evoke a proportion of correct responses from 50% to 100% (see Figure 2-8). The 75% threshold estimate was obtained from this task by repeating each amplitude modulation magnitude multiple times to calculate the proportion of correct responses for magnitude level.

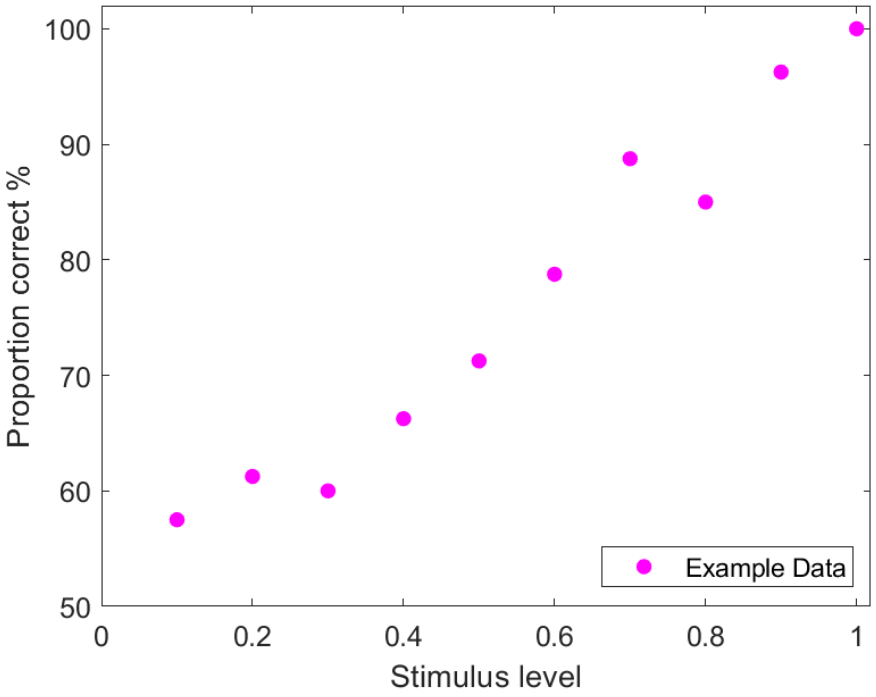

Figure 2-8. Example results from a method of constants experiment. The proportion of correct responses is plotted as a function of stimulus level. The magenta circles represent the proportion of correct responses for each level.

This experimental procedure was selected for two primary reasons. Firstly, it served as a practice for participants to become familiar with perceiving both easy and challenging stimuli to minimise participant noise in subsequent trial blocks when different experimental designs were employed. Secondly, the procedure was used to screen participants and determine if a 75% threshold could not be attained within the possible parameter levels, resulting in their exclusion from the study.

Using a fixed set of stimuli minimises the potential impact of individual differences among observers, and reported effects are a consequence of the manipulated variable. This method also reduces the need for a large number of participants since each level is repeated many times to accurately estimate the proportion of correct responses. However, this means that the method can be time-consuming, where multiple presentations increase the duration of the experiment. Furthermore, this methodology has a limited range of stimuli intensities,

which may not accurately capture a wide range of proportion correct responses. The fixed set of stimulus levels may also not be sensitive enough to detect subtle changes in sensitivity when increments are too large. Despite these limitations, the method of constants remains a valuable experimental design methodology for exploring the relationship between amplitude modulation magnitude and shape-from-shading depth perception.

Therefore, employing this method to screen participants and provide practice with a diverse range of stimuli with varying perceptual difficulty proved advantageous for subsequent threshold estimation using alternative psychophysical methods. As the primary objective of this methodology was practice, rather than precise threshold estimation, it involved presenting a sinusoidal plaid at 11 distinct levels ranging from 0 to 0.9, with intervals calculated using the square root of 2. Each level was repeated 10 times (110 trials total) to calculate the proportion of correct responses at each constant level, ranging from chance to perfect.

2.2.2 Up/Down Staircase Method

The up/down staircase method is a psychophysical procedure used to estimate perceptual thresholds (Cornsweet, 1962). Based on the participant's response in the previous trial, the staircase moves upward or downward in difficulty. If the stimulus is detected or discriminated in the previous trial, the staircase moves downward, making the stimulus harder to see. If the stimulus is not detected or discriminated, the staircase moves upward, making the stimulus perceptually easier to detect. Objective threshold measurement is taken by adjusting the perceptual difficulty of the stimulus until a specified threshold is met. In the case of the 3-down, 1-up staircase method used in the experiments, a 79.4% threshold was estimated. This means the stimulus amplitude decreased when three correct responses were recorded and increased when one incorrect response was recorded, as demonstrated in Figure 2-9.

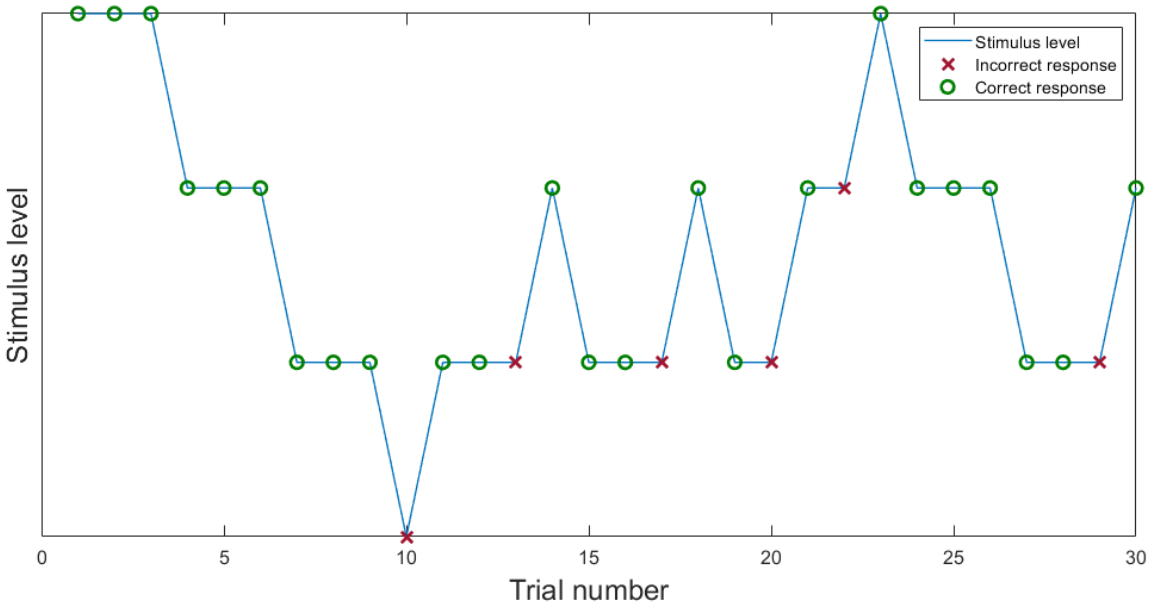

Figure 2-9. An example of a 3-down 1-up staircase procedure. The staircase procedure begins with a relatively high stimulus intensity, which is initially easy for the observer to discriminate, then decreases in intensity over time for every three correct responses.

In addition to the 3 down-1 up rule, the staircase step size was also modulated. Specifically, the step size was halved for the first four instances where the staircase reversed direction. After these four instances, the step size was modified by 4, 2, 2, and 1 dB, respectively. The 3 down-1 up rule and the modulation of the step size are two strategies that ensure that the staircase converges on an accurate threshold estimate. By decreasing the stimulus amplitude after three correct responses and increasing it after one incorrect response, the 3 down-1 up rule aims to adjust the task difficulty quickly in response to the participant's performance. Similarly, the reduction in step size aims to adjust the task difficulty more precisely by halving the step size for the first few reversals and then using a predetermined step size modification.

This adaptive method is an effective way of estimating perceptual thresholds because, after a few reversals, the stimulus level remains close to the threshold level, allowing for a more precise threshold value to be estimated. This contrasts with non-adaptive procedures, where stimuli are presented at fixed levels and may not be close to the

threshold, resulting in more trials to estimate the threshold. This makes staircase procedures more efficient than non-adaptive ones using fixed stimulus levels. However, perceptual errors can heavily influence an up/down staircase method, particularly if the participant becomes fatigued or loses motivation during the trials. Additionally, the adaptive nature of the staircase procedure means that it may not be suitable for estimating thresholds in cases where the participant's performance is highly variable or unstable, and the choice of parameters, such as the step size and the number of reversals, can affect the accuracy and efficiency of the threshold estimation.

2.2.3 Quest Staircase

The Quest staircase is a Bayesian adaptive method for estimating perceptual thresholds in psychophysics research (Watson & Pelli, 1983). Unlike the 3-down, 1-up staircase procedure, which is a rule-based adaptive method, the Quest staircase uses a statistical model to adjust the difficulty of the stimulus in response to the participant's overall performance. A Quest staircase is a running fit method, which continuously updates the model based on the participant's responses as the trials progress. The model assumes that the participant's responses follow a psychometric function, which relates the stimulus intensity to the probability of a correct response. It then estimates the parameters of this psychometric function based on the participant's responses and uses this information to determine the next stimulus intensity. A threshold is estimated by specifying the psychometric fit parameters (slope, guess rate and lapse rate) before the staircase has commenced (Watson & Pelli, 1983). After each trial, the likelihood function is calculated based on the existing data of the staircase. The stimulus intensity is then set for the subsequent trial based on the threshold estimate calculated from the previous trials.

This method differs from traditional up/down staircases in several ways. One distinction is that the step sizes in a Quest staircase are not predetermined and decrease as the staircase runs. This adaptability allows the Quest staircase to converge more quickly and efficiently on an accurate threshold estimate. Another distinction of a Quest staircase is that

an estimated threshold is input as the starting point for the staircase, which in this thesis was provided from the method of constants trials. This way, our pre-existing knowledge of the individual observer's threshold estimate will inform the more precise threshold estimate (from Quest). By incorporating the estimated threshold from the method of constant trials, the Quest staircase can obtain a posterior probability distribution of the threshold parameter values. This distribution provides a measure of uncertainty around the threshold estimate, which is an important parameter in interpreting the results of the experiments.

To ensure that each observer's starting point was unique to their performance in the method of constants task and to minimise the probability of poorer performance being a result of the starting stimulus magnitude being too difficult for the observer, it was deemed more appropriate to use both a Quest and method of constants design.

2.3 Equipment

2.3.1 Display Monitor

The visual stimuli were generated using the open-source package Psychopy© (Peirce et al., 2019). Vpixx (Vpixx Technologies Inc.), a specialised hardware system, provided precise control over stimulus presentation by increasing the dynamic range of the stimuli while also supporting high spatial and temporal resolutions. The stimuli were presented on a CRT monitor (Viewsonic P225f) running on a Mac OS X El Capitan v10.11 operating system. The monitor used had a display screen width of 39cm, a resolution of 1280 x 1024 pixels, and a pixel size of .0356 x .0356 cm, with an overall screen refresh rate of 75Hz.

In some empirical chapters, the maximum spatial frequency of the CRT monitor used to display visual stimuli may be limited by the size of individual pixels. However, this limitation can be addressed by increasing the viewing distance for participants. Increasing the viewing distance allows more pixels to represent a given visual stimulus, allowing for a more precise representation.

2.3.2 Gamma Correction

Accurate measurement of luminance output on the monitor is essential for the in-person experiments conducted in the empirical chapters, as even small changes in luminance can significantly affect the results. Therefore, it was necessary to calibrate the monitor before implementing each in-person study to monitor any deviations in the luminance output. This was achieved using a gamma correction function to characterise the non-linear relationship between voltage input and luminance output (Denis G Pelli & Zhang, 1991). The inverse of this gamma correction function is then used to provide the values required to build the look-up table (LUT).

Equation 4 specifies the relationship between the requested intensity, V, and the luminance output, L. The constants included in the equation are as follows; a describes the minimum luminance value that can be displayed on the monitor, k is the scaling factor that adjusts the range of V to match the range of L. b represents the range of the requested intensity values, γ represents the gamma value that accounts for the non-linear relationship between voltage input and luminance output. Using this equation, we can calculate the appropriate luminance output for a given requested intensity, considering the minimum luminance value, the scaling factor, and the gamma value.

$$L(V) = a + (b + k\,(V))^{\gamma}$$

Equation 2-3

When calibrating the monitor for the in-person experiments, a luminance patch was presented in the centre of the screen using an inbuilt function in PsychoPy©. The patch consisted of 500 x 500 pixels and was presented at 32 evenly spaced calibration points between 0-1, with measurements taken using a photometer at a distance of 57cm from the monitor. Three luminance values were recorded at each calibration point, and the mean was

calculated. The measurements were recorded separately for the three colour channels (RGB), and the overall output luminance was calculated.

Using the toolbox in PsychoPy©, a gamma function was produced to reflect the non-linear relationship between voltage input and luminance output. This function was then inverted in Equation 2-4 to produce the LUT to correct the input voltage and produce the correct output luminance. The corrected voltage-to-luminance relationship is linearised by the inversion of the gamma function, ensuring that the monitor is properly calibrated for the in-person experiments.

$$LUT(V) = \frac{\left((1-V)b^{\mathrm{g}} + V(b+k)^{\mathrm{g}}\right)^{\frac{1}{\mathrm{g}}} - b}{k}$$

Equation 2-4

2.3.3 Spatial Calibration

A spatial calibration was implemented in the experiments to ensure consistency and accuracy in the presentation of visual stimuli. The purpose was to verify that the size of the pixels on the monitor was consistent and square. The spatial calibration was conducted on 3/7/2017 using the specified monitor.

The spatial calibration procedure ensures that the size and shape of the stimuli displayed on the monitor were precise and consistent throughout the experiments. During the calibration process, a square of a specified size was displayed on the monitor, and the height and width of each square were recorded. For each square window size, a total of three measurements were taken using a measuring tape, and the mean of these measurements was recorded in a table. Once all measurements were taken, the estimated pixel size was calculated based on the recorded values, as depicted in Table 2-1. This type of calibration was critical in accurately presenting visual stimuli and ensuring the reliability of the experimental results.

Table 2-1

Measurements taken at specific stimulus sizes during a spatial calibration.

Stimulus Size	Stimulus Width	Stimulus Height	Pixel Width	Pixel Height
700	254.5	258.5	0.0364	0.0369
512	180.5	180	0.0353	0.031
255	90	90.5	0.0352	0.0354
100	35.5	35	0.0355	0.03
		Average Pixel	0.0356	0.0356

Note. The measurements in the table were taken during the spatial calibration process and represent the mean of three measurements, with all values being recorded in millimetres (mm).

2.3.4 Experimental Setup

For the in-person experiments, participants viewed all conditions binocularly in a modified chinrest with an optical trial lens frame. The chinrest included an adjustable frame for chin height attached to a table using two G clamps, and the chin could also be adjusted forwards or backwards to ensure comfortable viewing through the lens frame and minimise any restrictions. The optical trial lens frame featured several adjustable elements, including pupil distance adjustment and adjustment for the viewing aperture to be closer or further away from the observer's eyes if glasses were worn. The frame could accommodate up to three trial lenses for precise vision correction.

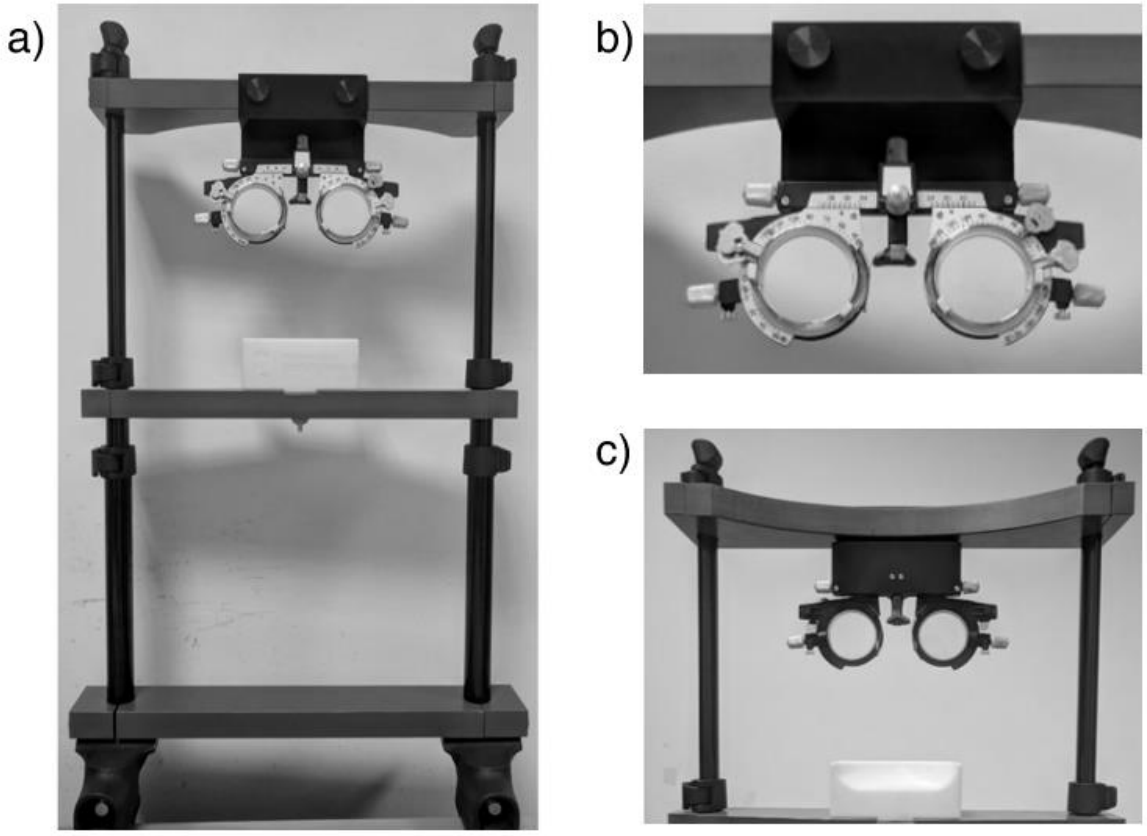

Figure 2-10. A depiction of the modified chinrest with optical trial lens frame developed for the in-person portion of experiments. a) captures the entire structure, b) provides a closer view of the optical trial lens frame and the adjustable elements, and c) shows the modified chinrest and lens frame from the participant's view.

The lens frame allowed for the correction of presbyopia, with the overall lens power required calculated as 1/distance (in metres). The lenses used for each experiment were specified in their respective chapters. Older adults viewed the stimuli through a positive and negative lens, and the sum of these two lenses provided the overall power to correct for presbyopia and determine the viewing distance. The viewing distance varied depending on the experiment, with a minimum viewing distance of 53.33cm. This was corrected for using two lenses with an overall power of 1.875 (+2.0 and -0.125). In cases where individuals required corrective glasses for distance vision, these were used in conjunction. To ensure a consistent viewing condition across age groups, younger adult participants were provided with a positive and negative lens, with an overall power of 0.

Longer viewing distances were required for some experiments to compensate for presenting high spatial frequency stimuli on the screen without distortion or clumping. Using longer viewing distances also allowed for the use of thinner lenses, reducing distortion. All adults were encouraged to wear their corrective lenses, if applicable, to ensure accurate vision correction.

During each experiment, participants were instructed to respond using a keyboard. They were encouraged to rest their fingers on the keys and to practice responding without looking at their fingers. This approach was adopted to ensure that they could maintain their focus on the fixation cross and the test stimuli that followed.

2.4 Statistical Analysis

2.4.1 Psychometric Functions

Data were obtained from a method of constants design where the proportion correct for each modulation depth level was fit to a curve to calculate thresholds at 75% proportion correct. All data was analysed and processed using Matlab© (MathWorks, 2012) using Palamedes Toolbox (Prins & Kingdom, 2009). A cumulative normal distribution psychometric function was used as the curve fitting tool. Due to the two-alternative forced-choice design, a guess rate (γ) of 0.5 was fixed. The lapse rate (λ) was varied for each curve-fitting analysis between the limits of 0 and 0.06. From this psychometric function, the threshold and slope of the curve were obtained for each condition. The psychometric function's goodness-of-fit was also measured, and the standard errors of the parameter were estimated using the bootstrapping method.

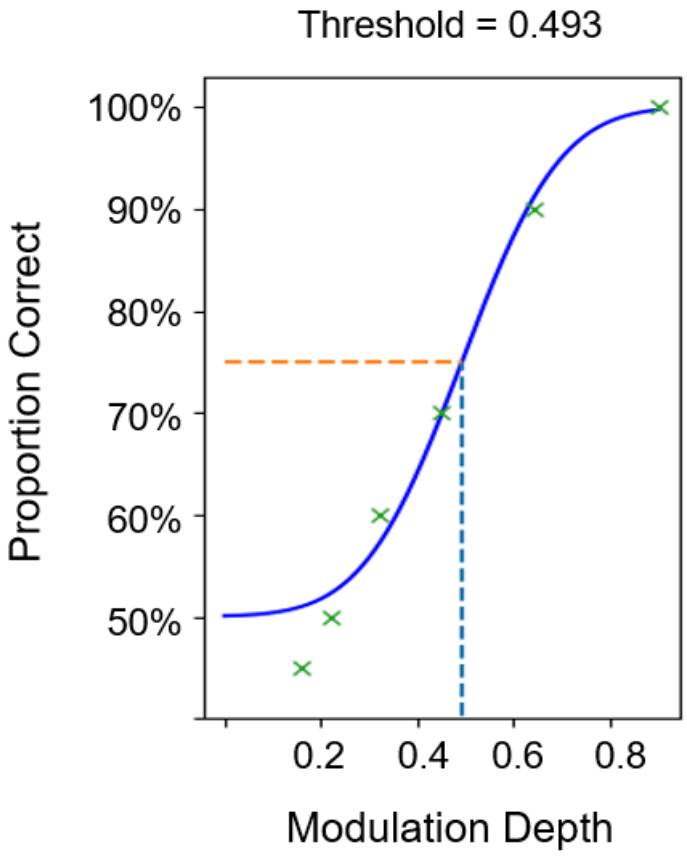

Figure 2-11. An example of a method of constants cumulative Gaussian curve fit. The curve fit shows an increase in correct responses as the stimulus level increases. The x-axis represents the stimulus level, while the y-axis represents the proportion of correct responses. In this example, the threshold estimate is 75%, indicating the stimulus level at which participants could detect the stimuli with 75% accuracy.

The likelihood function was used to estimate the parameters of threshold (α) and slope (β), where the maximum likelihood estimates of α and β are the calculated values that maximise the likelihood function. The equation below denotes the likelihood function of the four parameters, threshold (α), slope (β), guess rate (γ), and lapse rate (λ), where the probability of observation of the response y (correct/incorrect) on one specific trial k at a specified stimulus intensity x_k.

$$L(\alpha, \beta, \gamma, \lambda|y) = \prod_{k=1}^{N} p(y_k|x_k\,; \alpha, \beta, \gamma, \lambda)$$

Equation 2-5

The lapse rate parameter (λ) determines the proportion of lapses that participants make during the experiment. Although the value itself is not essential, it is vital to calculate an accurate estimate of lapses as this could systematically impact on the estimates for the other psychometric function parameters (α, β). Fixing the lapse rate to 0 would lead to a biasing of threshold and slope estimates, whereas slightly overestimating the lapse rate leads to lower biasing effects (Hall, 1981). In the present experiment, the lapse rate was not assumed to be equal between each experimental condition, and therefore the lapse rate was set to vary between 0-0.06 for each condition. Lapse rates greater than 0.06 were assumed to be incorrect as more considerable lapses would indicate that any thresholds obtained would be inaccurate. This way, the maximum likelihood of the participant's lapse rate between each condition is calculated rather than assumed, and further analysis of the lapse rate between conditions could be conducted (Kingdom & Prins, 2016).

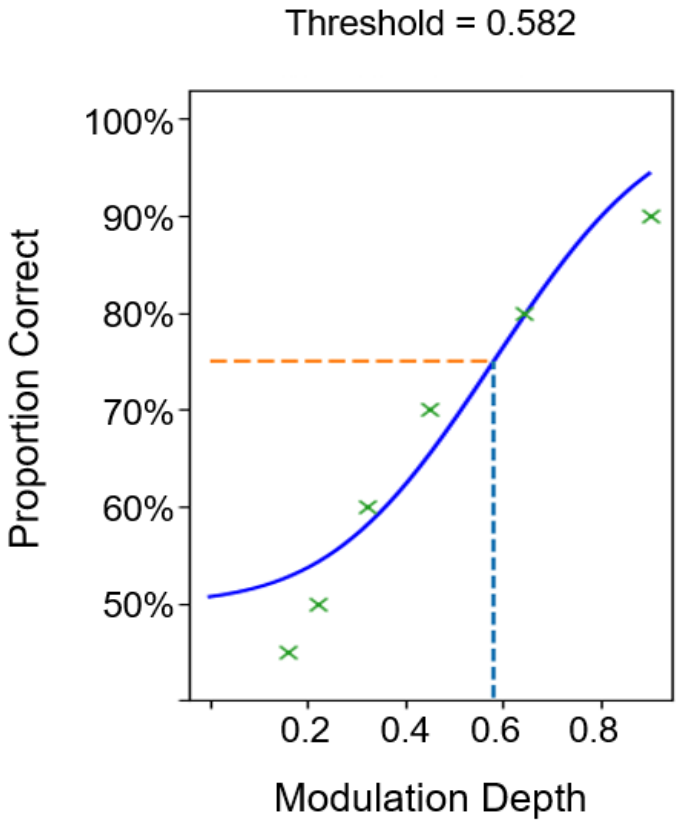

Figure 2-12. An example of a data set and psychometric function fit illustrates that, in some instances, the fit does not converge when λ is fixed at 0. The lack of convergence may occur when the initial estimate of λ is too far from the true value or when the function is not appropriate for the data.

To determine the magnitude of the error to which the calculated parameter estimates (α, β) were subject to a sampling distribution were obtained using a Parametric Bootstrap in Palamedes Toolbox (Prins & Kingdom, 2009). To estimate where most (68%) of the results would likely land for each scenario, the amount of variation in the estimates was measured. This calculation, known as the standard error of the threshold, was crucial in determining the 68% confidence intervals. The goodness-of-fit for the psychometric function model was subsequently assessed to determine if the curve closely aligns with the given dataset. This fit was considered 'close' if the observed values from the dataset largely correspond with the predicted values derived from the psychometric function. The disparities between the

observed and expected values were carefully examined to evaluate the fit accuracy of the model to the empirical data.

2.4.2 Thurstonian Scaling

Thurstonian scaling was employed in Chapter 5 to examine the perceived depth magnitude by paired comparisons. This methodology established a preference-based scale from paired comparisons between stimuli that don't inherently possess an empirical order. The decision to employ Thurstonian scaling for evaluating perceived depth magnitude was due to its ability to handle paired comparisons between stimuli that do not have an inherent empirical order. Unlike other scaling methods, Thurstonian scaling does not require a predetermined order or metric scale for the stimuli. Instead, it provides a means to establish a preference-based scale. The principles and assumptions for the most relevant cases were examined before applying this scaling technique. Thurstone's law of comparative judgment (LCJ) is a mathematical principle that embodies how individuals compare and evaluate different stimuli (Thurstone, 1929). The LCJ states that when individuals compare two stimuli, they do so by estimating the distinction between them on an underlying continuum. Therefore, comparisons are made between pairs regarding the magnitude of a given attribute on this continuum, which forms the basis of Thurstonian scaling methods (Thurstone, 1932, 1959). Thurstone assigned case numbers to specific models and their corresponding variations in the scaling procedure. Each scaling model assumes that judgments are transitive; if stimulus A is preferred to B, and B is preferred to C, then A is preferred to stimulus C. The sections below outline three specific cases (III, IV and V) whose assumptions are relevant to the current study.

Case III details a scenario where a single observation is made per condition, but the observer makes comparisons across all conditions, thus ranking each condition with one another. The model assumes that all the discriminal dispersions vary. Therefore, the model accounts for unequal variances in each condition. Case V is used in scenarios where multiple observations for each condition are made, allowing comparisons across conditions.

However, it operates under the assumption that the discriminal dispersions of all stimuli are the same and, therefore not accounted for in the model.

Lastly, case IV involves multiple independent observations per pairing condition without comparisons across pairing conditions. Each observation is independent and not influenced by the observer's responses to other conditions. This model outlines that the discriminal dispersions are not equal, but similar, and uncorrelated.

3 Perceptual and cognitive load on shape-from-shading of textured surfaces

This study aimed to investigate the impact of age on sensitivity to shape-from-shading, with examining the effect of first-order cues. The effects of a noise textures on performance and processing time were also examined. The chapter focused on the properties and applications of first-order vision, specifically how it facilitated depth perception through shape-from-shading and how it interacted with noise visibility and cognitive load. This was achieved through a modified visual N-back task where participants had to identify a concave stimulus among a group of convex stimuli. The depth cues were examined by monitoring performance for the depth cue alone, and with the addition of visual textures. The research shed light on the mechanisms that underlie our ability to perceive depth and offered valuable insights into the role of first-order vision in this process.[1]

3.1 Introduction

First-order vision is the visual process that detects luminance modulations (LM) and colour which facilitate detection of edges and contours (Ledgeway & Smith, 1994). These signals are therefore thought to play a key role in shape-from-shading, by conveying information regarding the distribution of light and dark areas on an object or surface (Kleffner & Ramachandran, 1992; Ramachandran, 1988).

[1] The experiments in this Chapter 4 were conducted online due to the global pandemic in 2020/2021 where in-person testing was not permitted by the University. The challenge in online settings is the inability to calibrate the luminance output of each participant's visual display accurately. This lack of calibration is important because AM stimuli are affected by luminance artifacts, which arise from non-linearities inherent in display monitors which could significantly alter the perception of AM stimuli, leading to unreliable data. To adapt to these constraints, the research plan was revised to focus on shape-from-shading in first-order visual components only, as these are less susceptible to variations in display calibration and therefore more suitable for online experiments.

As discussed in Chapter 1, LM modifies the local mean luminance within a specific region, which is thought to control the illumination and reflectance properties. Consequently, we would perceive regions with higher luminance values to have increased illumination and reflective qualities compared to areas with lower mean luminance (Schofield et al., 2006). This is corroborated by the statistical analysis of luminance properties in natural images, where a variation in the local luminance of a local region represents a change in depth or reflectance on the surface of an object (Kingdom, 2003; Schofield et al., 2017).

3.1.1 Light-from-above prior

When a stimulus possesses first-order visual cues for depth interpretation, the brain makes some assumptions about the light-source direction. This supports the idea that, when a light source is not immediately apparent in a stimulus, we implicitly assume the light is coming from above, a concept known as the light-from-above prior (Ramachandran, 1988). The light-from-above prior has been exemplified in various studies, including the one represented in Figure 3-1, which showcases identical stimuli, shaded with opposing LM polarities (Kleffner & Ramachandran, 1992). In the top panel of Figure 3-1a, the stimuli are perceived as convex, while in the lower panel, they appear concave. Under this assumption, the shading applied to an object can lead to opposing perceptions of depth, based on the light-source direction that the brain presumes, facilitating segregation.

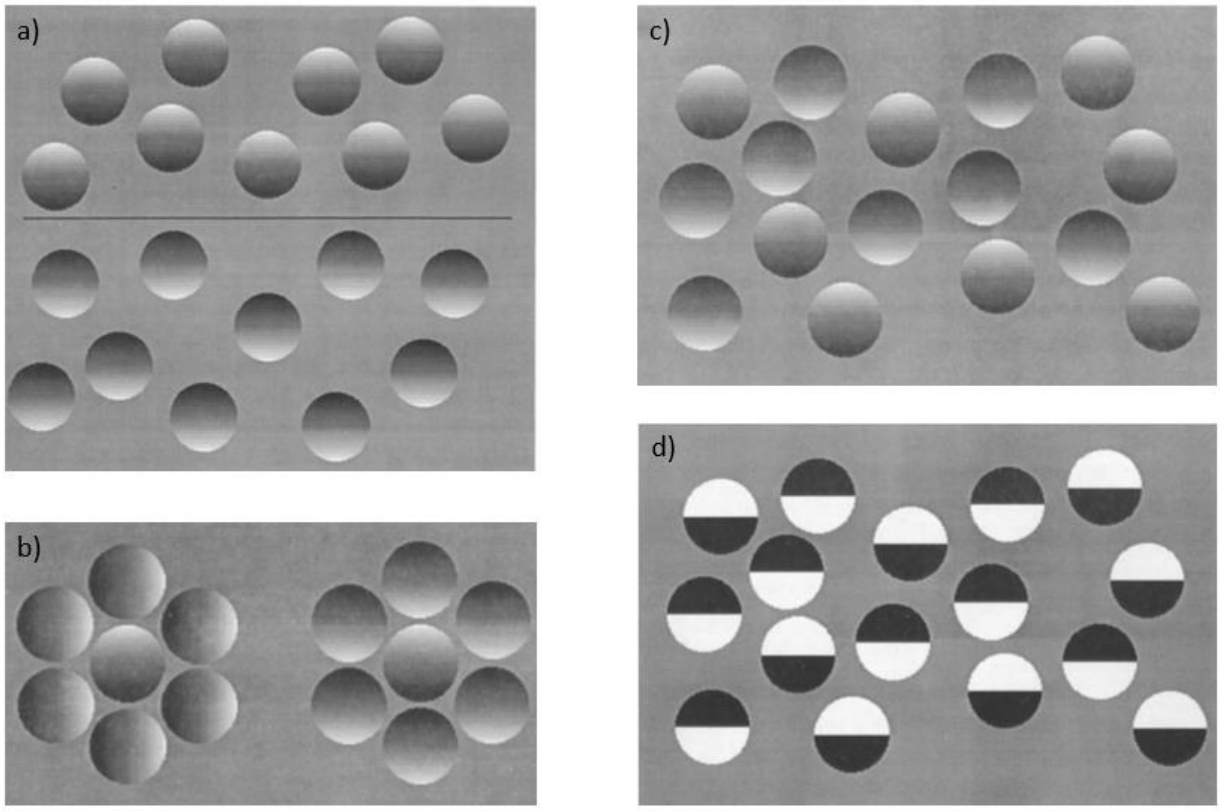

Figure 3-1. This figure demonstrates how shading alone can convey depth perception, utilising the light-from-above prior. a) displays stimuli that appear convex or concave in the top and bottom panel. b) illustrates the "centre-surround" interactions involved in perceiving shape-from-shading, where the centre stimulus in the left-hand group appears less convex than the same stimulus in the right-hand group. In c) stimuli with opposing luminance polarities is presented in a random array, while panel d) displays the same luminance polarities for the stimuli in c), but as a square wave, without depth cues. Note. Reprinted from "On the perception of shape-from-shading" by Kleffner, D. A., and Ramachandran, V. S., 1992, Perception & Psychophysics, 52(1), p.20-22.

To examine whether the facilitation of perceptual segregation of depth in the task was a consequence of depth cues, rather than LM polarity, the luminance cue was rotated by 90 degrees in Figure 3-1b. It is thought that ambiguity is introduced into the perception of depth, assuming the light-from-above prior, when conflicting polarities are presented. Figure 3-1b illustrates this phenomenon, where the left-hand group's surrounding stimuli have a rotated LM, which introduced depth ambiguity. In the right-hand group, less conflicting depth

cues facilitated perceptual segregation between convex and concave stimuli. As a result, the left-hand group exhibits diminished depth cues, leading to a decrease in segregation. This observation provides further support that depth cues, rather than LM polarity, facilitate perceptual segregation in the task. This finding is corroborated in cases where two opposing light sources illuminate identical objects, causing a human observer to accurately perceive the shape of only one of these objects, which suggests that shape perception is a global process (Kleffner & Ramachandran, 1992; Ramachandran, 1988).

The interaction between perceptual organisation and interpreting depth cues was further substantiated by examining the effectiveness of perceptual grouping in shape-from-shading stimuli. Whilst the stimuli in Figure 3-1c and Figure 3-1d have identical LM polarities, the control stimuli in Figure 3-1d do not convey depth information. The conclusions drawn from Figure 3-1d indicate that grouping stimuli based on luminance polarity is more perceptually challenging when compared to Figure 3-1c. This suggests that perceptual grouping is facilitated by shape-from-shading cues, rather than just the polarity of LM (Kleffner & Ramachandran, 1992). Studies using brain imaging techniques have provided support for this observation, showing that when individuals view displays that lead to weak and unstable depth perception, there is greater activation in area V1 when compared to stimuli that have stable depth cues (Humphrey et al., 1997).

3.1.2 Masking and pedestals in first-order channels

Previous studies suggest that first-order first-stage filtering is carried out by a single linear first-order channel (Westrick & Landy, 2013). Prior studies have demonstrated this whereby a modulation in luminance alone, enhances the illusion of depth more effectively than AM contrast (Schofield et al., 2006). This remains true when a noise texture is present, however this in turn could mask luminance signal and potentially obscure depth cues. This effect of masking typically occurs when the spatial frequency of the LM overlaps with spatial frequencies within in a noise texture. This then interferes with the perception of LM that is conveying the depth cue. It is thought that the overlap in spatial frequencies results in first-

order channels having difficulty in segregating and individually processing the two first-order cues. As a result, sensitivity of LM may be reduced due to the presence of the noise. This supports the notion that the processing of first-order visual information is carried out by first-order channels only.

Conversely, visual noise may also enhance depth cues in first-order modulated stimuli. In the context of luminance modulations, it was observed sensitivity of LM was facilitated in the presence of a LM background, serving as a pedestal (Schofield & Georgeson, 1999). In this study, a background LM and carrier were presented, while in the other interval, background and test modulations were superimposed. It was observed that when the background and test gratings had the same spatial frequency and phase, sensitivity of LM was enhanced. This pattern of results demonstrate that LM sensitivity initially improves at low contrast visual background textures, however, as contrast increases, sensitivity decreases. Further examination of the dipper function supports these findings, suggesting that the background texture (i.e. the mask) lowers the signal threshold thus facilitating perception, which then attenuates when the spatial frequency of the mask and signal differ by 0.5 octaves (Legge & Foley, 1980). Furthermore, a Gaussian noise texture added to a LM grating was also found to effectively mask only the spatial frequencies within the grating bandwidth (Pelli & Blakemore, 1990; Solomon, 2000). Therefore, it was proposed that masking of a LM grating is possible when a commonality in the spatial frequencies within the noise and the stimulus is present and at contrast levels above-threshold. Considering this, the question arises as to whether the use of a noise texture alongside a LM grating will impact younger and older adults in sensitivities in first-order shape-from-shading depth cues.

3.1.3 Age-related changes in shape perception

Tasks like shape perception that involve multiple processes, are likely to be influenced by numerous factors that change as we age. The ageing process is thought to

interact with these visual processes and alter functions such as visual acuity and contrast sensitivity. Age-related changes such as reduced visual acuity and increased lens opacity are thought to contribute to patterns of visual ageing in older adults (Glasser & Campbell, 1998; Owsley et al., 1983).

Studies investigating sensitivity to shape-from-shading cues found that older adults have reduced sensitivity compared to younger adults, suggesting a deterioration with age. Norman & Wiesemann (2007) propose that shape-from-shading perception was impacted by ageing, which resulted in decreased accuracy when discriminating local surface orientation of a shaded stimulus in older adults (mean age= 71.2, SD = 5.0) in comparison to younger adults (mean age = 24.0, SD = 2.9). As discussed in Chapter 1, research supports that sensitivity of first-order cues decreases with age due to increased lens opacity, resulting in reduced retinal illuminance (Owsley et al., 1983; Sutter et al., 1995). This reduction in illuminance may explain spatial vision deficits observed in older adults, particularly at higher spatial frequencies. In turn, this deficit could result in reduced perception of fine details within a stimulus, such as shading. Further research into contributing factors concluded an age-related deterioration in perceptual tasks, even when cognitive demand remained constant, implying that the age-related impairment is due to perceptual constraints rather than cognitive demand (Schneider & Pichora-Fuller, 2000). Constrastingly, it was observed that older adults had preserved shape perception when viewing static stimuli with shading. However, performance declines when moving objects were presented, implying that the reduced ability to perceive shape from motion in older adults is likely caused by a decline in detecting and discriminating motion (Norman et al., 2008).

3.1.4 Introduction to the study

Despite the substantial body of research on age-related cognitive and perceptual decline, the precise nature of their interaction is yet to be fully understood, and more notably how these factors influence shape-from-shading perception. Prior studies have primarily focused on perceptual and cognitive factors in isolation, whereas understanding how

cognitive and perceptual factors interact and influence the perception of shape-from-shading may provide a more comprehensive understanding of age-related changes in these areas.

The following study aimed to explore factors influencing depth perception of a stimulus by examining the visual and cognitive requirements of the task and how these factors change with age through a series of online experiments. The primary objective focused on examining how additive noise impacts on sensitivity of first-order shape-from-shading cues. Additionally, noise contrast was manipulated to further investigate the perceptual challenges associated with perceiving a shape-from-shading stimulus. The study hypothesised that increased visibility of a noise texture would lead to more significant impairment in shape-from-shading perception at high spatial frequencies when compared to older adults. It was also predicted that when cognitive demands were elevated, older adults would experience a more significant decline in performance. Therefore, a secondary objective was to explore the interaction between perceptual quality and task difficulty in both younger and older adults.

3.2 Methods

In the following section, the methods utilised for conducting the series of online experiments will be outlined.

3.2.1 Equipment

The experiments outlined in this study were designed for online participation in a participant's personal environment. This introduced the limitation of varying display monitor properties, including resolution, size and luminance, as well as inconsistent viewing distances. To address the issue of monitor resolution, a spatial calibration method was employed. An accessible technique that allowed participants to calibrate their monitors independently involved adjusting the size of a rectangular stimulus displayed on the screen to match the dimensions of a standard-sized bank card. Participants used keyboard inputs to alter the width and height of the rectangle. Once satisfied with the size, a verification step

required participants to confirm the stimulus matched the height and width of their bank card and restart the spatial calibration if necessary. This approach ensured the consistency of size and shape for test stimuli throughout the trials. Additionally, participants were asked to position themselves to be an arm's length so that stimuli could be spatially calibrated (approximately 63cm). Although a gamma-corrected monitor could not be implemented a generic correction, close to the sRGB specification for gamma commonly used in many monitors was applied. ($\gamma = 2.2$).

3.2.2 Procedure

The study employed a visual search task, in which four stimuli were presented during a trial: three distractors and one target. Participants were instructed to respond to the location of the target stimulus. The target was described as being concave, whereas distractors were described as convex in the participant instructions. Participants were required respond to the location with a keyboard press, in a 4-alternative forced choice task (4afc). The stimulius location was randomised within their quadrant with an unlimited duration (see Figure 3-2). A trial concluded once a response was recorded, and a subsequent trial was presented after an inter-trial-interval (ITI) of 500ms. The target location was randomly assigned for each trial where each quadrant displayed the target for approximately ¼ of the total test trials.

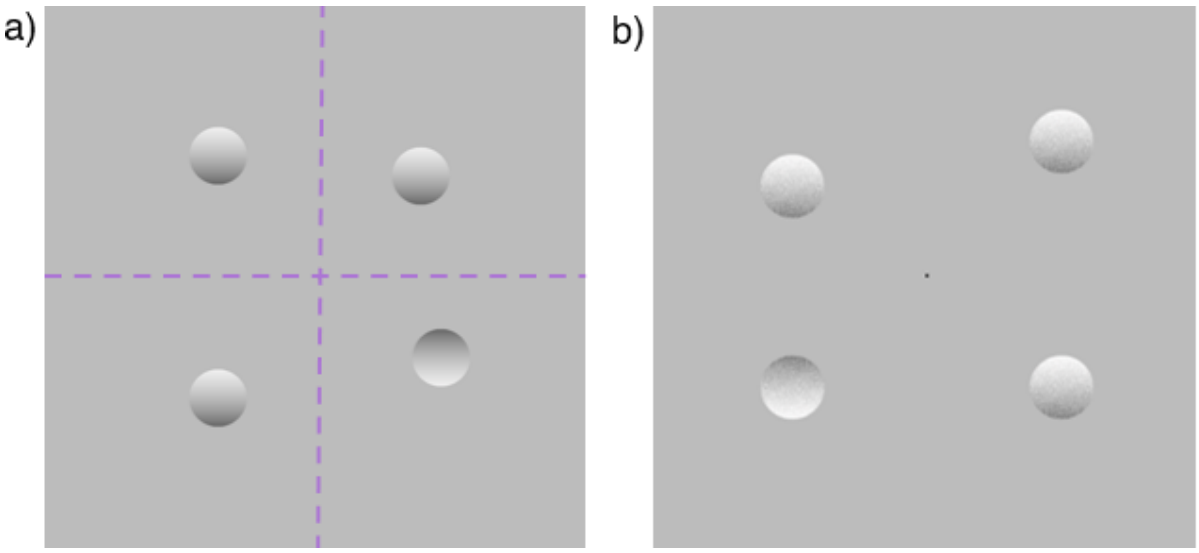

Figure 3-2. An example trial in a visual search task, presenting three convex stimuli and one concave stimulus, each in a separate quadrant of the screen. The placement of the stimuli within each quadrant is indicated by the dashed purple line a). b) depicts a trial where stimuli were presented with additional binary noise texture, and both figures have been rescaled for illustrative purposes.

3.2.3 Stimuli

The study presented stimuli composed of a vertical linear ramp luminance gradient, which spanned the full available luminance range of the display, that ranged from 0 to 100% with a frequency of one cycle per stimulus. These stimuli were presented through a circular window and polarity was oriented at either 0 degrees (convex) or 180 degrees (concave), depending on whether they were a target or distractor. The stimuli were presented at a size of 30mm x 30mm and viewed from an approximate distance of 63cm, which was equivalent to 2.73 x 2.73 degrees of visual angle (v/deg), therefore a luminance modulation of 0.37 cycles per degree (cpd) was presented in the study.

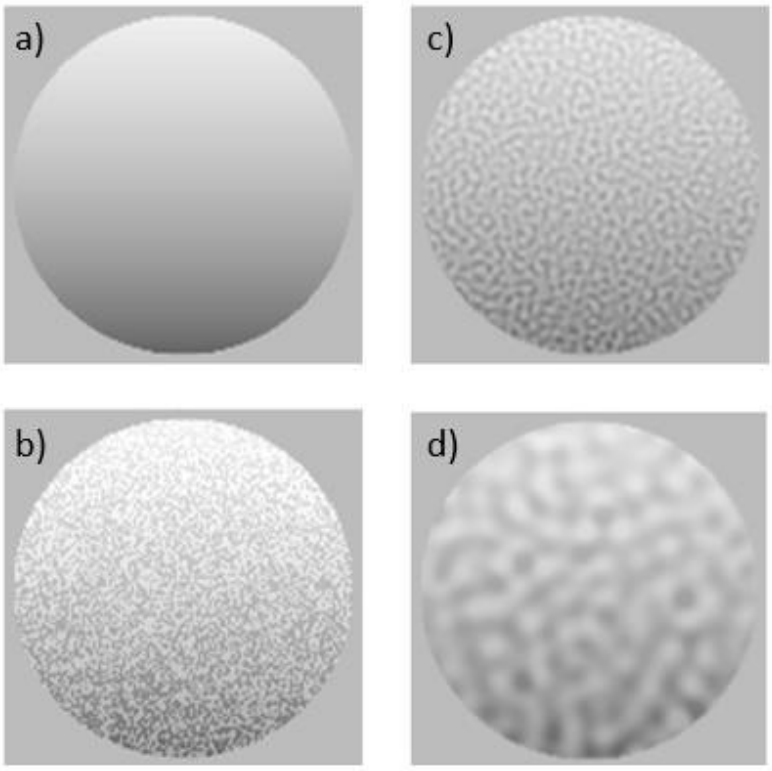

Figure 3-3. Examples of the stimuli used in the study, including a) a luminance gradient (1 cycle per stimulus), whereas b) binary noise, c) fine-scale isotropic noise, and d) coarse-scale isotropic noise were added to a luminance gradient (1 cycle per stimulus).

Figure 3-3 highlights the stimuli displayed in the experimental trials in order to investigate the impact of sensory load. The perceptual qualities of the stimuli were altered by the addition of a noise texture. A binary texture with approximately 2x2 pixel components, an isotropic texture with a central spatial frequency of 12 cpd, and 4 cpd (one-octave bandwidth) were added to the luminance gradient and presented at the specified viewing distance. Both the luminance gradient and additive noise were carefully balanced to have equal perceptual power during presentation. Additional information regarding the composition and presentation of these stimuli can be found under their corresponding experiment headings.

3.2.4 Participants

In order to investigate the effects of age on sensory and cognitive factors, two age groups were recruited via Prolific for each online study. Younger adults were defined as

individuals aged 18 to 24, whereas older adults were recruited from individuals aged 60 or above. For each experiment, a new set of participants were recruited, resulting in the group mean age was different for each experiment.

3.2.5 Experimental parameters

Specific details regarding the parameters used for each online study will be provided under their respective subheadings to highlight the distinctive parameters of each experiment.

3.2.5.1 Experiment I. Exploring masking effects in shape-from-shading of a textured stimulus

To explore the effects of masking, participants completed two experimental conditions. The first condition utilised stimuli with a luminance modulation, as detailed in the stimuli section above. In a second condition a (~2x2 pixel) binary texture was added to the luminance gradient at an opacity of 50%. The contrast of the noise texture was set to 0.561 root-mean-square (rms). The study comprised 66 test trials for each condition (132 total), participants were randomly allocated to a counterbalanced group. A total of 40 participants were recruited online (20 older and 20 younger adults).

3.2.5.2 Experiment II. Broadband and narrowband visual textures on shape-from-shading

To investigate the impact of narrow- and broadband noise textures on shape-from-shading, a binary and isotropic visual texture were employed. An isotropic noise texture with a central spatial frequency of 12 cpd with a one-octave bandwidth (full width half height) was added to the luminance gradient, with opacity set to 50%. The parameters of the binary noise texture were replicated from experiment I, however, because of the different luminance properties of the two noise types, the overall contrast of both noise textures was adjusted to 0.52 rms. The two conditions were counterbalanced and a total of 40 participants (20 older, 20 younger) were recruited for the study.

3.2.5.3 Experiment III. Investigating the relationship between sensory and cognitive load in shape-from-shading

The relationship between sensory and cognitive load was explored by using a 4 and 12 cpd isotropic noise textures that were added to a luminance gradient (one-octave bandwidth). Additionally, the noise texture was presented under both high and low contrast conditions for the visual texture. The overall contrast of the noise for each age group was established through a pilot data to ensure visibility of textures across age groups was matched (see Figure 3-4)

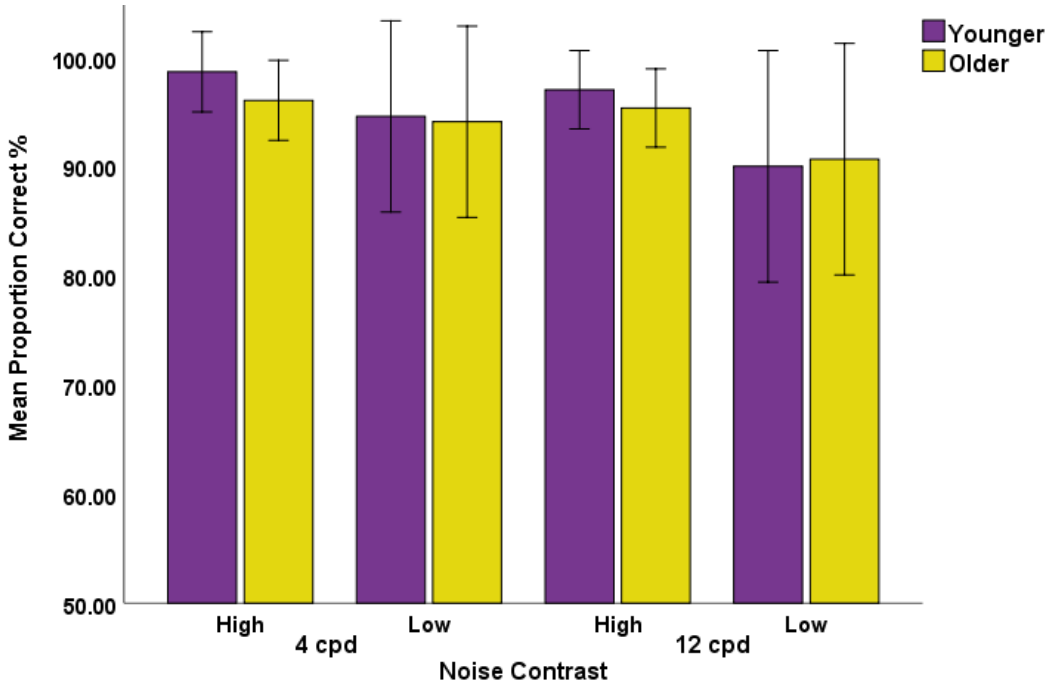

Figure 3-4. The average proportion correct for younger and older adults in a pilot study, aimed at determining matched noise texture visibility for each age group. Note. The data shown consists of 6 participants (3 older, 3 younger). Error bars represent standard error of the mean. Note. Refer to Table 3-1 for corresponding rms contrast values for each participant group under 'high' and 'low' conditions.

In the pilot study, 6 participants (3 older, 3 younger) completed a series of noise contrast detection tasks in a 4-alternatice forced choice task (4afc) task at various noise contrast levels. In this task, participants were asked to identify a specific texture. While all

four stimuli involved luminance modulations, the target was specific texture with the additive luminance modulation. For both spatial frequencies, doubling the overall noise contrast led to a stimulus that was perceptually easier to detect, with similar proportions correct for both younger and older adults. A t-test was conducted to ensure that performance between younger and older adults was not significantly different for each their corresponding conditions ($p > 0.05$). Reducing the overall contrast by half, was more challenging to detect but remained consistently visible to all participants. The contrast levels were therefore determined in for each spatial frequency condition for each age group, as presented in Table 3-1. The contrast levels for the participant groups were adjusted based on their respective percentages of correct responses in the pilot task.

Table 3-1.

Contrast levels (rms) used for each noise texture and age group.

	Younger		Older	
	High	**Low**	**High**	**Low**
4cpd	0.25	0.1	0.375	0.15
12 cpd	0.3	0.12	0.5	0.25

40 participants (20 older, 20 younger) were recruited for the experiment which involved three tasks with the first task being the visual search task, as described in the two previous experiments. The second and third tasks were modified visual N-back tasks. In the second task, participants were asked to respond to the location of the target (concave stimulus), however, rather identifying its position during each trial, participants were asked to identify whether the target was in the same or different location as the previous trial in a 2-alternative-forced-choice (2afc) task. Similarly, the third task was a visual 2-back task where

participants were required to respond based on whether the target stimulus was located in the same or a different position compared to its placement two trials prior. In the 0-back trial, stimuli had an unlimited presentation period whereas stimuli were presented for a 1000ms in the 1-back and 2-back trials an ITI of 500ms.The three tasks were conducted for the four spatial frequency/contrast combinations under counterbalanced conditions using a Latin squared design to account for practice effects.

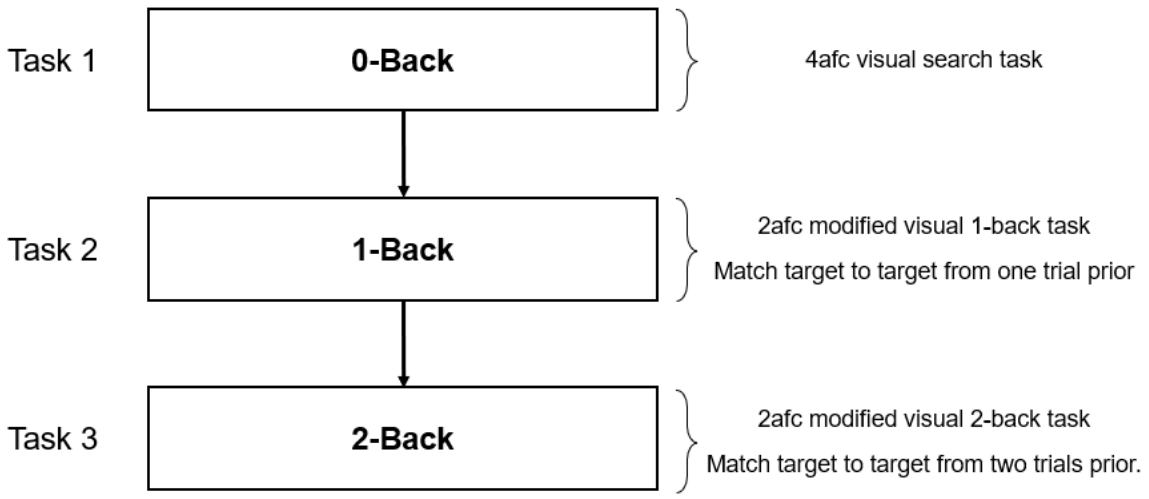

Figure 3-5. The sequence of tasks for each condition, commencing with a 4-alternative forced choice (4afc) visual search task, followed by 1-back and 2-back tasks. The 1- and 2-back tasks used a 2-alternative forced choice (2afc) design, which involved matching a target stimulus to the corresponding one from the n'th trial prior. This sequence of tasks is reiterated for each stimulus condition.

3.3 Results

3.3.1 Masking effects

To explore the effects of masking, accuracy and reaction times were examined for the gradient-only and gradient and binary noise stimuli. As illustrated in Figure 3-6, the mean accuracy (± standard error) for older adults in the gradient-only condition was 99.85% (± 0.08) which remains constant in the binary noise condition, 99.65% (± 0.16). In contrast, the

younger adults exhibited lower overall performance, with a mean accuracy of 98.65% (± 0.35) in the gradient-only condition and 97.80% (± 0.52) in the binary noise condition.

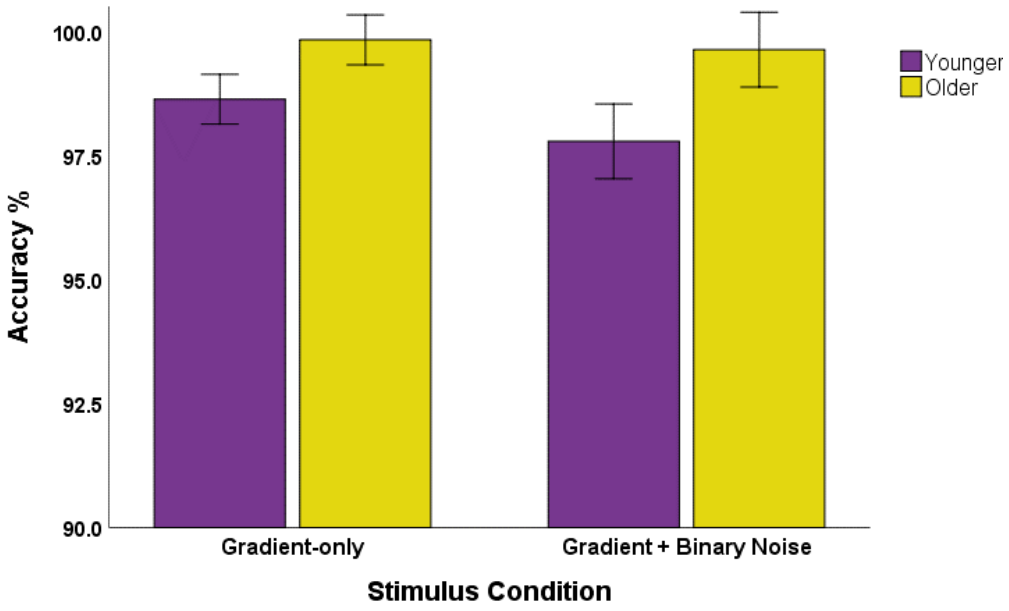

Figure 3-6. The average accuracy for each age group, where younger adults are represented by the purple bar and older adults by the yellow bar. Error bars represent 95% confidence intervals. Note. This figure represents the raw data for all observers before the analysis was conducted.

Significant outliers were identified by examining boxplots and defined as values occurring beyond three times the box length. In the dataset, two outliers were identified in accuracy scores in the younger adult dataset were removed from the analysis (N = 38). A ceiling effect was evident from the strong negative skew of the dataset. Therefore, a transformation was deemed appropriate in order to interpret the distribution of the means accurately (Fox, 2016). Due to the extreme skewness of the dataset an inverse log transformation was applied to the dataset (see Equation 3-1). Where the constant C represents the highest score in the entire dataset, and x denotes the score of an individual participant.

$$\log 10(C + 1 - x)$$

Equation 3-1

After the transformation was applied, it was determined that accuracy was lower in conditions where binary noise was present (98.73% ± 0.26), when compared to luminance-only gratings (99.25% ± 0.18), $F(1, 36) = 4.32$, $p < .05$, partial $\eta^2 = 0.11$. Additionally, a significant main effect of age group on accuracy was reported, $F(1, 36) = 14.98$, $p < .001$, partial $\eta^2 = 0.294$. However, there was no significant two-way interaction between noise condition and age group on accuracy scores, $F(1, 36) = .60$, $p = .44$, partial $\eta^2 = .02$.

Inspection of reaction times as depicted in Figure 3-7, shows a reverse pattern of results. Older adults had notably slower reaction times (± standard error) in both the gradient-only condition at 1531.16ms (±126.18) and binary noise condition at 1513.37ms (±114.42). Younger adults displayed consistently faster reaction times in both conditions at 666.82ms (±278.4) in the gradient-only condition and 957.12ms (±765.81) in the binary noise condition.

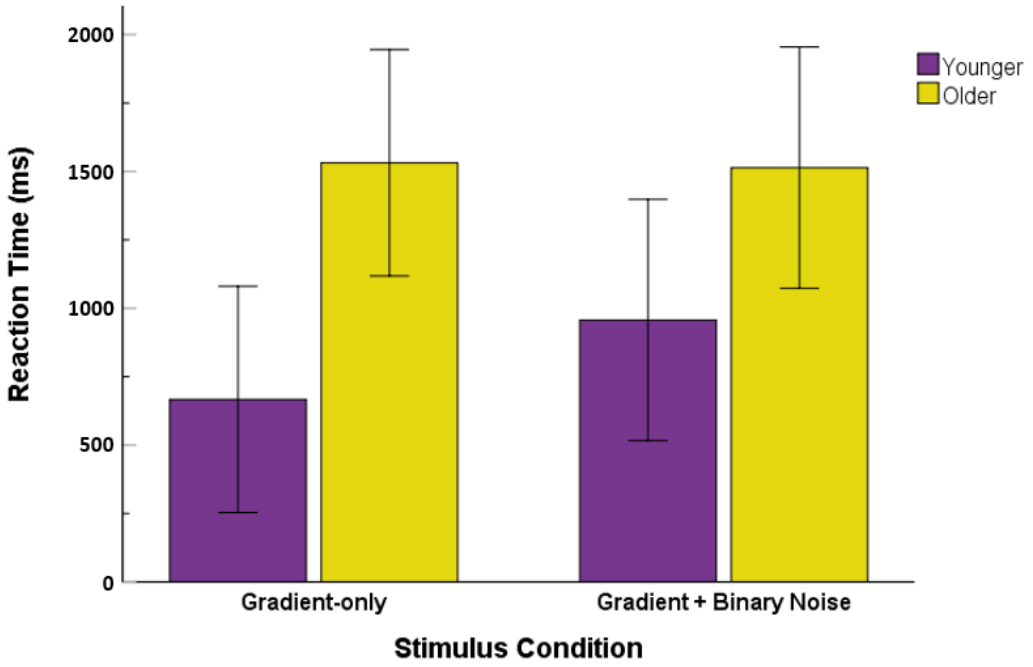

Figure 3-7. Mean response times for each age group in experiment I. Error bars represent 95% confidence intervals of the mean for each group. Note. This figure represents the raw data for all observers before the analysis was conducted.

The dataset for reaction times contained three outliers, these participants were subsequently excluded from the analysis (1 younger, 2 older). The distribution of reaction times revealed a strong positive skew which led to the decision of transforming the data, for more accurate insights. Therefore, the dataset was transformed before further analysis, $log10(x)$. A significant main effect was reported, where the use of a binary noise addition to a luminance grating increased reaction times overall, $F(1, 35) = 16.46$, $p < .001$, partial $\eta^2 = .32$. Also, younger adults had faster response times in both conditions compared to older adults, $F(1, 35) = 16.55$, $p < .001$, partial $\eta^2 = .32$. However, there was no significant two-way interaction between the noise condition and age group for reaction times, $F(1, 35) = 3.74$, $p = .06$, *partial* $\eta^2 = .097$.

3.3.2 Broadband and narrowband visual textures

To investigate how the use of broadband and narrowband visual texture influences shape-from shading, accuracy and reaction times were analysed for binary noise and 12 cpd isotropic noise stimuli added to a luminance gradient. As illustrated by the mean accuracy in Figure 3-8, the older adults exhibited slightly elevated performance (mean ± standard error of 98.78% ± 0.77) in the binary group condition, when compared to the younger adults (97.55% ± 0.49). However, in the isotropic noise condition, differences in performance were minimal, older adults had a mean accuracy of 94.28% (± 2.05) whereas younger adults' mean accuracy was 94.25% (± 2.40)

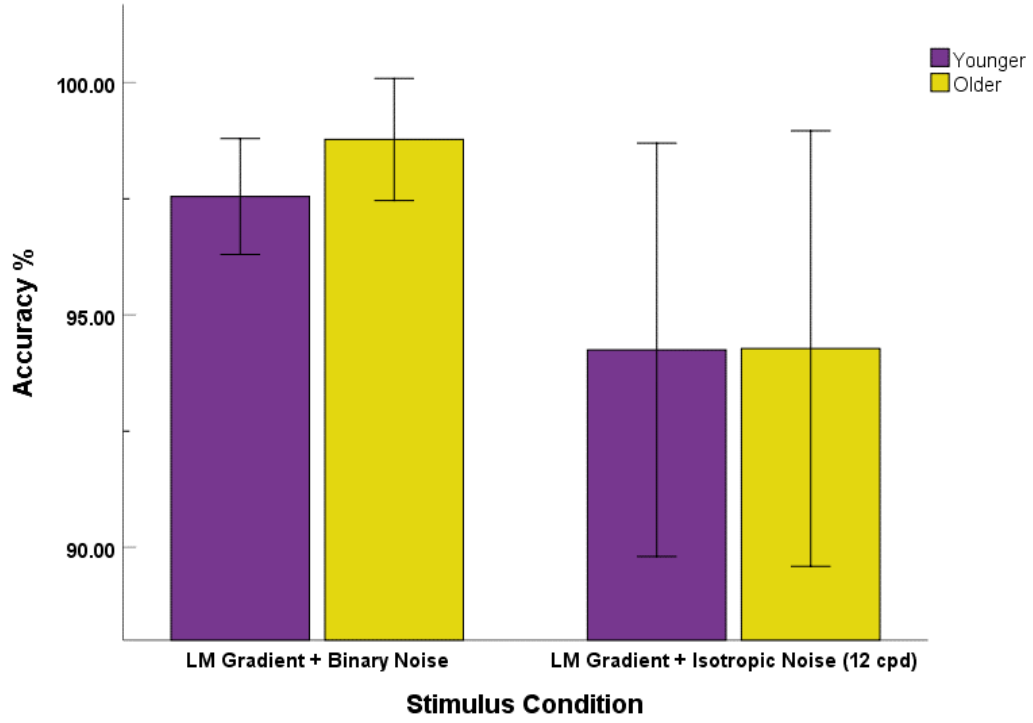

Figure 3-8. Comparison of performance in younger and older adults' accuracy, for binary noise and isotropic noise textures. Error bars represent 95% confidence intervals. Note. This figure represents the raw data for all observers before the analysis was conducted.

Three participants from the dataset (2 older, 1 younger) whose accuracy was identified as an outlier were removed from the analysis (N = 37). An extreme negative skew was observed due to a ceiling effect. Therefore, to normalise the distribution of scores, a transformation was applied (see Equation 3-1). The analysis revealed that participants

demonstrated greater accuracy in conditions where a binary noise texture was added to the luminance gradient, $F(1, 35) = 9.03$, $p < 0.005$, *partial* $\eta^2 = 0.21$. Furthermore, a significant main effect of age on accuracy was reported, $F(1, 35) = 7.03$, $p < .05$, *partial* $\eta^2 = 0.17$. However, a non-significant interaction between noise condition and age group was reported, $F(1, 35) = 1.09$, $p = 0.1$, *partial* $\eta 2 = 0.03$.

Upon examination of reaction times between the two age groups, as depicted in Figure 3-9, it was observed that younger adults responded faster in both the binary condition, with a mean reaction time (± standard error) of 884.76ms (± 63.96) and in the isotropic condition, 1054.90ms (± 54.59). In contrast, older adults had average response times of 1284.38ms (±106.31) in the binary condition, which increased to 1729.65ms (±194.21) in the isotropic noise condition.

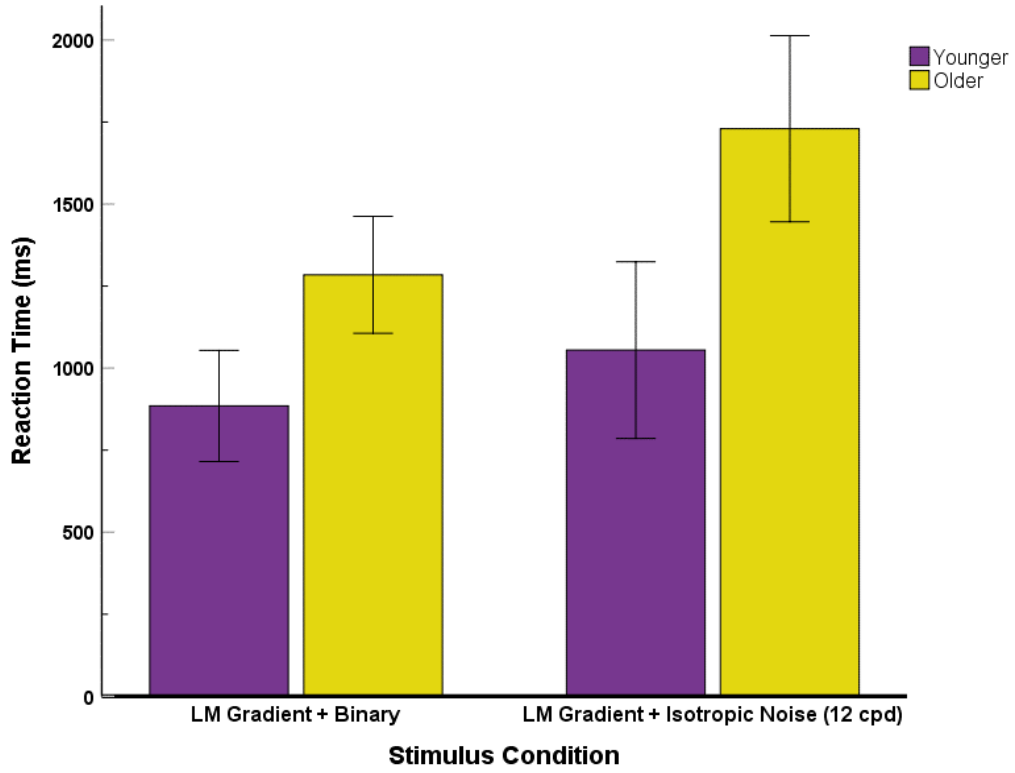

Figure 3-9. Mean reaction times of younger and older adults when comparing difference in binary noise and 12 cpd isotropic noise stimulus conditions. Error bars represent 95% confidence intervals. Note. This figure represents the raw data for all observers before the analysis was conducted.

Prior to analysis, two older adults' data were removed from the study due to outlier reaction times (N = 38). In contrast to the previous experiment, the data were normally distributed, as determined by a Shapiro-Wilk's test ($p > 0.05$), indicating that a transformation was not necessary before further analysis.

A significant interaction between noise stimulus and age group for reaction times was identified, $F(1, 36) = 4.58$, $p < 0.05$, partial $\eta^2 = 0.11$. It was found that older adults had slower reaction times (1607.02ms ± 107.11) compared to younger adults (969.83ms ± 101.62) in both conditions, $F(1, 36) = 13.24$, $p < 0.001$, partial $\eta^2 = 0.27$. Also, binary noise conditions elicited faster responses (1084ms ± 60.62) than the isotropic noise condition

(1392.28ms ± 96.38) for both age groups, $F(1, 36) = 4.58$, $p < 0.05$, partial $\eta^2 = 0.11$. However, the post-hoc tests revealed significant differences in reaction times were present in the older adult group between the two conditions ($p < 0.001$), whereas younger adults reaction times did not significantly differ between conditions.

3.3.3 Sensory and cognitive load manipulations on shape-from-shading

To explore the interaction between sensory and cognitive load on shape-from-shading, accuracy and reaction times were examined in this online study. Firstly, when examining the accuracy for each age group, a pattern emerged where a reduction in accuracy was a result of an increase in N-back task condition, as summarised in Figure 3-10. For younger adults, a mean accuracy (± standard error) of 97.57% (± 0.62) in the 0-back task, which decreased to 89.72% (± 2.32) for the 1-back task and further dropped to 78.05% (± 3.02) in the 2-back task. Similarly, older adults followed a similar trend with a mean accuracy of 97.59% (± 0.62) in 0-back trials, which dropped to 87.89% (± 2.32) in the 1-back task, and further decline to 74.08% (± 3.02).

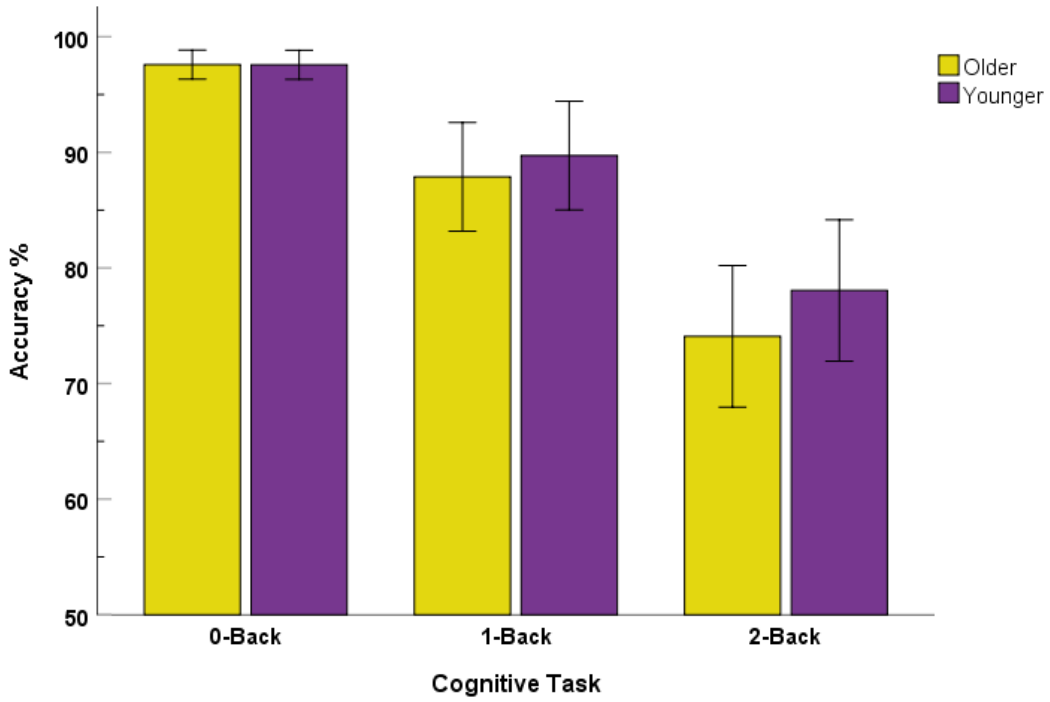

Figure 3-10. A bar chart illustrating the average accuracy scores for both younger and older adult groups in each cognitive task condition, error bars denote 95% confidence intervals. Note. This figure represents the raw data for all observers before the analysis was conducted.

The distribution of data within each subset was a cause for consideration due to ranging from moderate to extreme skewness (-0.51 to -3.72). Consequently, a log transformation was implemented on all subsets to address the distribution and unequal skewness, $\log 10(C + 1 - x)$. Although some datasets still reported a significant negative skew after transformation, it was concluded that the subsequent analyses would be adequately robust to highlight interactions, and additional transformations might potentially mask these (Field, 2013). Therefore, significant interactions reported were followed up with non-parametric post-hoc tests to address this. One outlier was identified from the subsets, consequently the participant's data was removed before analysis (1 older adult).

A three-way ANOVA, which included task (three levels: 0, 1, 2 back), spatial frequency (two levels: 4, 12) and contrast (high, low) as factors, yielded no significant three-way interaction ($p > 0.05$). However, an interaction between age group and cognitive task

was reported, $F(2,74) = 3.203$, $p < 0.05$, partial $\eta^2 = 0.08$, where younger and older performance significantly declined as task load increased. This suggest that as the task's cognitive complexity increases, older adults tend to experience a more rapid decline in performance. When consulting this interaction in Figure 3-11 it is apparent that in the 0-back task performance is marginally elevated in the older adult groups, however as cognitive load increases in the two subsequent conditions we see in inverse of this relationship, where younger adults outperform older individuals. Upon comparison with Figure 3-10, Figure 3-11 reveals a slight difference in accuracy scores for the 0-back task. This variance can be attributed to the exclusion of an outlier in the older adult group and the application of a log transformation to the dataset.

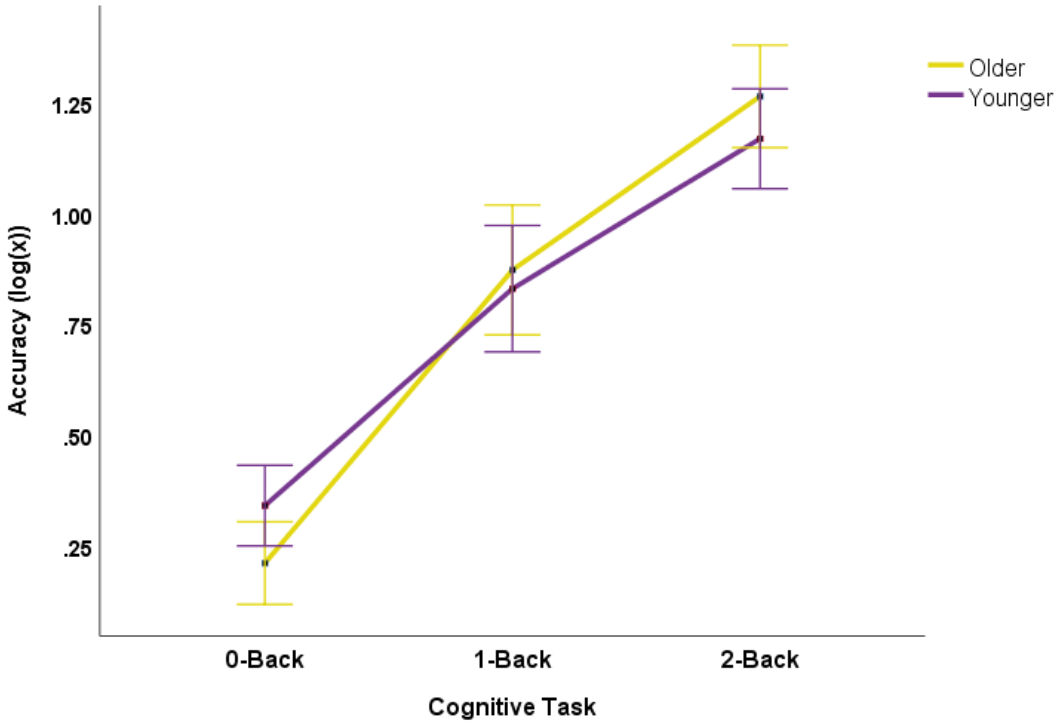

Figure 3-11. Illustration of the interaction between age and cognitive load. Accuracy scores are an inverse of log(x) transformation, thus higher scores correlate to poorer performance. Error bars indicate 95% confidence intervals.

This two-way interaction was further substantiated by non-parametric pairwise comparisons of raw accuracy scores. These comparisons revealed a significant decrease in younger adults' scores from the 0-back to the 2-back task ($p < 0.05$) and from the 1-back to the 2-back task ($p < 0.001$). In contrast, older adults exhibit a significant difference between the 1-back and 2-back tasks ($p < 0.001$), but not between the 0-back and 1-back task.

Additionally, a significant main effect of cognitive task on accuracy was observed, $F(2,74) = 15.10$, $p < 0.001$, partial $\eta^2 = 0.29$. A non-parametric Friedman test on raw scores confirmed this finding, $\chi^2(2) = 70.49$, $p < .0001$. Pairwise comparisons of the median with a Bonferroni correction further revealed that accuracy in the 0-back task declined from 98.53% to 91.81% in the 1-back task ($p < 0.001$), which then declined further in the 2-back task 79.04% ($p < 0.001$). The overall pattern of results indicates a clear relationship between the

task interaction and age effect. This highlights the influence of age and its interaction with cognitive load on perceptual performance.

A consistent pattern emerged when examining reaction times. Both younger and older adults showed a gradual increase in reaction times in the N-back task condition as depicted in Figure 3-12. In younger adults this increase is marginal, with mean response times (± standard error) going from 660.58 ms (± 47.45) in the 0-back task to 789.60 ms (± 63.14) in the 1-back task, and finally an increase to 852.94 ms (± 79.58) in the 2-back condition. In contrast, older adults exhibited slower responses and also more pronounced increases between conditions, with reaction times of 873.90 ms (± 47.46) in the 0-back, 1035.75 ms (± 64.14) in the 1-back, and 1186.67 ms (± 79.58) in the 2-back condition.

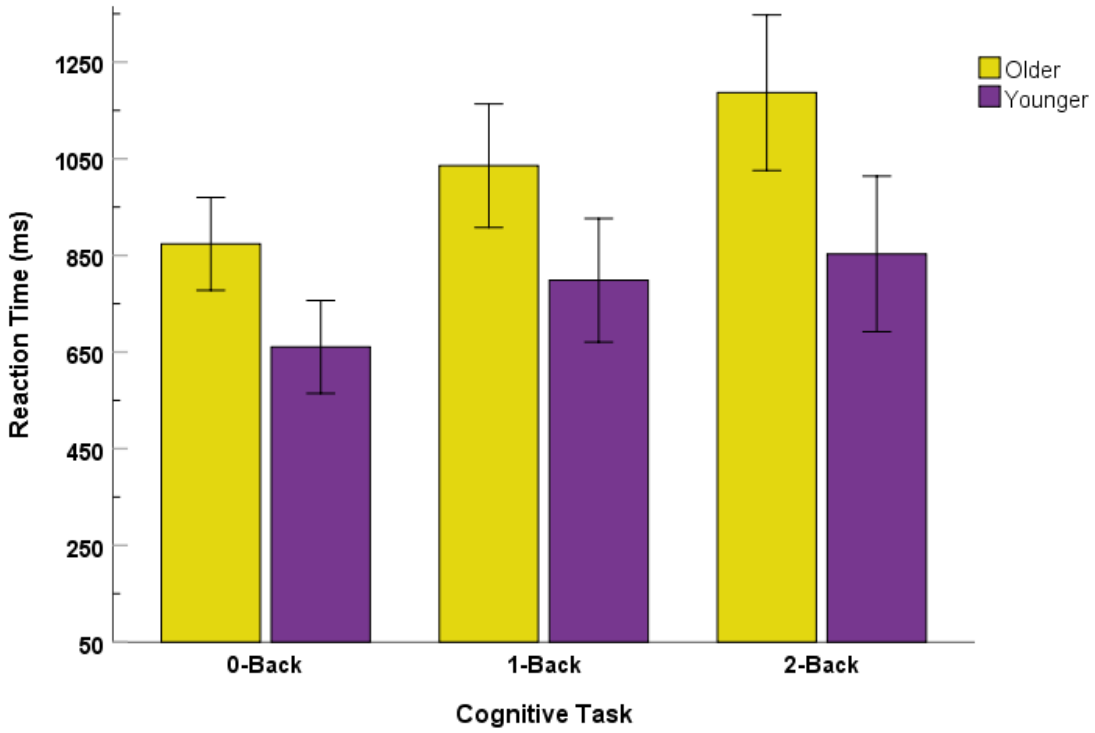

Figure 3-12. Mean reaction times for each age group across the three cognitive tasks, error bars indicate 95% confidence intervals. Purple bars represent younger adult data, whereas yellow bars denote older adults.

Before examining differences in reaction times, three outliers were excluded (2 older, 1 younger). A log10(x) transformation was applied to the reaction time data to address the

varied positive skewness within each subset. Therefore, significant interactions were supplemented with non-parametric post-hoc tests. Older adults were found to have significantly slower reaction times across all conditions compared to younger adults, $F(1,35) = 10.41$, $p < 0.05$, partial $\eta^2 = 0.139$. Furthermore, it was discovered that cognitive task significantly influenced reaction times, with an increasing trend as described above, $F(2,70) = 17.07$, $p < 0.001$, partial $\eta^2 = 0.196$. This trend was supported by a non-parametric comparison of the raw (median) reaction times, $\chi^2(2) = 28.95$, $p < .0001$, with an increase in reaction times from 719.41ms in the 0-back task, to 921.58ms in 1-back task ($p < 0.005$), and a subsequent rise to 1033.64ms ($p < 0.05$) in the 2-back task. However, a non-significant interaction was reported between age group, task type, noise spatial frequency and noise contrast ($p > 0.05$).

This indicates that cognitive load might have a more pronounced impact on first-order shape-from-shading perception with first-order modulations, compared to visual sensitivity. Consequently, it seems that cognitive load and age may interact.

3.4 Discussion

The present study aimed to investigate factors influencing shape-from-shading by examining both the visual characteristics of the stimulus and the cognitive demands of the task. The impact of these factors on performance in different age groups was assessed through a series of online experiments designed to provide insight into the contributions of shape-from-shading perception in terms of perceptual quality and cognitive demand and how these differ with age. Furthermore, the study aimed to provide further clarification on theories of perceptual and cognitive ageing, as discussed in the introduction, in order to better understand their contribution and potential interaction to the decline in visual perception that accompanies healthy ageing.

3.4.1 Masking of LM shape-from-shading cues with broadband noise.

The first objective centred on exploring the masking of first-order luminance gradients and their subsequent influence on shape-from-shading signals. This was achieved by comparing performance in luminance-only gradients, with a selection of visual textures with different spatial frequency properties. The first experiment compared performance on luminance-only gratings and a luminance grating with an additive binary noise texture. The findings revealed that the addition of the visual texture led to reduced accuracy and slower reaction times. The results suggest that poorer performance and response times were due to an inhibitory effect addition of a binary noise texture. This supports the concept of masking, where common spatial frequencies between the signal and mask impair differentiating and processing the two luminance cues in first-order channels. As a consequence, sensitivity of a luminance gradient would be reduced with the addition of noise (Foley & Legge, 1981; Pelli & Blakemore, 1990; Solomon, 2000). In this experiment, binary noise was utilised due it possessing equal energy across spatial frequencies. This was to ensure that both age groups were presented with noise of the same perceptual quality accounting for age-related losses in high frequency sensitivity, thus allowing for any masking and/or pedestal effects to be evident in both groups. As previously discussed, noise textures have also been shown to enhance depth cues in first-order modulated stimuli in certain cases (Foley & Legge, 1981; Kontsevich & Tyler, 1999). This pedestal effect is believed to occur when the luminance signal falls below the just noticeable difference (JND) threshold. On the other hand, masking is thought to take place when contrast levels surpass the JND threshold. In this context, the observed masking effect is likely present because the luminance signal exceeds the JND threshold. This masking of a luminance gradient lends further support to visual processing models that propose separate channels in the visual system for first- and second-order information (Schofield, 2000; Schofield & Georgeson, 1999).

3.4.2 Age-related changes in sensitivity of first-order information

Inconsistencies within the study emerge from the observed pattern of results, where older adults had significantly better performance in both conditions but took longer to respond during the trials. It is possible that older adults exercised greater caution before providing a response, resulting in fewer errors and lapses when compared to the younger adult group. This explanation aligns with observed slower reaction times among older adults. Moreover, a ceiling effect was observed for both younger and older adults, suggesting that variations in accuracy were likely attributable to lapses and errors in responses rather than perceptual challenge. It is possible that the observed pattern of results can be attributed to the common-cause hypothesis. This theory suggests that a central function, such as processing speed, contributes to cognitive and perceptual decline in older adults (Lindenberger et al., 2001; Salthouse, 1996). Evidence for this hypothesis comes from research investigating the decline in processing speed among older adults. It was found that extending stimulus presentation time, enhanced older adult performance to levels similar to younger adults (Bennett et al., 2007; Raghuram et al., 2005). The sensory deprivation hypothesis suggests that deterioration of perception may contribute to the gradual degradation of neural stimulation and plasticity, thus depleting cognitive ability (Lindenberger & Baltes, 1994). Researchers have explored the link between sensory decline and cognitive ability by manipulating sensory load. Studies in auditory perception have shown that older adults' cognition is negatively affected by a reduction in signal-to-noise ratio (Pichora‐Fuller et al., 1995). However, older adults are more effective at using contextual cues than younger adults in high noise conditions and when the signal-to-noise ratio is increased, their performance is similar to that of younger adults. Similar results have also been observed by manipulating visual noise, where older adults performed similarly to younger adults when noise was reduced and were reported to use contextual cues more than younger adults (Speranza et al., 2000).

While there is a well acknowledged association between visual deficits and ageing, the ability to perform such tasks may not be solely dependent on the visibility of stimuli (Lindenberger et al., 2001). Tasks involving the identification of convex and concave stimuli require a level of perceptual organisation to group or segregate stimuli based on their properties (Kleffner & Ramachandran, 1992). When examining shape recognition, research has shown that ageing negatively impacts the performance of older adults, indicating a potential decline in visual memory (Norman et al., 2015). Furthermore, stimulus durations for older adults may influence shape perception in contour discrimination tasks, even when controlling for factors such as retinal illuminance (Roudaia et al., 2011). Similarly, an observer's cognitive ability is likely to influence performance of complex tasks. Research has established a relationship between perception and cognition in ageing, with visual and auditory acuity being identified as potential indicators of executive functioning in later life (Lindenberger & Baltes, 1994). This implies that cognition may play a significant role in older adults' perception, particularly of complex stimuli.

3.4.3 Differences in perception of shape in narrowband and broadband noise.

In the exploration of the effects of broadband noise and narrowband noise with high spatial frequencies, it was reported that performance declined for both groups when an isotropic noise texture was presented. Further investigation of reaction times revealed an interaction between age group and noise, where older adults exhibited longer response times in the isotropic noise condition, while younger adults' reaction times did not significantly differ. The initial hypothesis suggested that the visibility of a fine-grained isotropic noise texture would be less visible to older adults resulting in reduced masking effects and less impairment in the task. However, the results suggest reduced sensitivity of the shape-from-shading cue in the isotropic noise condition, when compared to the binary noise for older adults. The findings indicate that perhaps a broadband visual texture conveys more information about shape-from-shading in first-order visual channels than a narrowband texture, and therefore when the bandwidth is constrained to one octave at a spatial

frequency identified as leading to poorer perceptual sensitivity for older adults in a CSF, a drop off in sensitivity occurred. Furthermore, it is thought that internal visual noise increases with age, which could elevate performance in high noise conditions as older adults may be more be accustomed to perceiving stimuli with external visual noise (Yan et al., 2020). Owing to this additional internal visual noise, older adults could require a high a higher intensity of noise to mask a grating compared to younger adults (Arena et al., 2013).

3.4.4 Age and Cognition interaction in shape-from-shading

The objective sought to investigate interactions between sensory load, and tasks with increasing cognitive demands and age-related differences. It was concluded that both younger and older adults' performance worsened as cognitive load increased, which was reflected in both accuracy and response times. The study found that noise contrast and spatial frequency did not have a significant interaction with age on performance. This suggests that cognitive load may have a stronger impact on first-order shape-from-shading perception with first-order modulations than visual sensitivity.

A significant interaction between age group and cognitive load was observed for accuracy. This suggests that cognitive resources might be required for this task. Further examination suggested that the effects of cognitive load drove this interaction on performance. However, no significant difference in performance for older adults in the 0-back and 1-back tasks was reported, while younger adults did display a significant difference in performance between these tasks. This interaction is consistent with previous literature suggesting that cognitive performance varies between younger and older adults. This supports the notion that ageing may affect capacity for increasing cognitive demands in older adults, whereas sensory perception is preserved. The observed findings lend support to the cognitive load theory, which suggests a trade-off between cognitive load and visual perception. According to this hypothesis, an increase in cognitive load can result in a trade-off with diminished perception (Li et al., 2001; Lindenberger & Baltes, 1994). This hypothesis sheds light on the trade-off, demonstrating that when cognitive demands in the 0-back task

were minimal, performance was comparable across age groups. Moreover, the hypothesis proposes that enhanced perception does not necessarily lead to improved cognitive performance. The findings lend support to this hypothesis by demonstrating an independence between sensory load and cognitive performance. This suggests that the perceptual quality of the stimulus did not trade off with improved cognitive performance, indicating an independence between these aspects of performance.

However, caution should be exercised in interpreting these results. It is unclear how specific this observation is, for example, participants may have instinctively moved closer to the display in conditions where stimuli were perceptually more challenging to see. A variation in viewing distance throughout the study could have reduced the mean differences between conditions and increased variability, resulting in the absence of a statistically significant interaction of spatial frequency and contrast of the noise texture on performance. Also, monitor size and resolution could not be standardised across participants, as previously mentioned. To address this issue, a large sample of participants was used in a mixed-design study, ensuring a baseline for each task to account for these variations. However, when comparing groups, the design may be more susceptible to these variations. The assumption was made that the variation in monitor size, resolution, and luminance settings is approximately equal between the two groups, although this is not measured. Consequently, it is crucial to consider the possibility that age-related differences in performance could be confounded by display settings, both when significant differences are reported and when they are not. To address these limitations of inconsistent viewing conditions, it is recommended that future replications of this study be conducted in a controlled lab-based environment, which would allow for better management of extraneous factors and provide more reliable results.

Excluding participants based on fitting a normal distribution is a debated issue. However, in these studies, all the stimuli presented were supra-threshold, which means they were well above threshold for detection. This was necessary due to the nature of online

studies, which introduced high variability of display monitor properties between participants. Therefore, a strict exclusion criterion was necessary for two reasons. Firstly, it was essential to ensure that all included participants were genuinely engaged with the task. Online environments can present unique challenges in maintaining participant engagement, excluding participants that are passively answering trials was necessary. Secondly, due to the inability of conducting in-person visual assessments at that time, the exclusion criteria aimed to ensure that participants did not have undisclosed visual impairments that could affect their performance. Future validation of these results through traditional psychophysical methods would confirm any interactions between sensory and cognitive load.

3.4.5 Conclusions

The findings of this study suggest an age-related effect on cognition in shape-from-shading perception. The effect of cognitive load on sensitivity to shape-from-shading appeared more pronounced in older adults, which lends support to the cognitive load hypothesis. Notably, the use of a visual noise texture effectively masked the shape-from-shading cues, with the spatial properties of the two textures masking these cues in distinct ways. The results suggest an interaction between the spatial properties of the noise, specifically in terms of bandwidth. Another aspect to consider was the potential impact of noise texture on either masking or enhancing depth cues. The masking or facilitation effects of noise texture on sensitivity to shape-from-shading were investigated by adding a luminance modulation instead of multiplication. Consequently, exploring sensitivity to shape-from-shading by modulating the texture itself would provide further insights, to ascertain whether the masking effects remains consistent.

4 Piloting and methodology refinement for psychophysical studies

In this chapter, I will provide a comprehensive overview of the piloting and refinement of my experimental method for estimating thresholds for second-order vision. The process of piloting took place over the first 18 months of my PhD, during which I developed a robust method for data collection. The chapter will present each study in chronological order, highlighting the specific methodology used for data collection, summarising the results, and providing a brief discussion of the limitations of each pilot and the conclusions drawn for subsequent experiments. Additionally, this chapter will outline the refinement of my data analysis for the data collected in each pilot and detail how I determined that a combination of threshold estimates from a method of constants and staircases was the most appropriate for my study**.**

4.1 Background

Previous research has investigated the impact of various factors on the sensitivity of shape-from-shading cues, including the orientation of the surface, the type of lighting conditions, and the spatial frequency of the noise carrier. It has been shown that the orientation of the surface can influence the perception of shape-from-shading, with oblique surfaces being more difficult to perceive than horizontal or vertical surfaces (Appelle, 1972). Additionally, different types of lighting conditions, such as diffuse or specular illumination can affect form perception and elicit perceptual biases in interpretation (Liu & Todd, 2004). Finally, the spatial frequency of the noise carrier has been found to impact the sensitivity of shape-from-shading cues, with high spatial frequencies enhancing performance in human and non-human primates (Cavonius & Robbins, 1973; Weinstein & Grether, 1940).

4.2 Pilot Study I. Exploring Sensitivity Limits in a Method of Constants Study

The primary objective in this pilot study was to examine the impact of the spatial frequency of a noise carrier on the sensitivities to shape-from-shading and to assess the limits and range appropriate for young adult observers when conducting experiments assessing sensitivity of shape-from-shading with a method of constants design. Achieving an appropriate balance between these two types of cues is highly sensitive and can be easily influenced by various experimental factors such as display luminance, pixel size, and laboratory lighting conditions. Therefore, it is important to ensure that the range of sensitivity captured in a method of constants design includes responses from chance to perfect levels of performance. To address this issue, a pilot study was conducted to determine the range of levels required to capture the full range of sensitivity in shape-from-shading cues using a method of constants design. This pilot study focused on young adult observers and aimed to provide a foundation for further investigation in this area with older adults in subsequent chapters of this thesis.

4.2.1 Methods

4.2.1.1 Stimuli

In the pilot study, a sinusoidal plaid was presented using an isotropic noise carrier that was presented at four spatial frequency intervals. As described in 2.1.4, a sinusoidal plaid consisted of two compound gratings, composed of a luminance and amplitude modulation that differ in their phase relationships, in-phase and anti-phase. These compound gratings are layered over the visual texture at two adjacent orientations, 45° and 315° to form a sinusoidal plaid. In Figure 4-1, the range of spatial frequencies used in this study varied from a coarse texture of 1.5 cpd to intermediate textures of 3 and 6 cpd, to a fine texture of 12 cpd. The spatial frequency of the noise carrier determined the level of ‘detail’ in the texture, with lower spatial frequencies corresponding to coarser textures and higher spatial frequencies corresponding to finer textures. The carrier used in this study had

a frequency bandwidth of 1 octave (full width, half height) and the overall root-mean-square (RMS) contrast was 0.4.

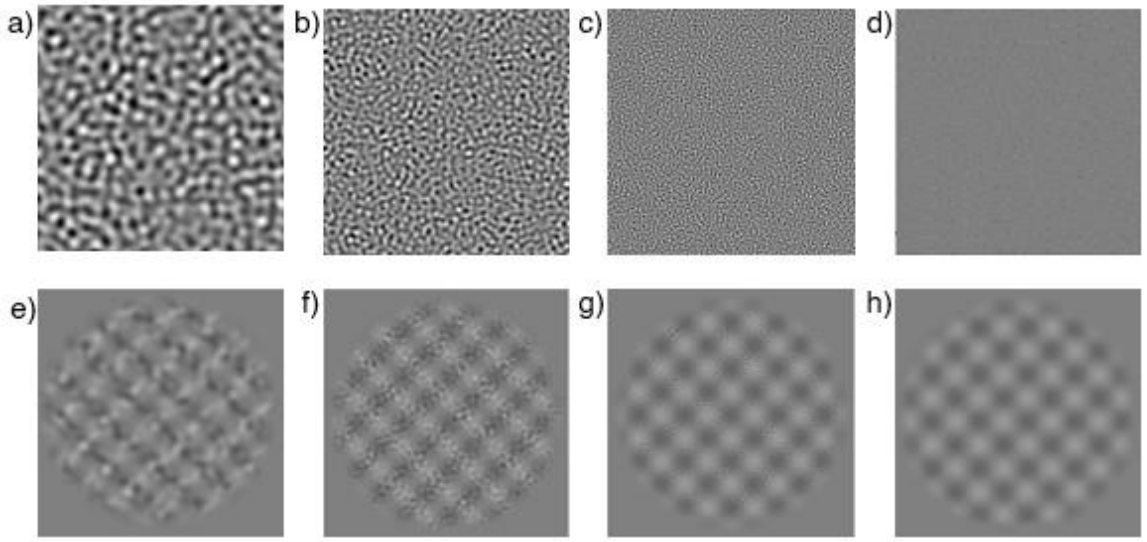

Figure 4-1. Isotropic noise textures and corresponding sinusoidal plaids at four different spatial frequencies, with each spatial frequency being one octave higher than the previous (a doubling in spatial frequency). The top row (a-d) displays the isotropic noise carriers without luminance or amplitude modulation, and the bottom row (e-h) shows their corresponding sinusoidal plaids. The visual texture of the a) 1.5 cycles per degree (cpd) carrier appears relatively coarse, while the b) 3 and c) 6 cpd carriers have decline in texture coarseness. The d) 12 cycles per degree texture is the finest of the four. All stimuli were drawn to the specified spatial frequencies and viewing distance and have been resized for this figure.

In addition to the spatial frequency of the noise carrier, the sinusoidal plaid stimulus used in this study also controlled for orientation and contrast. The plaid stimulus was created by overlaying two sinusoidal gratings that were perpendicular to each other (i.e., a phase difference of 90°). The contrast of the plaid pattern was adjusted to ensure that it was above the threshold but not saturated. The luminance component was scaled to 0.1 for each oblique and remained constant throughout the experiment. Stimuli were presented at an overall size of 8° (after a reduction of 2° due to the contrast gradient of a raised cosine window) and at a viewing distance of 80cm. The spatial frequency of the sinusoidal modulations was set to 0.75 cycles per degree, equating to 6 cycles per observable

stimulus. In the experiment, the luminance-modulation (LM) depth was kept constant, while amplitude-modulation (AM) depth was varied.

4.2.1.2 Participants

A total of eight adults (three male, five female) participated in the pilot study, with a mean age of 24.38 years (SD = 2.45). All participants reported normal or corrected-to-normal vision and were asked to wear corrective lenses if required. Before beginning the experiment, participants underwent a brief training session to familiarise themselves with the stimuli and task. They were shown an example of each stimulus type and given instructions on how to perform the task. This training session aimed to reduce any potential confounds due to unfamiliarity with the stimuli or task, and to ensure that participants were able to perform the task accurately and consistently throughout the experiment.

4.2.1.3 Design/Procedure

The current study employed a within-subjects design to examine the effects of noise carrier spatial frequency on sensitivity of shape-from-shading using a sinusoidal plaid stimulus. During the task observers were asked to determine the orientation of the coarse-scale undulations that appeared to have greater depth, in a two-alternative forced-choice (2afc) method (see Schofield et al., 2017).

As discussed in 4.2.1.1, spatial frequency of the stimulus texture was presented at four levels ranging from coarse to fine textures. The experiment utilised a method of constants design, in which the strength of amplitude modulations was manipulated to estimate thresholds in detection. The design included 12 amplitude modulation depth levels at logarithmic intervals spanning the entire range of monitors luminance capability (0%, 4%, 6%, 8%, 11%, 16%, 22%, 32%, 45%, 64% and 90%). These were repeated 20 times per interval, with a total of eight blocks (two blocks for each spatial frequency level), and the presentation order of each interval was randomised for each trial. The conditions were randomised using a Latin square design to prevent any order effects, and participants were

randomly assigned a viewing order. This design ensured that each stimulus was presented an equal number of times in each possible position within the sequence, minimising the impact of any potential order effects on the results.

4.2.2 Results

The results indicate that the AM thresholds followed a consistent pattern, with higher threshold estimates observed for the noise carrier conditions with spatial frequencies of 1.5 and 12 cpd, compared to the intermediate spatial frequency conditions of 3 cpd and 6 cpd. This sensitivity trend is illustrated in Figure 4-2. These findings suggest that sensitivity of shape-from-shading cues increases with an increase in the spatial frequency of the noise carrier, which is reflected in a decrease in threshold value. However, this sensitivity trend does not continue in the 12 cpd condition, where a sharp increase in threshold values indicates a decline in sensitivity of shape-from-shading cues. Additionally, the 1.5 cpd and 12 cpd conditions showed greater variability in their threshold estimates, indicating that sensitivity of shape-from-shading cues was less consistent in these conditions across participants compared to the intermediate spatial frequency conditions.

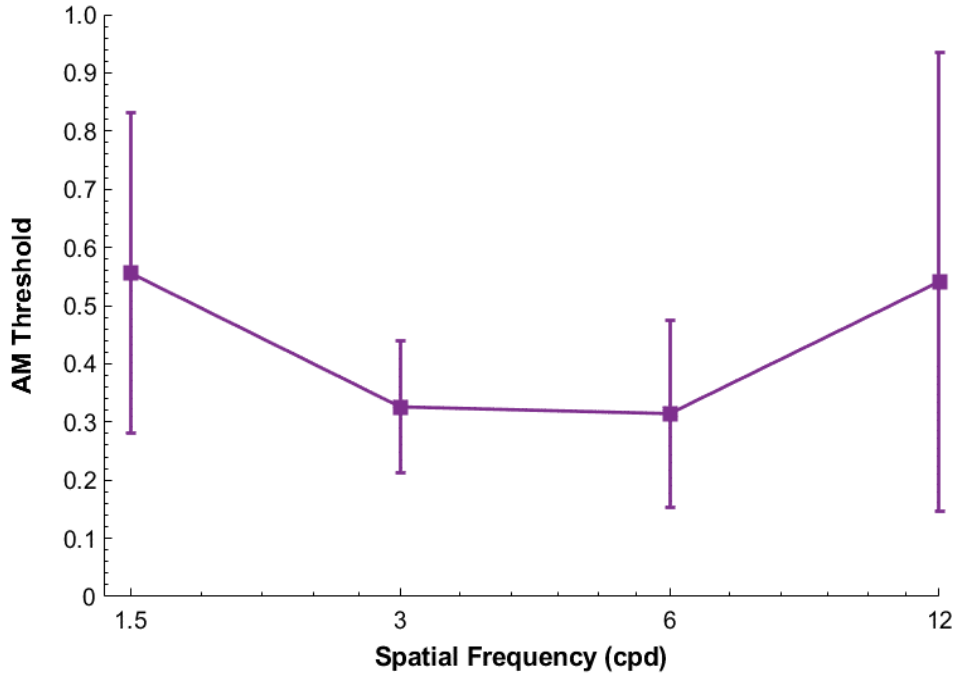

Figure 4-2. Results illustrate AM thresholds for each condition, presented as mean thresholds for all participants. The variability in the thresholds is represented by the standard error bars.

The presented data represents mean ± standard deviation values for the AM thresholds. The threshold values decreased from 0.56 ± 0.09 in the 1.5 cpd condition to 0.33 ± 0.05 in the 3 cpd condition, further to 0.31 ± 0.06 in the 6 cpd condition and increased again to 0.54 ± 0.12 in the 12 cpd condition. A one-way repeated measures ANOVA was conducted to test whether there was a statistically significant difference in the thresholds among the four spatial frequency conditions. The data were normally distributed, as assessed by a Shapiro-Wilk test ($p > .05$), and no outliers were detected. The assumption of sphericity was met, as indicated by Mauchly's test of sphericity ($\chi 2(5) = 6.03$, $p = .31$). The results did not reveal any significant effects of the spatial frequency of the noise carrier on the AM thresholds, $F(3,21) = 2.34$ $p = 0.1$, partial $\omega^2 = .002$. Suggesting that changes in spatial frequency of the noise carrier did not produce any statistically significant changes in the AM thresholds.

To further understand the individual differences in threshold estimates due to the high variability, and to analyse any potential trends across participants, the data was examined on an individual basis. The individual thresholds presented in Table 4-1 allowed further examination of whether individual participants' threshold estimates were consistent with the overall trend in the group data. Table 4-1 provides the individual thresholds for each participant. Overall, the thresholds were lower for the two intermediate conditions. However, for participant P6, the threshold in the 12 cpd condition was greater than 100%. Additionally, the proportion of deviance analysis revealed that in the 6 cpd condition, the psychometric function did not provide a good fit to the data (<.05).

Table 4-1

Individual AM thresholds for each participant in the four spatial frequency conditions.

	Thresholds			
	1.5 cpd	**3 cpd**	**6 cpd**	**12 cpd**
P1	0.22827*	0.18708	0.43876	0.2272
P2	0.86483*	0.24026	0.18511	0.2067
P3	0.6218	0.48714	0.21748	0.32324
P4	0.38202	0.38908	0.15058	0.15378
P5	0.62084	0.29195	0.37157	0.57671
P6	0.89892	0.47451	0.3529*	1.263
P7	0.15773	0.22021	0.61599	0.92397
P8	0.67201	0.3172	0.18169	0.65365

Note. The data is presented as mean ± standard error, and the proportion of deviance analysis results are also provided. * Proportion of deviance <.05

The lapse rates displayed in Figure 4-3 exhibit a similar trend to the threshold estimates, whereby they decrease from 0.05 ± 0.02 in the 1.5 cpd condition to 0.04 ± 0.02 in the 3 cpd condition, and to 0.039 ± 0.02 in the 6 cpd condition, with a subsequent increase to 0.906 ± 0.01 in the 12 cpd condition. The data were normally distributed, and no outliers were detected, as confirmed by a Shapiro-Wilk test ($p>.05$). Mauchly's test of sphericity indicated that the assumption of sphericity was met $\chi 2(5) = 5.33$, $p = .38$.

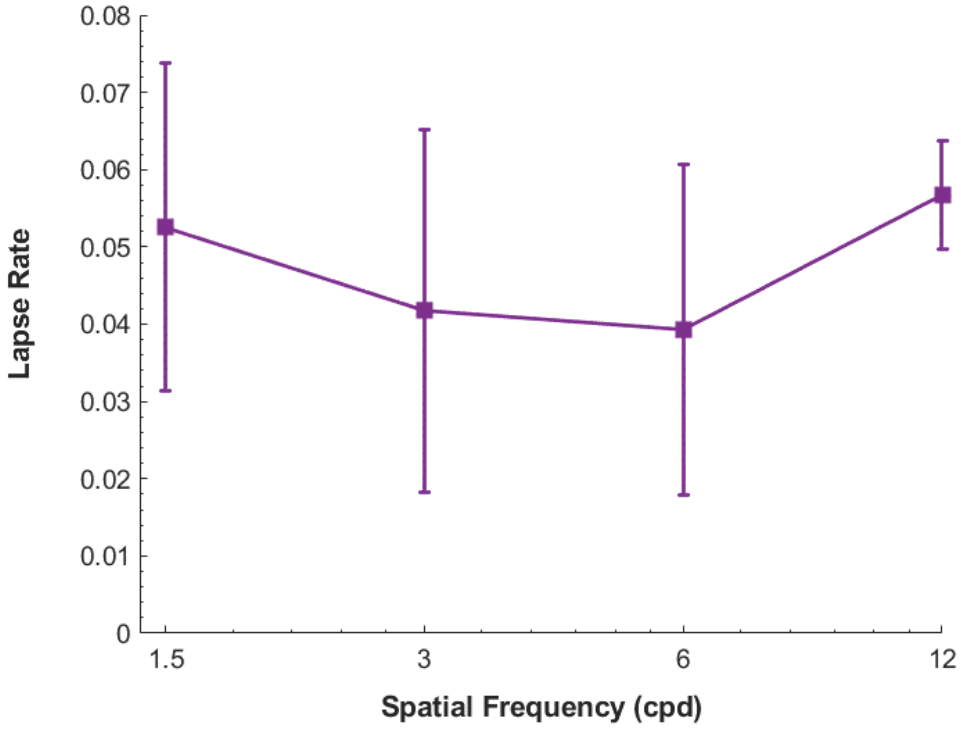

Figure 4-3. The estimated lapse rates, as measured by the proportion of trials in which participants responded incorrectly even when the stimulus was detectable. The error bars represent the estimated standard error of the mean (lapse rate).

A one-way repeated measures ANOVA revealed no significant difference in lapse rates due to changes in noise carrier spatial frequency, with a p-value of 0.11. These results suggest that the lapse rates were consistent across the different noise carrier spatial frequency condition, $F(3,21) = 2.31$, $p = 0.11$, partial $\omega^2 = 0.25$.

The median reaction times presented in Figure 4-4 were assessed to identify any significant effects as a function of spatial frequency and reflect reaction times when the AM depth was set to 90%. The reaction times displayed a pattern similar to lapse rates and thresholds. Reaction times were reduced from 793.03 ± 264.82 in the 1.5 cpd condition to 684.44 ± 136.6 in the 3 cpd condition and further to 681.62 ± 113.76 in the 6 cpd condition. However, reaction times increased to 768.6 ± 127.81 in the 12 cpd condition.

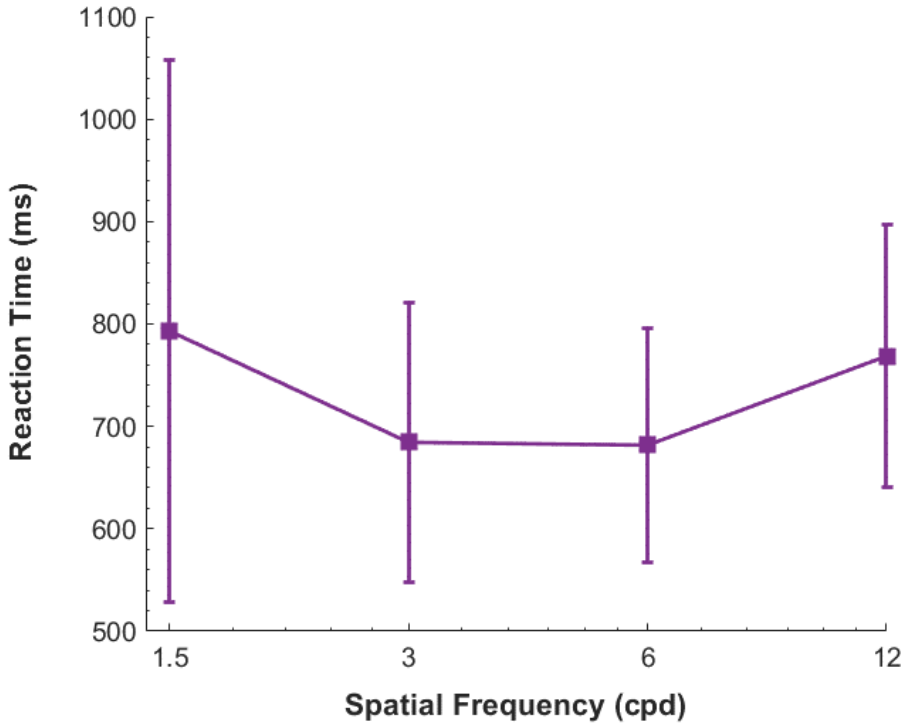

Figure 4-4. The median reaction times across the four conditions at an amplitude modulation of 90%. The standard error of the mean is indicated by error bars.

To investigate the impact of spatial frequency on the average median reaction time, a one-way repeated measures ANOVA was performed. One outlier was excluded from the analysis, and the data was found to be normally distributed in each condition, as confirmed by the Shapiro-Wilk test ($p > .05$). Mauchly's test for Sphericity indicated that the assumption of sphericity was not met $\chi 2(5) = 11.54$, $p \leq .05$. A Greenhouse & Geisser (1959) correction was applied, resulting in an epsilon, ε, value of 0.51. Ultimately, the analysis revealed a non-significant effect of carrier spatial frequency on reaction time, with $F(1.54, 9.25) = 3.83$, $p = 0.07$, and partial $\omega^2 = 0.39$.

4.2.3 Interim Discussion

The results conclude a non-significant difference between the experimental conditions. Therefore, the experimental hypothesis that an increase in spatial frequency of the noise carrier would result in an increase in sensitivities to amplitude modulations (resulting in lower thresholds) was not supported. However, the pattern of results in terms of

amplitude modulation threshold estimates showed an increase in sensitivity from 1.5 cpd to 3 cpd and further increased sensitivity from 3 cpd to 6 cpd. Although these results were non-significant, the general pattern of threshold estimates is consistent with previous research (Dakin & Mareschal, 2000; Dövencioğlu et al., 2013; Felipe, Buades, & Artigas, 1993; Schofield et al., 2017; Sutter et al., 1995).

The non-significant results of this pilot study may largely be attributed to its small sample size, which resulted in an underpowered design. Thus, while the findings did not reach statistical significance, the range and spread of the data suggest that significant differences might be observable with a more adequately powered study. In this thesis, Chapter 4 and 5 have explored this by increasing the sample size. Therefore, despite the lack of statistical significance, the trend in AM threshold estimates may still hold valuable insights. The increase in sensitivity observed when transitioning from 1.5 cpd to 3 cpd and subsequently from 6 cpd to 12 cpd suggests that there might be an underlying relationship between spatial frequency and amplitude modulation sensitivity. This pattern could be attributed to the characteristics of the human visual system, where the processing of spatial information is known to be influenced by factors such as spatial frequency and contrast. The patterns observed in the findings extend beyond amplitude modulation threshold estimates, as they also align with the results obtained for lapse rates and median reaction times. The high variability and slower reaction times observed in the 1.5 cpd condition suggest a lower sensitivity of stimuli at this frequency compared to the 3 and 6 cpd conditions. Similarly, the marginal increase in reaction times at 12 cpd suggests that the visual system may be less efficient at processing stimuli at this frequency also. These findings indicate an optimal range of spatial frequencies for which the visual system is most sensitive, with sensitivity decreasing at both lower and higher frequencies. The results also highlight the importance of considering individual differences in spatial frequency sensitivity when studying visual perception. The consistency across multiple measures strengthens the notion that the

relationship between spatial frequency and amplitude modulation sensitivity might be more nuanced than the current study's statistical outcomes suggest.

The reduction in sensitivity of amplitude modulations in the 12 cpd condition was anticipated, as previous research has indicated that an increase in spatial frequency leads to a tapering off of sensitivity in adults (Dakin & Mareschal, 2000; Sutter et al., 1995). However, the high variability within this condition prompted further investigation. Upon examining the stimuli presented in the 12 cpd condition, it became clear that the CRT monitor’s resolution resulted in a visual texture of 12 cpd, comprising only three pixels per cycle at the current viewing distance. This limitation could have distorted the first- and second- order signals and potentially contributed to the greater variability in thresholds observed at 12 cpd. Further investigation into appropriate stimuli parameters given the screen resolution will be vital before conducting further experiments using this paradigm.

In addition to the pattern of sensitivity threshold estimates, it was noted that the thresholds seemed considerably higher compared to those found in studies with similar experimental parameters and stimuli (Schofield et al., 2017). The higher thresholds observed in all conditions might be attributed to the luminance constraints of the monitor used in the experiment. Limitations in the display's luminance range could have affected the visibility and contrast of the visual stimuli, subsequently influenced participants' performance, and led to elevated thresholds. Therefore, it is essential to consider the impact of display characteristics when interpreting the results and comparing them to findings from other studies.

More likely, the elevated thresholds are also likely attributable to participants being under-practised before taking part in the study. Research employing a similar experimental paradigm has demonstrated that perceptual learning of visual textures does not transfer between distinct visual textures and that the learning process is relatively slow, with performance plateauing after approximately 100 trials (Dövencioğlu et al., 2013). In the current pilot study, participants were given 15 practice trials with a binary noise texture,

meaning that perceptual learning of this noise carrier may not have transferred to the experimental conditions. Providing only 15 practice trials for naïve observers is likely insufficient to yield reliable and consistent thresholds. In future research utilising this paradigm, it would be beneficial to ensure that participants receive adequate practice for each experimental condition before estimating their thresholds.

4.3 Pilot Study II. Obtaining Reliable Thresholds from Experienced Observers

Drawing on the insights gained from the previous pilot study, pilot study II was designed to address the limitations identified in the initial study and aimed to acquire more reliable thresholds by involving two experienced vision observers who had completed over 1000 trials of practice. These observers were better equipped to provide consistent results due to their extensive experience with similar experimental paradigms. The experimental methods in pilot study II incorporated several adjustments to improve the overall reliability and validity of the findings. These changes were implemented to address concerns related to under-practice. Another aspect addressed the monitor constraints identified in the first pilot study, which may have impacted the visibility and contrast of the visual stimuli, leading to higher, more variable threshold estimates. To display stimuli with greater fidelity, the experimental setup was modified, which included changes to the stimuli parameters.

In addition to addressing the limitations identified, the results from pilot study II aimed to provide support for the range and intervals used in studies that employ this methodology in the empirical chapters 5 and 6. By obtaining reliable thresholds from experienced observers, insights into the appropriate range and intervals aim to produce precise and consistent thresholds in the empirical chapters.

4.3.1 Methods

In this section, the methods employed in pilot study II are outlined. Many of the parameters used in this study are similar to those in pilot study I; therefore, not every detail

will be repeated here. Instead, the focus will be on highlighting the key parameters and differences in methodology that distinguish this study from the initial pilot.

4.3.1.1 Stimuli

Similar to pilot study I, a sinusoidal plaid was presented using an isotropic noise carrier, manipulated to display the stimulus at four spatial frequencies: 0.75, 1.5, 3 and 6 cpd. The frequency bandwidth of the carrier was set to 1 octave (full width, half height). The overall rms contrast was 0.4, and the luminance sinusoid was scaled to 0.1 for each oblique. Stimuli were presented through a raised cosine window at a larger stimulus size of 10° and viewed at a distance of 80cm. The spatial frequency of the sinusoidal modulations was set to 0.375 cycles per degree, equating to 3.75 cycles per observable stimulus size.

4.3.1.2 Participants

Two observers participated in the study; participant HB (female, aged 25) and participant HA (female, aged 44). Both had corrected-to-normal vision and wore corrective lenses during participation. It is worth noting that both participants had extensive prior experience with similar experiments and experimental paradigms, classifying them as 'experienced' observers.

4.3.1.3 Design

In this pilot study, a within-subjects design was employed to investigate the effect of stimulus texture changes on the observer's ability to detect amplitude modulations. Participants underwent an extended training period of 100 trials before completing a method of constants design at each of the four spatial frequencies. The manipulation of amplitude modulation strength was carried out in the same manner as in pilot study I at 12 intervals, remaining consistent with the previous experiment.

4.3.2 Results

Upon examining the threshold estimates, as depicted in Figure 4-5, the thresholds follow a consistent pattern across different noise carrier conditions. In the 0.75 cpd condition,

both participants exhibited higher thresholds, suggesting a reduced sensitivity of amplitude modulations at this spatial frequency. A marked decline in thresholds was observed in the 1.5 cpd condition, indicating an increase in sensitivity as the spatial frequency of the noise carrier increased. Interestingly, the 3 cpd and 6 cpd conditions yielded relatively similar thresholds for both participants, suggesting that sensitivity of amplitude modulations plateaued at these spatial frequencies.

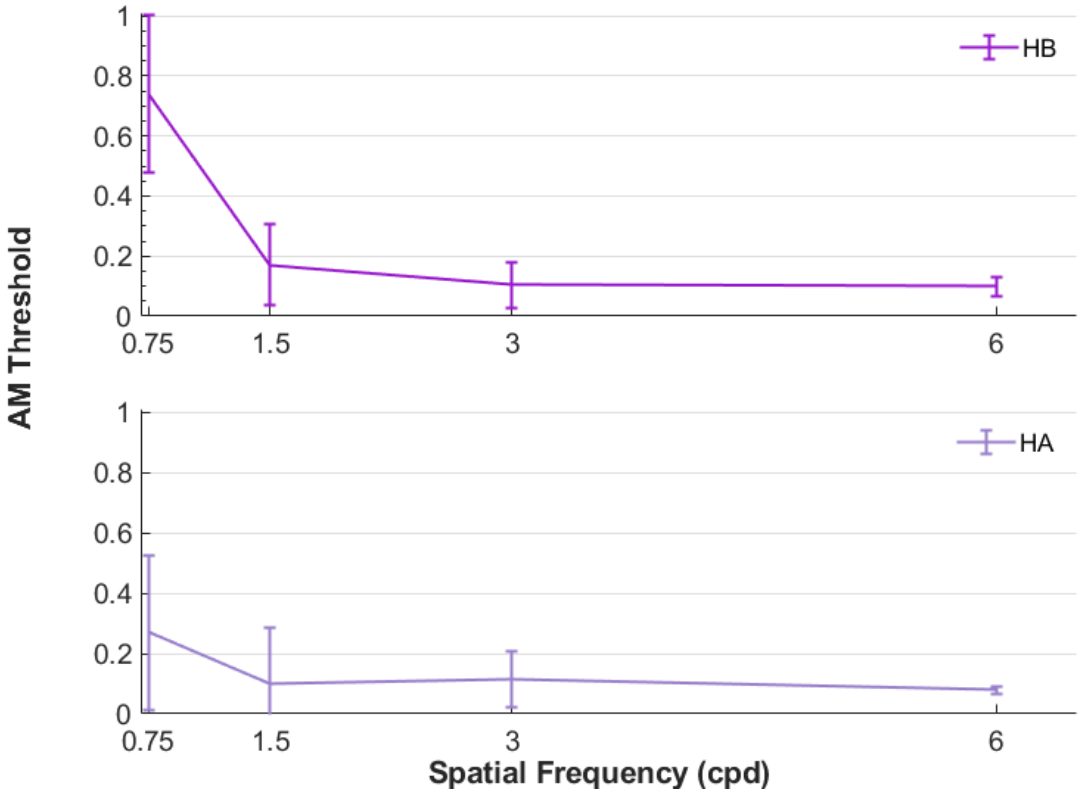

Figure 4-5. AM estimated thresholds across different noise carrier conditions for both participants, represented as separate graphs. Error bars represent standard error of the threshold estimates, calculated using Bootstrapping (1000 iterations).

Based on the threshold estimates shown in Figure 4-5, all estimated thresholds were below 1.0, when compared to the initial pilot study. Greater variability in threshold estimates was observed in the 0.75 cpd condition. A single case of an unsuitable psychometric function poorly fitting the data set was identified (Observer HA, 3 cpd).

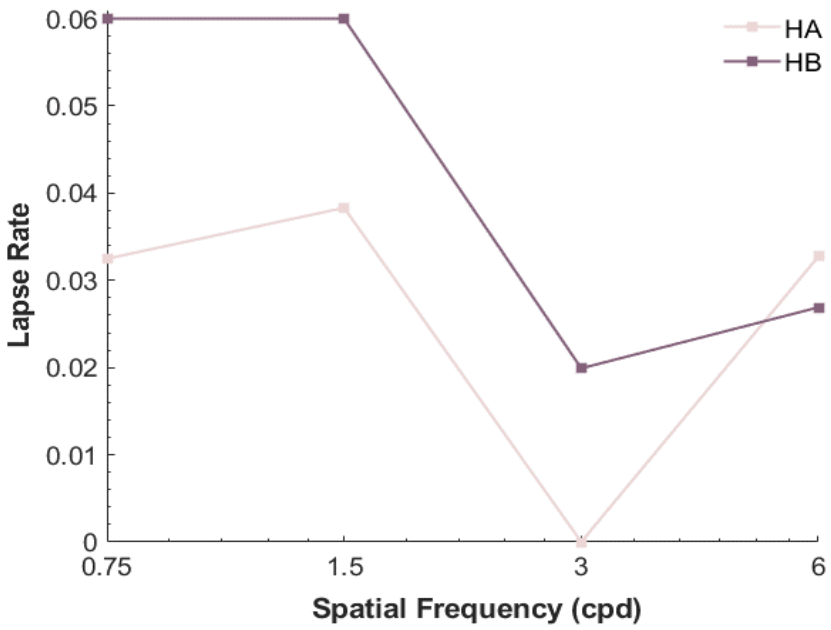

Figure 4-6. The estimated lapse rates for each condition are shown for the two observers, HA and HB, with each observer's data represented as a separate line.

As shown in Figure 4-6, the estimated lapse rates follow a pattern where the lapse rates in the 0.75 cpd and 1.5 cpd conditions are higher than those in the 3 cpd and 6 cpd conditions. However, the difference in estimated lapse rates between the four conditions was not statistically significant, $F(1,1) = 5.95$, $p = .25$, partial $\omega^2 = .86$. Again, given the small sample size of two participants, the study was likely underpowered to detect any significant differences.

4.3.3 Interim Discussion for Pilot Study II

The results from pilot study II indicate that the spatial frequency of the noise carrier shows some variation in sensitivity of amplitude modulations in shape-from-shading stimuli. Specifically, observers had more difficulty detecting modulations in amplitude in the conditions with low spatial frequencies of the noise carrier (0.75 cpd). These patterns of findings are consistent with previous research, suggesting that the spatial frequency of the noise carrier can affect sensitivity of second-order visual properties. The estimated lapse rates also followed a similar pattern to that seen in pilot study I, with higher lapse rates in the

lower spatial frequency conditions. However, again, there was no statistically significant difference between the four conditions.

It is worth noting that a small sample size will result in low statistical power, making it difficult to detect any significant differences in threshold estimates between conditions. Therefore, the lack of statistically significant results in this analysis may be due to the study being underpowered rather than an absence of any true effects of spatial frequency on sensitivity of shape-from-shading. Studies with larger sample sizes will address this limitation in the empirical chapters and provide more conclusive evidence regarding the effects of carrier spatial frequency on sensitivity of shape-from-shading.

The pattern of threshold estimates is consistent with previous research on amplitude modulations, with higher threshold estimates observed for very coarse noise carriers and an increase in sensitivity as the carrier spatial frequency increases (Manahilov et al., 2003; Schofield & Georgeson, 2003). These findings suggest that the spatial frequency of the noise carrier plays a crucial role in the perception of amplitude modulations.

The ratio of noise carrier-to-envelope has also been shown to be a critical factor in the sensitivity of amplitude modulations, with a gradual decline in threshold observed as the ratio increases (Dakin & Mareschal, 2000; Jamar & Koenderink, 1985). The present pilot study investigated a range of carrier-to-envelope ratios, from 2:1 to 16:1, which were selected based on the constraints of the spatial resolution of the display monitor and viewing distance used in the study. It is worth noting that previous research has also shown the decline in threshold plateaus at high ratios of carrier-to-envelope spatial frequencies, with deterioration only observed at ratios of 32:1 and higher (Sutter et al., 1995). However, ratios greater than 16:1 were not investigated due to limitations in the viewing distance and stimulus size. Adjusting the experimental parameters was considered in subsequent chapters to investigate higher ratios and obtain reliable threshold estimates from these conditions.

4.4 Discussion

In each pilot study, the primary aim was to investigate the relationship between spatial frequency of the noise carrier and AM depth threshold estimates. The first pilot study used a sinusoidal plaid stimulus to examine the effect of different spatial frequencies of the noise carrier on amplitude modulation thresholds, while the second pilot study used a similar approach but with a different range of spatial frequencies and examined whether more experienced observer's and more practice would result in less variable threshold estimates. The results of both studies revealed a similar pattern of threshold estimates, where lower spatial frequencies of the noise carrier were associated with reduced sensitivity, and intermediate spatial frequencies resulted in greater sensitivity. However, neither study found statistically significant differences in threshold estimates across conditions, which may be due to the small sample size of two participants. Further research with a larger sample size is needed to confirm these findings and to investigate the potential relationship between spatial frequency, and amplitude modulation threshold estimates more thoroughly.

In pilot study I, the estimated lapse rates did not differ significantly between conditions. However, the same pattern was observed in pilot II, where observers had more difficulty in detecting amplitude modulations in conditions with lower spatial frequencies of the noise carrier. These findings are consistent with previous research that has shown the importance of the ratio of the noise carrier to the envelope spatial frequencies on sensitivities to amplitude modulations (Dakin & Mareschal, 2000; Jamar & Koenderink, 1985; Sutter et al., 1995).

The carrier-to-envelope ratios investigated in the pilot study II were lower than those that have been shown to result in a decline in sensitivity, suggesting that the ratios tested may not be perceptually challenging enough. However, we see that when the ratio of 1:32 was presented in pilot I, we had a drop off in sensitivity. It is unclear whether the observed high threshold estimates in the 12cpd condition in pilot I are due to differences in spatial frequency or distortion of the carrier caused by the constraints of the monitor's resolution. It

is possible that with a larger range of ratios, displayed with greater fidelity, a significant effect may have been observed.

The patterns observed in both pilot studies are consistent with previous research and provide important insights into the factors that affect sensitivities to amplitude modulations, although the findings were non-significant, this is likely due to small sample sizes. The following chapters will build upon these findings by investigating a wider range of spatial frequencies and exploring the role of other perceptual factors. These pilot studies provided insights into the relationship between spatial frequency and amplitude modulation threshold estimates and lay the groundwork the subsequent research in this thesis.

5 Perceived depth magnitude of luminance and contrast-modulated noise textures

This chapter investigates the impact of age-related changes in sensitivity of shape-from-shading. Chapter 3 demonstrated an interaction between the perception of first-order shape-from-shading cues and noise textures for younger and older adults. It was concluded that the visibility of a noise texture impacted sensitivity of shape-from-shading. Consequently, the aim was to broaden the scope by integrating additional cues into this relationship, achieved by modulating a noise carrier using second-order amplitude contrast. Specifically, the role of texture modulated by first- and second-order shape-from-shading cues and how sensitivity of this changed with age. By incorporating these additional factors, further understanding of ageing of the visual system can be explored was therefore explored.

5.1 Introduction

The findings in Chapter 3 suggest that shape-from-shading perception was influenced by masking for both younger and older adults. That study also found that older individuals demonstrated comparable or even heightened sensitivity of shape-from-shading cues relative to younger adults, particularly in conditions where cognitive load was not manipulated. Additionally, the study revealed significant differences in sensitivity when examining broadband and narrowband noise textures. Moreover, the comparison of narrowband textures at contrasting spatial frequencies was not feasible due to the discussed limitations of conducting online research, necessitating further investigation in this area.

Chapters 5 and 6 of this thesis explore the effects of amplitude-modulated (AM) contrast on shape-from-shading perception. The interaction between AM and a noise carrier signal, offer further insights into the mechanisms underlying our interpretation of depth.

Chapter 5 specifically investigates the impact of AM within the context of single grating stimuli. Chapter 6 then extends this exploration to more complex visual stimuli, sinusoidal plaids. Constituted of superimposed gratings with varying orientations, plaids present a more intricate platform for evaluating the role of AM depth modulation. Consequently, these two chapters collectively aim to enhance our understanding of the role and impact of shape-from-shading with first- (LM) and second-order (AM) stimuli, and how these change with age.

5.1.1 LM and AM cues in shape-from-shading

Masking and facilitation within first- and second-order modulations provides further insights into how the two visual streams process modulations. In motion, luminance modulations cancel each other's effects when presented with opposing directions, which is also observed when AM contrast- and luminance-modulated gratings that are presented at the same spatial frequency (Lu & Sperling, 1995). This observation suggests the existence of either a fully or partially shared underlying mechanism governing both processes. Initially, AM and LM stimuli may be processed through distinct pathways but then converge during a later pooling stage (Wilson, Ferrera & Yo, 1992). This integration during late pooling could then lead to effective masking, where the presence of one type of stimulus modulates or alters the perception of the other. Additionally, in some cases where a first-order noise texture is used in conjunction with modulations in AM contrast and luminance, it can assist in the detection of modulations rather than obscure it (Dakin & Mareschal, 2000). This is further supported by research on the effects of static luminance and AM contrast- gratings. When a stimulus is composed of both gratings, the phase of these two gratings can either facilitate or impede the perception of depth, where an in-phase grating gives the illusion of depth, whereas anti-phase is perceived as a flat surface (Georgeson et al., 2009; Schofield et al., 2017).

5.1.2 Perceived depth magnitude of shape-from-shading

As previously established, shape-from-shading perception is the process of discerning the shape and depth of a stimulus based upon its shading when other shape cues, such as edges, are absent (Christou & Koenderink, 1997). Chapter 3 explored how luminance modulations convey information about shape, owing to the light-from-above prior (Kleffner & Ramachandran, 1992). However, changes in luminance are also likely associated with variations in visual texture (Kingdom, 2003).

In Chapter 1, it was proposed that the human visual system can perceive static stimuli by processing key visual cues such as luminance and contrast. The ability to distinguish between illuminance and material changes with high accuracy was also discussed (Sun & Schofield, 2011). The relationship between first- and second-order properties of natural images demonstrated a positive correlation which signified a change in illumination, while a negative correlation was associated with material changes (Johnson & Baker, 2004). This observation implies an association between the first- and second-order visual cues, where their statistical relationship can be replicated to ascertain the origins of changes in luminance and reflectance (Kingdom, 2008).

Variations in illumination and material properties exhibit distinct statistical relationships concerning amplitude (AM) and luminance modulations (LM) (Schofield et al., 2006). As illustrated in Figure 5-1, the interaction between these modulations, particularly an in-phase relationship (LM+AM), enhanced the perceived depth of a surface. However, when the gratings are anti-phase (LM-AM), it conveyed a change in texture rather than illumination. As a result, these contrasting relationships are thought to enhance the perception of shape versus material changes to the observer, in relation to the light source (Kingdom, 2003).

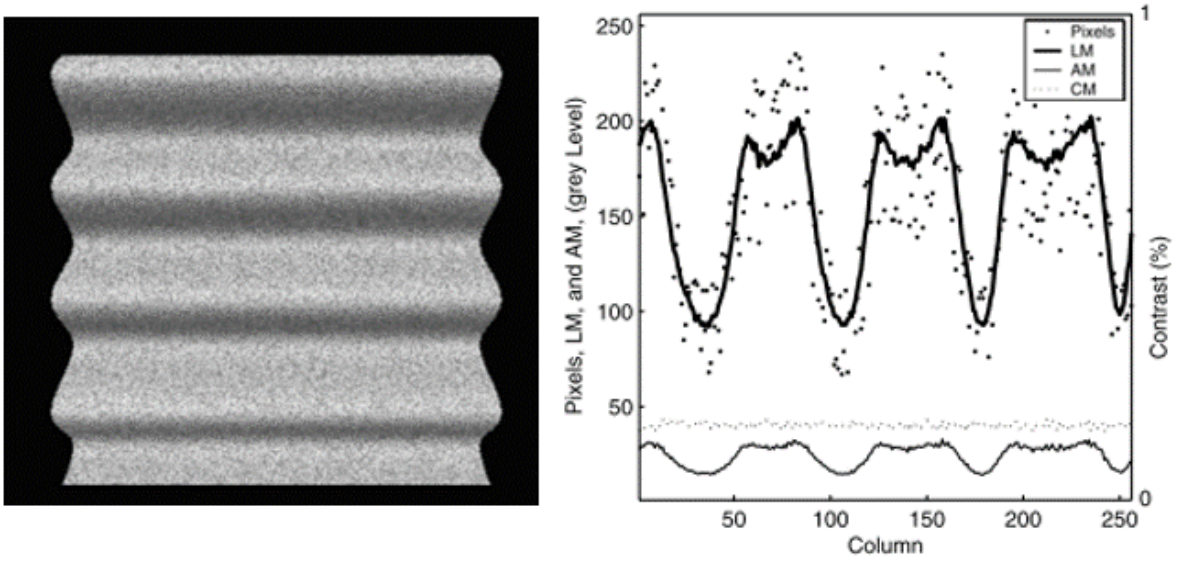

Figure 5-1. A depth-modulated albedo textured surface, illuminated by a light source. The surface exhibited a diffuse albedo texture, consisting of changes in illumination which consequently influenced the shape perception. Note. Adapted from “Local luminance amplitude modulates the interpretation of shape-from-shading in textured surfaces” by Schofield, Hesse, Rock & Georgeson, 2006, Vision Research, 46(20), p.3464.

The statistical relationship between LM and AM in natural scenes has been defined in prior research, but the perception of depth in human observers based on this relationship is yet to be fully characterised for older adults. Depth mapping provides insights into investigating this relationship, where the perceived depth magnitude (PDM) of a grating can be assessed through observers estimating the depth at specific points within the sinusoidal modulation (Schofield et al., 2006). In Figure 5-2a, a reference location was selected on the test stimulus. For plaids stimuli, the intersection of the central peaks of the two obliques was marked, and for single oblique stimuli a central luminance peak and a nominal peak were marked. Observers were then instructed to identify which of the markers appeared closer to them in depth. Responses identifying the marker as closer were scored as +1 and responses a marker as further away were scored as -1 resulting in a mean score for each test phase for the perceived surface gradient. As depicted in Figure 5-2a, it was found that when gratings were shown simultaneously, observers perceived in-phase obliques to have

greater PDM than anti-phase obliques. However, when gratings were presented separately, the distinction between in-phase and anti-phase was reduced, with LM-AM appearing relatively depthy.

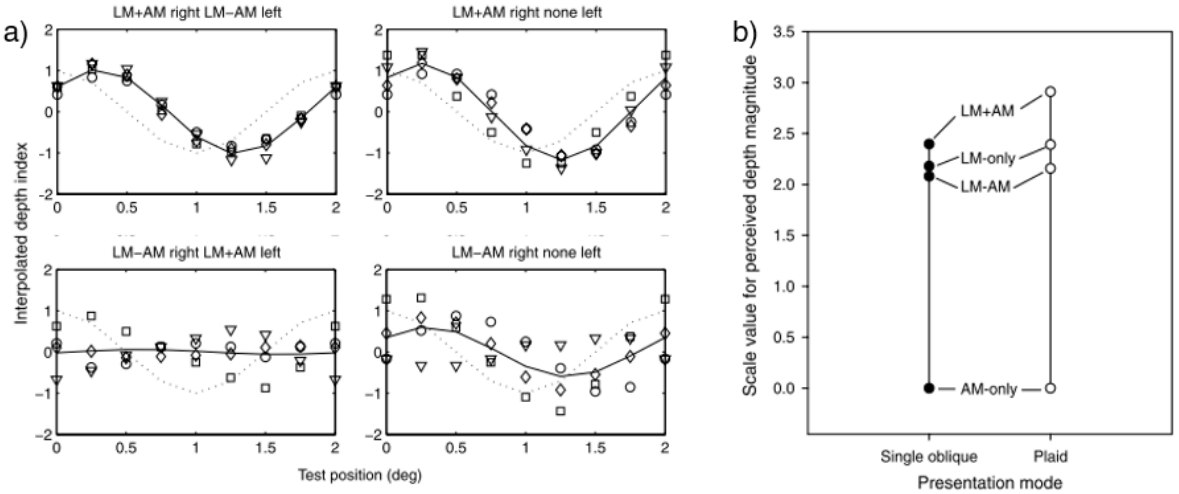

Figure 5-2. (a) Depth profiles for LM+AM and LM-AM at uniformly distributed points along the sinusoidal modulation. The left column denotes the depth index of gratings presented simultaneously and the right column for individual plaids. The x-axis represents the nominal test position in relation to a single cycle of the luminance signal, measured in cosine phase units, and the interpolated depth index is presented on the y-axis (b) Scaling plots for a paired comparisons task, comparing PDM for single interval and two-interval presentations of gratings. Note. Reprinted from “Local luminance amplitude modulates the interpretation of shape-from-shading in textured surfaces” by Schofield, Hesse, Rock & Georgeson, 2006, Vision Research, 46(20), p.3464.

Tasks using a paired comparisons design provides further insights, revealing a similar trend when both in-phase and anti-phase gratings are presented within a single interval. Figure 5-2b demonstrates that PDM was heightened compared to stimuli presented at separate intervals. Further comparisons found that LM gratings presented independently had greater PDM than AM-only gratings (Schofield et al., 2006). This finding suggests that shape-from-shading cues originate from variations in local mean amplitude and are enhanced by the presence of LM.

5.1.3 Does ageing affect shape-from-shading perception?

Vision undergoes significant changes with ageing, characterised by minimal reductions in sensitivity at low spatial frequencies and an increasing deficit at high spatial frequencies throughout adulthood (McGrath & Morrison, 1981; Skalka, 1980; Sloane et al., 1988). Thus, ageing is often linked to a reduction in processing fine-scale visual details. This phenomenon could potentially impair the processing of second-order visual cues, thereby influencing depth perception (Schofield et al., 2017).

Texture also plays a vital role in conveying depth information and is thought to be impacted by ageing. Textures are typically categorised as narrowband or broadband, each carrying distinct implications for depth perception. Narrowband textures concentrate their energy within a limited range of spatial frequencies. Broadband textures contain energy across a wide range of spatial frequencies and offer rich information about an object's surface and depth (Schofield et al., 2017). This decline in contrast sensitivity thresholds as a function of high carrier spatial frequencies could potentially be a result of internal noise within the visual system and neural processing deficits (Pardhan, 2004). In this paper, it was suggested that older adults demonstrated neural deficits at lower spatial frequencies and optical deficits at high frequencies, suggesting that both factors contribute to age-related changes in visual acuity and contrast sensitivity. The influence of these factors appears to be spatial frequency dependent, suggesting changes in function in the visual cortex. While these changes may not involve cell loss, they may contribute to changes in second-order processing (Rapp & Gallagher, 1996; Weale, 1975). The perception of second-order signals is thought to be more adversely affected by ageing due to the optical and cortical requirements. This is supported by the hypothesis that even though there's some shared low-level processing between first- and second-order stimuli, the more complex analysis required by second-order stimuli is more vulnerable to the effects of ageing (Faubert, 2002; Habak & Faubert, 2000).

5.1.4 Is there a relationship between shape-from-shading perception and first- and second-order vision?

The interaction between first- and second-order cue sensitivity and depth perception is suggested to change with age (Sun & Schofield, 2011). In shape-from-shading studies using first order (LM) and second-order (AM) stimuli, the perception of anti-phase gratings was unaffected by the carrier frequency for younger adults, maintaining a consistently flat appearance (Schofield et al., 2017). However, the perceived depth of in-phase gratings increased as carrier spatial frequency increased for younger adults, whereas older adults exhibited selective perceptual difficulty at high carrier frequencies. Therefore, carrier sensitivity is thought to impact sensitivity of AM modulations.

As discussed in chapter 1, linear mechanisms are thought to detect first-order cues, while second-order cues require further processing, therefore interacting with visual textures differently (Cavanagh & Mather, 1989; Schofield & Georgeson, 2003). Despite this, second-order cues require a first-order carrier which therefore impacts sensitivity of AM cues, further supporting the relationship between sensitivities to first- and second-order cues.

5.1.5 Introduction to the Study

Although previous research has explored the presentation of gratings simultaneously or in separate intervals, the PDM of gratings that are presented in one interval but are spatially independent has not been examined. Therefore, the present study sought to determine, whether the heightened PDM of in-phase gratings remained apparent when presented simultaneously with, but spatially separated from anti-phase gratings. The relationship between age and shape-from-shading perception was investigated by manipulating spatial properties of a visual texture used for shading cues. Amplitude modulation (AM) thresholds were measured to justify higher AM testing levels for older adults than for younger adults. For a more thorough assessment, younger adults were tested at both levels. Noise thresholds were also evaluated to potentially elucidate the reduced AM

perception observed in older adults. As older adults typically have lower sensitivity of high frequency carriers (i.e. noise), AM perception may be compromised due to reliance on perception of the noise as a carrier. The study aimed to determine whether combinations of LM and AM manipulations of a noise texture led to masking or facilitation of a shape-from-shading stimulus. It was predicted that younger and older adults will exhibit greater PDM for in-phase gratings and reduced PDM for LM-only gratings when the noise carrier is visible. Whereas a reduction in PDM for in-phase gratings was predicted for older adults as contrast sensitivity attenuates at high carrier spatial frequencies.

5.2 Methods

5.2.1 Design/Stimuli

The present study consisted of three tasks that examined: contrast sensitivity, amplitude modulation sensitivity, and perceived depth magnitude of gratings through paired comparisons. Each task was conducted under three conditions of noise spatial frequency, with the order counterbalanced and randomly assigned to observers. Observers viewed the screen binocularly (further details provided in 5.2.3) and fixated on a central target before each trial. To ensure consistent viewing, participants made responses after the presentation period. A 1000ms inter-trial-interval followed each trial, during which a coarse-scale isotropic noise with a central spatial frequency of 0.5 cpd was presented to prevent effects of negative after-images interacting with sensitivity for the following trial. An isotropic narrowband noise carrier was utilised and presented at 4, 8 and 12 cpd for each of the following tasks.

5.2.2 Participants

A total of 34 participants, ranging in age from 18 to 26 and 61 to 82 completed the study, with 17 individuals constituting the younger group and 19 in the older group. Participants went through a brief training period before commencing the experiment. This included a short verbal introduction to each task and 12 practice trials for each condition, as

well as being shown a physical representation of how the stimuli used in the depth judgments talk might appear in a real-world context.

5.2.3 Equipment

Stimuli were generated using Psychopy © (Peirce, 2007) and run on a Mac OS X El Capitan v10.11 (Apple Inc) operating system. Stimuli were presented using a Bits++ (Cambridge Research Systems) stimulus processor on a CRT monitor (Viewsonic P225f, display screen width 39cm, 1280 x 1024 pixels, pixel width = 0.0178° x .0178° at a 160cm viewing distance) with an overall screen refresh rate of 75Hz. Participants were positioned 160cm from the monitor using a modified chinrest with an adjustable optical trial lens frame. All participants had vision corrected to normal standards and, wore their prescribed glasses throughout the experiment if required. Younger adults viewed the stimuli through two optical lenses, +0.12 and -0.12, to create an aperture but no correction. Older adults viewed the stimuli through two optical lenses, +0.12 and +0.5, (total power +0.67) to correct for presbyopia. Further to this, all participants incorporated their respective distance corrections, involving either a single lens for older adults or bifocal/varifocal lenses as required. Participants provided their responses via a keyboard, and the study was conducted in a room with controlled lighting.

5.3 Experiment I: Sensitivity of LM and AM Cues

5.3.1 Methods

To evaluate sensitivity of noise texture, a noise target was presented for 1000 ms to either the left or right of a central fixation point (p = 0.5), whereby observers made responses over the location of the target (2afc). An example of each trial is depicted in Figure 5-3. Two, 3-down-1-up (3D1U) staircases, each with 12 reversals each were completed concurrently for each condition. During the first 4 reversals of each staircase, the difference in intensity was reduced with a specified pattern of 4, 2, 2, and 1 dB. To ensure accurate and reliable threshold measurements, the threshold estimate of the final 8 reversals in the second

staircase were averaged to produce the threshold estimate (79.4%). The first staircase was used as a practice to familiarise participants with the task and stimuli. This approach helped to mitigate the influence of initial learning and task familiarisation on the data. As a result, the data obtained from the second staircase had smaller error margins.

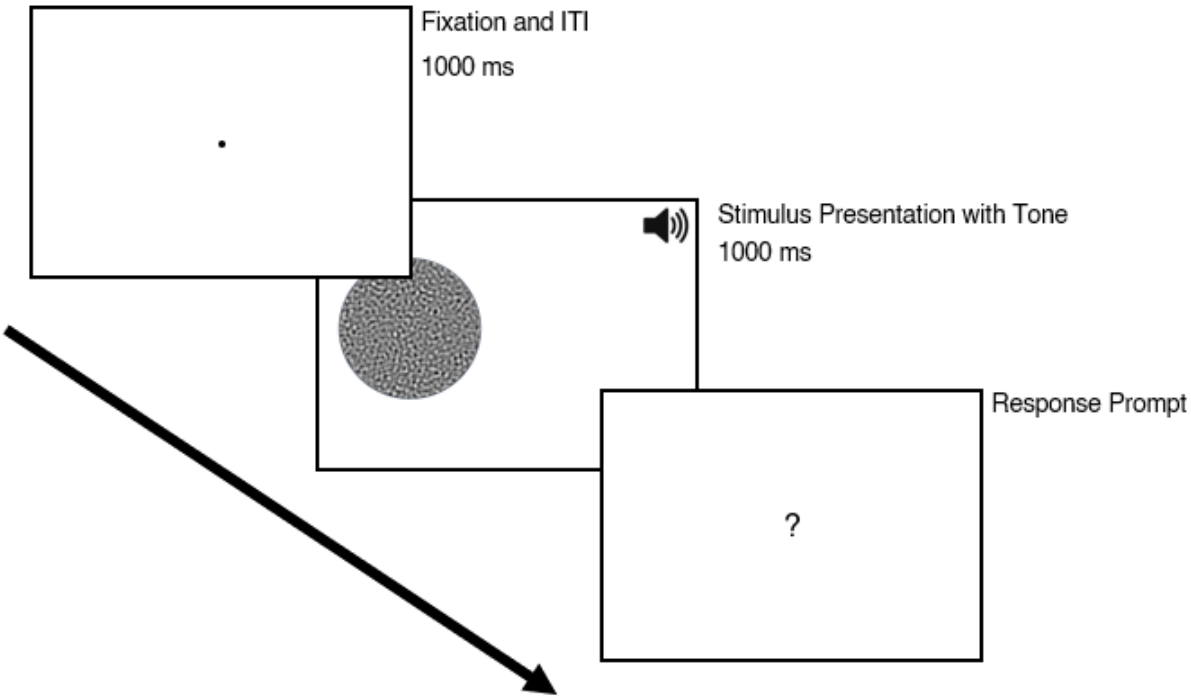

Figure 5-3. An example trial in assessing contrast sensitivity of narrowband noise, in which the stimulus was presented on either the left or right side of the fixation point, followed by an on-screen response prompt.

A tone was used to signal the beginning of each trial, thereby alerting participants to anticipate the appearance of the next stimulus presentation, even during trials where the stimulus was not visible to the participant.

In order to investigate the sensitivities of amplitude-modulated noise carriers, a two-interval forced choice (2ifc) experimental design was employed. A noise texture, with a diameter of 5° and rms contrast of 0.4 was presented during each interval through a raised cosine window on opposing sides of a central fixation point, for a duration of 1000ms. During

one interval chosen at random (p = 0.5), an AM sinusoidal grating oriented at 15°, was presented, thus altering the local contrast amplitude of the noise carrier, whilst keeping the overall luminance the same in each interval (see Figure 5-4). The frequency of the AM grating was kept constant at 0.6 cpd, equating to 3 cycles per presentation.

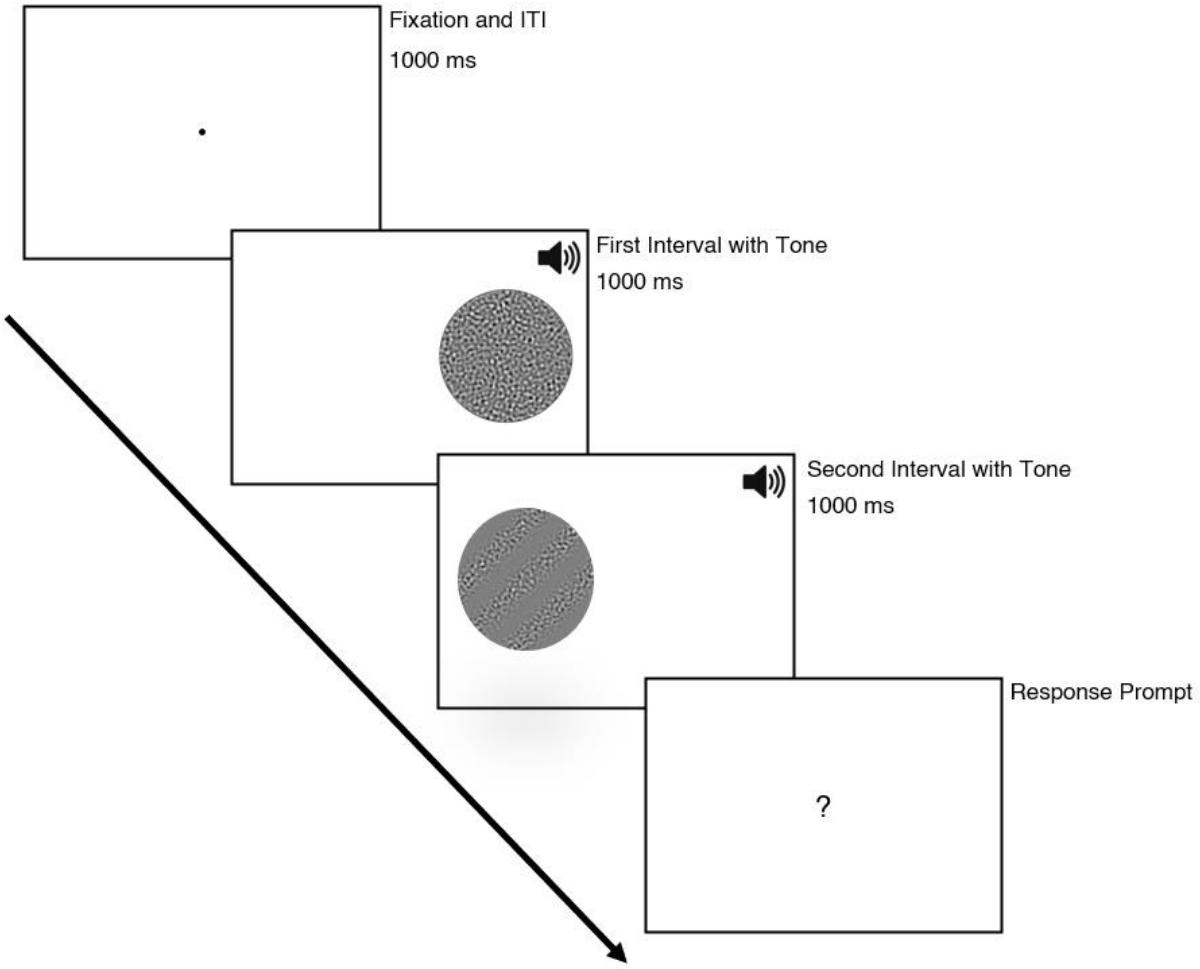

Figure 5-4. The progression of a 2ifc trial investigating sensitivity of amplitude modulations. The figure shows a stimulus being presented to either side of a central fixation point during each interval, followed by an on-screen response prompt.

Each interval was also accompanied by a tone to notify participants of a stimulus presentation. Analogous to the contrast sensitivity task, two 3D1U staircases were

employed, where AM strength was varied to estimate thresholds based off the last 8 reversals.

5.3.2 Results

5.3.2.1 Contrast Sensitivity of Narrowband Noise Textures

The findings from the task looking at contrast sensitivity of noise textures indicate that as spatial frequency increases, sensitivity declines (refer to Figure 5-5). Post hoc tests revealed for the younger adults, mean threshold estimates (± standard error) did not significantly differ ($p > 0.05$) in all conditions. In the 4 cpd condition, a threshold of 0.06 (± 0.39) was reported, this increased to 0.082 (± 0.046) in the 8 cpd condition, and a further increase to 0.086 (± 0.047) in the 12 cpd condition. However, the older adults demonstrated a pronounced rise in thresholds from 0.036 (± 0.038) in 4 cpd to 0.152 (± 0.045) in 8 cpd ($p < 0.001$), and a further increase to 0.359 (± 0.046) in the 12 cpd condition ($p < 0.001$).

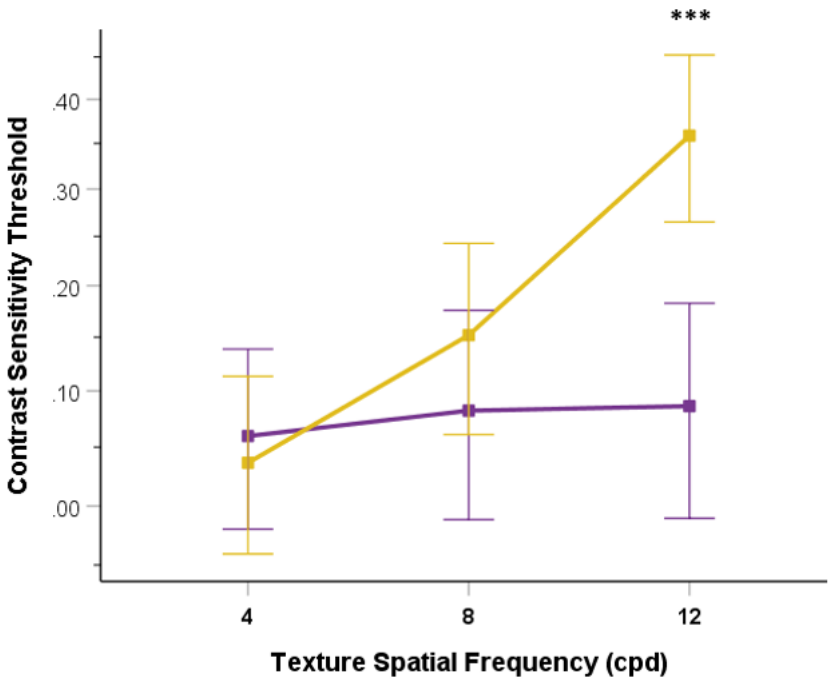

Figure 5-5. Group average of contrast sensitivity thresholds for younger adults, indicated by the purple line, and for older adults, represented by the yellow line as a function of noise texture spatial frequency. Note. *** denotes a significant difference between group means ($p < 0.001$).

It was concluded that age group influenced the sensitivity of the noise textures, especially when the noise texture presented was a fine-grained texture as in the 12 cpd condition. Here, younger adults demonstrated a slight change in sensitivity, whereas older adults experienced a significant drop in sensitivity, $F(1.17, 38.68) = 12.49$, $p < 0.001$, partial $\eta^2 = 0.275$. Furthermore, significant differences in sensitivity between the two age groups was only found in the 12 cpd condition ($p < 0.001$).

5.3.2.2 Amplitude Modulation Sensitivity as a Function of Carrier Spatial Frequency

Findings from the amplitude modulations sensitivity task also demonstrated that as the spatial frequency of the noise carrier increased, the older adults exhibited a decrease in sensitivity, resulting in raised thresholds (see Figure 5-6). Greatest sensitivity for older adults was observed at 4 cpd. Mean threshold estimates (± standard error) were 0.181(± 0.008) which increased to 0.272 (± 0.041) at 8 cpd (n.s., $p > 0.5$) which then further rose to 0.442 (± 0.056) when the carrier spatial frequency was presented at 12 cpd ($p < 0.001$). Younger adults presented a differing trend, where thresholds did not significantly differ ($p > 0.05$), thresholds in the 4 cpd condition were slightly elevated at 0.161 (± 0.008), with a minimal increase in threshold at 0.141 (± 0.041) in the 8 cpd condition, with similar threshold averages in the 12 cpd condition at 0.135 (±0.057).

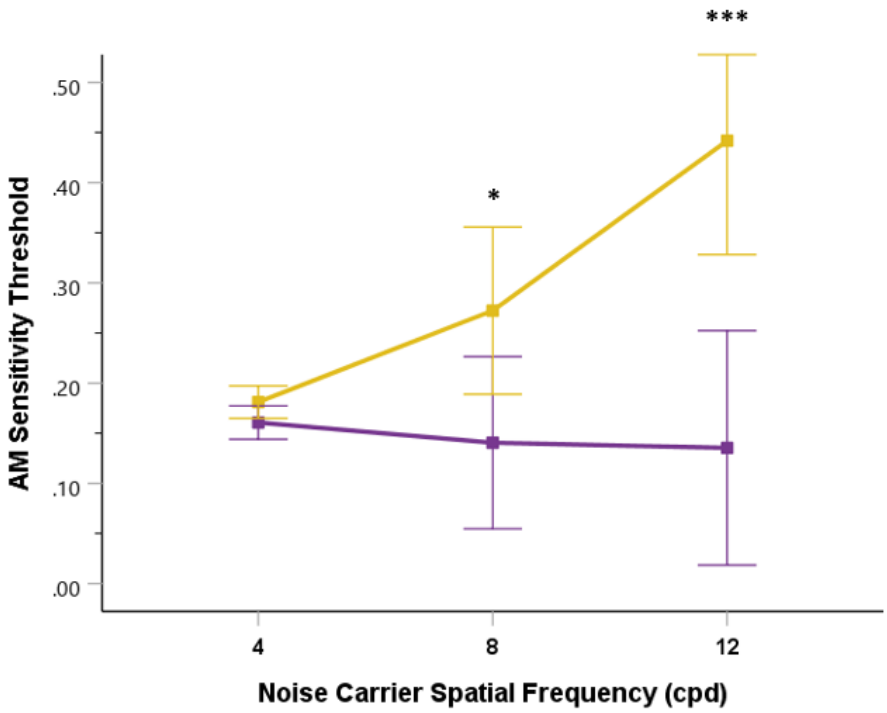

Figure 5-6. Amplitude modulation sensitivity thresholds for younger (purple) and older (yellow) adults as a function of the spatial frequency of the noise carrier. Note. * denotes a significant difference between age-group means ($p < 0.05$), and *** $p < 0.001$.

The observations illustrated in Figure 5-6 suggest a strong effect of older age on amplitude sensitivity, particularly when presented with high spatial frequencies, whereas younger age is associated with greater sensitivity for fine grained textures compared to older adults, $F(1.59, 52.23) = 10.87$, $p < 0.001$.

5.3.3 Discussion

5.3.3.1 Deteriorated contrast sensitivity in older adults at high spatial frequencies

This pattern of results in the contrast sensitivity task is consistent with the CSF which indicates a peak in sensitivity around 4 cpd for adults, followed by sensitivity decreases for lower and higher spatial frequencies. The effects of age and perception of higher spatial frequencies on contrast sensitivity is a central theme in this experiment where a significant reduction in sensitivity was observed for older adult. This assertion of specific losses in age-related sensitivity are supported in the literature, especially at high spatial

frequencies(Owsley, 2011; Owsley et al., 1983; Robson, 1966) . The perceptual difficulty was shown at 12 cpd for older adults, and differences in sensitivity between the two age groups were significant. This decline in sensitivity at higher spatial frequencies is understood to be due to physiological changes in the eye due to ageing or changes in neural processing within the visual system, which leads to decreased neural efficiency or heightened internal noise (Allard & Faubert, 2006; Elliott, 1987; Yan et al., 2020).

5.3.3.2 Consequential decline in amplitude modulation sensitivity for older adults

Older adults displayed a significant decrease in AM sensitivity thresholds in line with increases in carrier spatial frequency, a pattern reminiscent of the one observed for contrast sensitivity thresholds. In contrast, younger adults' sensitivity remained stable across all conditions, which deviates from previous studies that assessed AM thresholds concerning carrier spatial frequency.

While it could be posited that AM sensitivity is linked to the carrier's sensitivity, suggesting that diminished visual sensitivity results in lower AM sensitivity, this does not entirely account for the marked degradation observed in older adults at higher carrier frequencies. The significant sensitivity differences between age groups at 8 and 12 cpd imply that poorer perception of the carrier cannot fully explain the thresholds measured at these levels when differences are only observed at 12 cpd for contrast sensitivity. This may be due to ageing-related cognitive changes that exacerbate AM perception sensitivities observed in older populations.

A decline in contrast sensitivity and amplitude modulation (AM) sensitivity among older adults, especially notable at higher spatial frequencies was observed. This has important implications for the subsequent paired comparisons study. Given that older adults exhibit such a marked reduction in sensitivity of the carrier, amplitude modulation, which is intrinsically reliant on noise as its carrier, will also be less perceivable. Therefore, to ensure an adequate comparison across age groups, the AM levels were set higher for older adults in the paired comparison study for depth judgements.

This finding underlines the significance of adjusting experimental conditions in research involving different age groups, particularly when it concerns vision and perceptual tasks. Given that these results highlight age-related decline in sensitivity, they justify the need for appropriate adjustments to cater to the perceptual differences between age groups.

Following this rationale, the paired comparison study was designed to provide a comparative evaluation of performance and processing time across younger and older adults while considering their individual differences in perceptual sensitivity. The methods used in the paired comparison study will be detailed in the following section.

5.4 Experiment II: Paired Comparisons of Shape-from-Shading Cue Components

5.4.1 Methods

To explore the perceived depth of shape-from-shading cues, a 2afc paired comparisons task was adopted. Each trial involved a pair of horizontal gratings with different cues and compositions. The pairs of stimuli were presented as horizontal gratings containing either an LM-only, AM-only, in-phase (LM+AM), or anti-phase (LM-AM) signal. The frequency bandwidth of the noise was set to 1 octave (full width, half height), and the overall rms contrast was 0.4. The spatial frequency of the sinusoidal modulations was set to 1.0 cycles per degree, equating to 5 cycles per stimulus size.

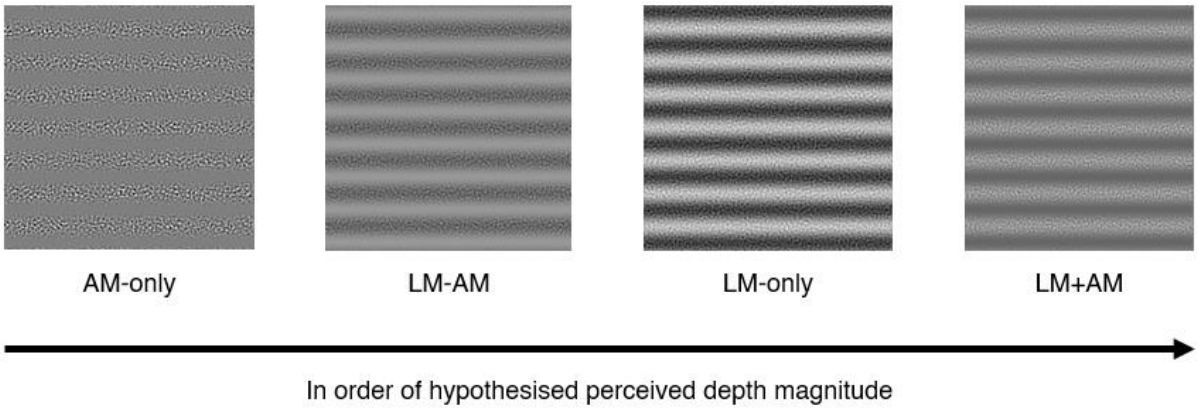

Figure 5-7. Representations of shape-from-shading cues presented in a paired comparisons task, ordered from left to right based on the perceived depth magnitude as established in prior research (Schofield, 2006).

During each trial, participants were simultaneously presented with two stimuli and made judgements based on which stimulus they perceived to have greater depth (see Figure 5-8). Stimuli were presented to either side of a fixation point until a response was recorded. Each stimulus pairing was presented 20 times in a randomised order.

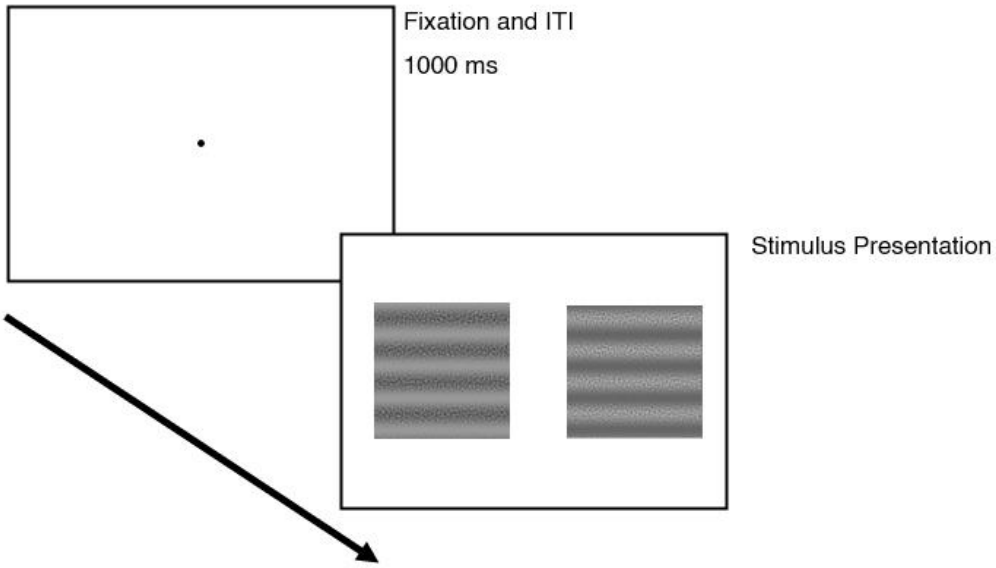

Figure 5-8. The procedure of a paired comparisons trial assessing PDM of shape-from-shading cues, whereby two stimuli are presented simultaneously for an unlimited duration until a response is recorded. In the example shown, an anti-phase stimulus (left) is presented simultaneously with an in-phase stimulus (right).

5.4.2 Analysis

Thurstonian scaling, used to assess perceived depth magnitude through paired comparisons, is based on the theoretical principles of Thurstone's law of comparative judgments. The specifics of these assumptions and case conditions were explained in Chapter 2. The experiment aligned with the assumptions of case IV, which posits that each pairing condition involves multiple independent observations without inter-condition comparisons. It also assumes that while the discriminal dispersions are not equal, they are similar and uncorrelated. Given these characteristics, case IV was deemed most appropriate for the analysis.

The proportions of each condition pairing were transformed into z-scores using the inverse cumulative normal function. In this model, the distance between two stimuli was calculated as follows.

$$\frac{S_i - S_j = (s_i + s_j) z_{ij}}{\sqrt{2}}$$

Equation 5-1

In this equation, S_i and S_j are the scale values of stimuli i and j, s_i and s_j are the discriminal variances for stimuli i and j, and z_{ij} is the z-score for the proportion of times stimulus i was judged greater than stimulus j. Thus, taking for account discriminative dispersion. Therefore, the scale value for a given stimulus was calculated below.

$$S_i = \left((s_i \sum_k z_{ik} + \sum_k (s_k z_{ik}) \right) / s\sqrt{2}$$

Equation 5-2

5.4.3 Results

Analysis of the paired comparisons task for shape-from-shading cues utilised Thurstonian Scaling, detailed in Section 5.4.2. This method involved calculating a preference-based order from the proportions derived from each stimulus pairing in Table 5-1, whilst accounting for variances of their distributions to produce a scale.

.

Table 5-1

Summary of proportion of trials where a given stimulus was reported to have greater PDM than the paired stimulus.

	Younger Adults						Older Adults		
	Low AM Stimuli (0.2 AM depth)			High AM Stimuli (0.6 AM depth)			High AM Stimuli (0.6 AM depth)		
	4 cpd	8 cpd	12 cpd	4 cpd	8 cpd	12 cpd	4 cpd	8 cpd	12 cpd
LM+AM vs AM-only	**0.909(±0.168)*** **	**0.918(±0.221)*** **	**0.947(±0.182)*** **	**0.914(±0.192)*** **	**0.934(±0.202)*** **	**0.907(±0.220)*** **	**0.889(±0.256)*** **	**0.886(±0.239)*** **	**0.928(±0.145)*** **
LM+AM vs LM-only	0.497(±0.102)	0.482(±0.095)	0.476(±0.099)	0.500(±0.181)	**0.555(±0.107)***	0.484(±0.098)	0.531(±0.205)	0.503(±0.142)	0.522(±0.111)
LM+AM vs LM-AM	0.465(±0.107)	0.494(±0.141)	0.509(±0.071)	0.570(±0.284)	0.545(±0.221)	0.539(±0.164)	0.500(±0.265)	0.464(±0.204)	0.547(±0.183)
LM-only vs AM-only	**0.912(±0.215)*** **	**0.929(±0.202)*** **	**0.935(±0.204)*** **	**0.905(±0.172)*** **	**0.907(±0.214)*** **	**0.855(±0.302)*** **	**0.886(±0.234)*** **	**0.867(±0.258)*** **	**0.928(±0.162)*** **
LM-only vs LM-AM	0.441(±0.124)	0.491(±0.097)	0.491(±0.083)	0.545(±0.201)	0.516(±0.169)	0.498(±0.126)	0.428(±0.246)	0.417(±0.207)	0.525(±0.135)
LM-AM vs AM-only	0.503(±0.021)	0.500(±0.035)	0.512(±0.042)	**0.636(±0.218)***	**0.645(±0.259)***	**0.659(±0.261)***	0.506(±0.024)	0.483(±0.042)	0.494(±0.045)

Note. The proportion of trials where the leftmost stimulus was reported to possess a greater PDM on average than the rightmost stimulus in column 1. A proportion is close to 1.0, signifies that the stimulus was consistently selected as having greater PDM in all trials for that condition. A proportion of 0.5 indicated that the two stimuli had similar PDM for all trials in that condition. Significant deviations from 0.5 were determined using one-sample t-tests where a significance level of *$p < 0.05$, and ***$p < 0.001$ are in bold and asterisked.

The raw proportions in Table 5-1 revealed patterns regarding the PDM across different stimuli. In-phase luminance-modulated and amplitude-modulated (LM+AM) gratings and LM-only gratings were perceived as having more depth than AM-only stimuli. This suggests that both LM+AM and LM-only stimuli should have higher positions on the PDM scale, whereas AM-only stimuli should be towards the lower end.

LM-AM stimuli were perceived as having roughly equivalent depth to both LM+AM/LM-only and AM-only stimuli. This suggests that LM-AM would occupy a mid-range position on the PDM scale. However, the exact positioning is challenging to predict based solely on proportions.

When studying younger participants in high amplitude modulation conditions, it was found that LM-AM differed from the usual pattern when compared to AM-only. Specifically, participants consistently perceived LM-AM as having more depth, indicating that in these conditions, LM-AM should be placed closer to LM+AM on the PDM scale.

5.4.3.1 Highest PDM scale values observed for LM+AM and LM-only gratings.

It was highlighted in Table 5-1 that across all participants, in-phase stimuli were consistently perceived as possessing greater PDM than AM-only stimuli ($p < 0.001$) across all spatial frequency conditions. An increase in the proportions of trials “favouring” the in-phase grating, compared to an AM-only was also observed from 4 cpd to 12 cpd, this pattern was consistent among the younger adults at low AM conditions and older adults. A similar pattern of results was also observed in conditions where LM-only gratings showed significantly greater PDM than AM-only.

In addition, proportions for PDM in LM-only gratings didn't significantly differ in comparison to both LM-AM stimuli and LM+AM gratings. However, one exception was observed in younger adults in the 8 cpd condition for stimuli with high AM depth in LM+AM and LM-only pairings. LM+AM stimuli also did not significantly differ in observed PDM when paired with LM-AM gratings across all conditions. Finally, the LM-AM scale values were not

significantly different in their PDM proportions from AM-only stimuli, aside from observations in the high AM depth condition for younger adults.

To produce a Thurstonian scale using the statistical model, case IV, the smallest scale value was calculated using Equation 5-2 and provided the baseline value for the scale. The distance between each subsequent stimulus were calculated using Equation 5-2 discussed in Analysis 5.4.2. The scaling values for each condition in conjunction with Table 5-1 will now be discussed.

5.4.3.2 Addressing Scaling Plots Axes Inversion

In considering Figure 5-9 and Figure 5-10, the range of the Thurstonian scaling values should be noted on the y axis. These figures present scale values ranging from 0 to -1.4, in contrast to the 0 to +1.3 range of scaling values in Figure 5-11. This inversion can be traced back to some key observations in the data. Specifically, small variances between some proportions of stimulus pairings for young adults in the low AM condition, and for older adults. Meanwhile, in other conditions, much larger variances were observed. It was hypothesised that these large imbalances in variances could impact the scale values. This arose from the Case IV's incorporation of variances for all stimuli pairings to calculate each data point. Most notably, case IV specified that these differences are assumed to be not equal but similar in size, which is not true for these datasets.

To investigate whether large differences in variance was producing the inversion of the scale values, an additional analysis was carried out. This involved removing all pairings with the stimulus that produced these small variances from the dataset, which was determined from Table 5-1 as LM-AM. Scale values were then calculated from the remaining stimuli pairings. The results of this reanalysis confirmed that without LM-AM stimulus the scaling values did not invert, and furthermore the order of the scale values was consistent to the order in Figure 5-9 and Figure 5-10.

5.4.3.3 Increased preference for stimuli containing LM and an overall reduction in variability at high spatial frequencies among older adults.

As highlighted in Table 5 1, a complementing pattern of results was illustrated in Figure 5-9 for older adults, whereby LM+AM and LM-only were perceived as having most depth for older adults. The scaling plots in the Figure 5-9 suggest that both AM-only and LM-AM gratings were perceived to have the least depth. Despite variations across spatial frequencies, the proportions presented in Table 5-1 indicate no significant differences in observed PDM between these two gratings. Another observation made from Figure 5-9 suggests that high spatial frequencies (12 cpd) led to increased depth judgements for stimuli containing an LM signal. However, reduced differences between the three stimuli containing an LM cue were also observed at 12 cpd (LM-only, LM+AM, and LM-AM). A further observation made from Table 5-1 showed that older adults exhibited reduced variability in the 12 cpd condition.

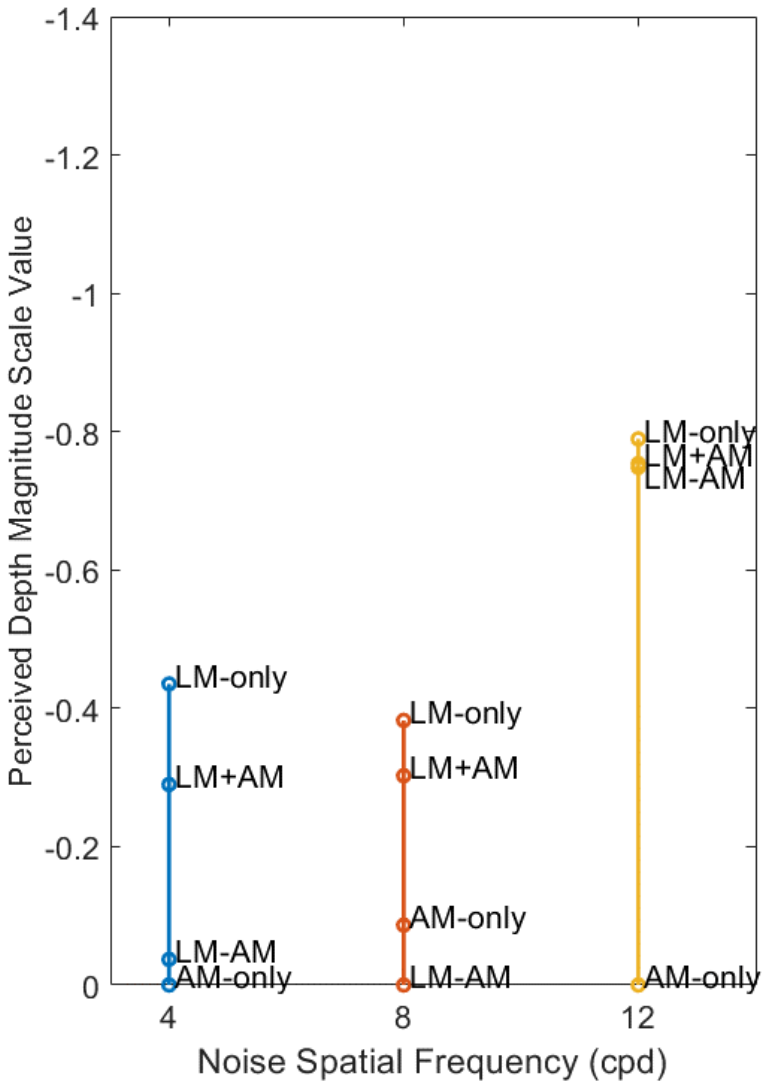

Figure 5-9. Thurstonian scale values for older adults for stimuli with an AM cue at a depth of 0.6, i.e., 60%. These scale values illustrate the perceived depth magnitude of each stimulus.

Big differences were observed between LM+AM and LM-AM at 4 and 8 cpd, but not at 12 cpd. At 4 and 8 cpd, LM-AM ranks at the bottom of the scale, whereas at 12 cpd, it aligns at the top with LM+AM. This pattern emerges when older adults struggle to perceive the AM cue clearly, reducing its influence and rendering all stimuli containing an LM cue similar.

5.4.3.4 Lower AM cues increase differences but reduce PDM of LM+AM signal

The findings in Figure 5-10 represent the distribution of scale values for younger adults for stimuli with a low AM cue (AM depth = 0.2). A contrasting pattern of results was observed whereby the scale values were notably more dispersed by comparison to Figure 5-11, suggesting larger observed differences between stimuli. A similar observation was also observed in Table 5-1.

which shows that the proportions for stimuli pairings generally deviate more from the central value of 0.5, when compared to younger adults in the high AM condition.

Moreover, these scaling plots exhibit similarities with those of older adults, in terms of marked differences in scale plots between LM+AM and LM-AM at 4 and 8 cpd. The younger adults, however, do not experience the loss of AM sensitivity at 12 cpd. As a result, the LM+AM and LM-AM scaling plots remain distinct at this frequency.

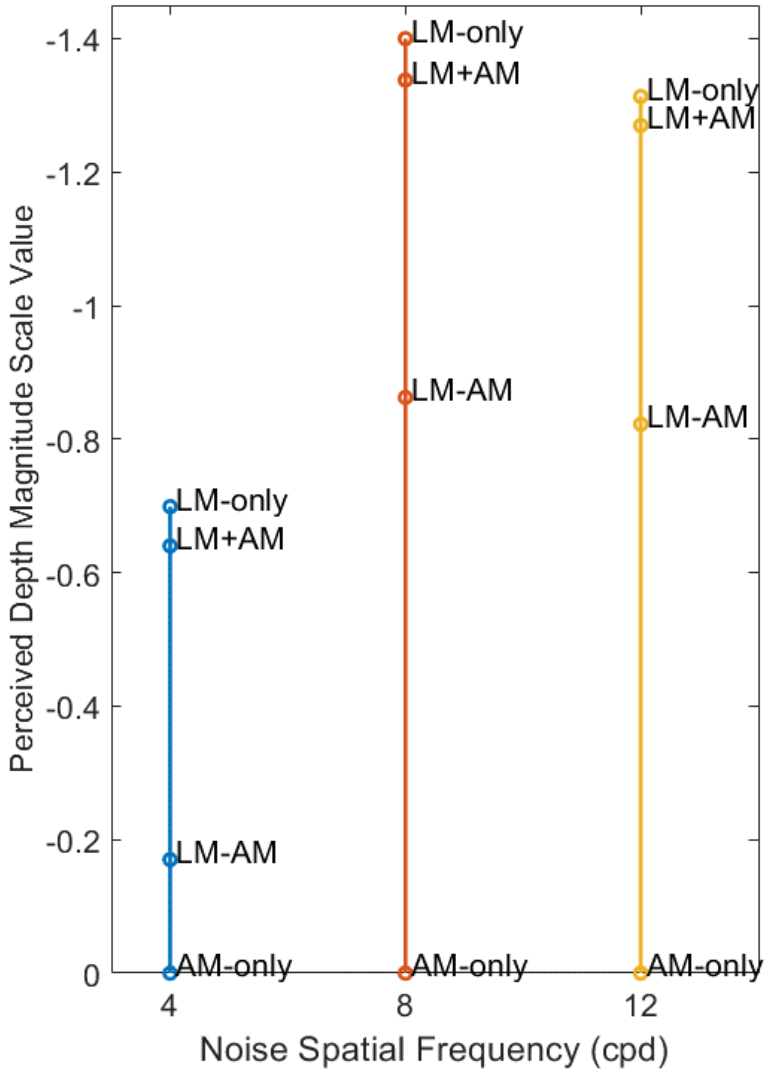

Figure 5-10. PDM Scaling values for younger adults for judgements made in the low AM condition.

The scaling plot suggests that that LM-only stimuli were perceived has having highest PDM. The scale values for LM+AM stimuli remained consistently lower than LM-only cues, where proportions range between 0.476 to 0.497. Furthermore, proportions for LM-only and LM+AM stimuli were not significantly different. It was also observed that AM-only gratings were reported to have the lowest PDM scale values, a trend which held across all three spatial frequency conditions. The scaling plots also show a relationship between

carrier spatial frequency and PDM scale values where plots were more dispersed in the 8 and 12 cpd conditions than in the 4 cpd condition.

5.4.3.5 LM+AM stimuli exhibit greater PDM for younger adults at intermediary carrier spatial frequencies with a high AM component.

Figure 5-11 summarises PDM scale values for younger adults observing stimuli with a matched AM intensity to the older adult condition (AM depth = 0.6). Here, the scale values for LM+AM stimuli indicate that younger adult perceived this to have greater PDM than other stimuli, with LM-only stimuli ranked second in the scale. When consulting Table 5-1, a significant difference between LM+AM and LM-only cues was observed in the 8 cpd condition, whereas conditions with a lower or higher carrier spatial frequency did not elicit this distinction. A further distinction was observed for younger adults in Table 5-1 between AM-only and LM-AM gratings, whereby an anti-phase stimulus was reported to possess significantly greater PDM ($p < 0.05$). Figure 5-11 further exemplifies that AM-only stimuli in the study were perceived with minimal PDM across all spatial frequencies.

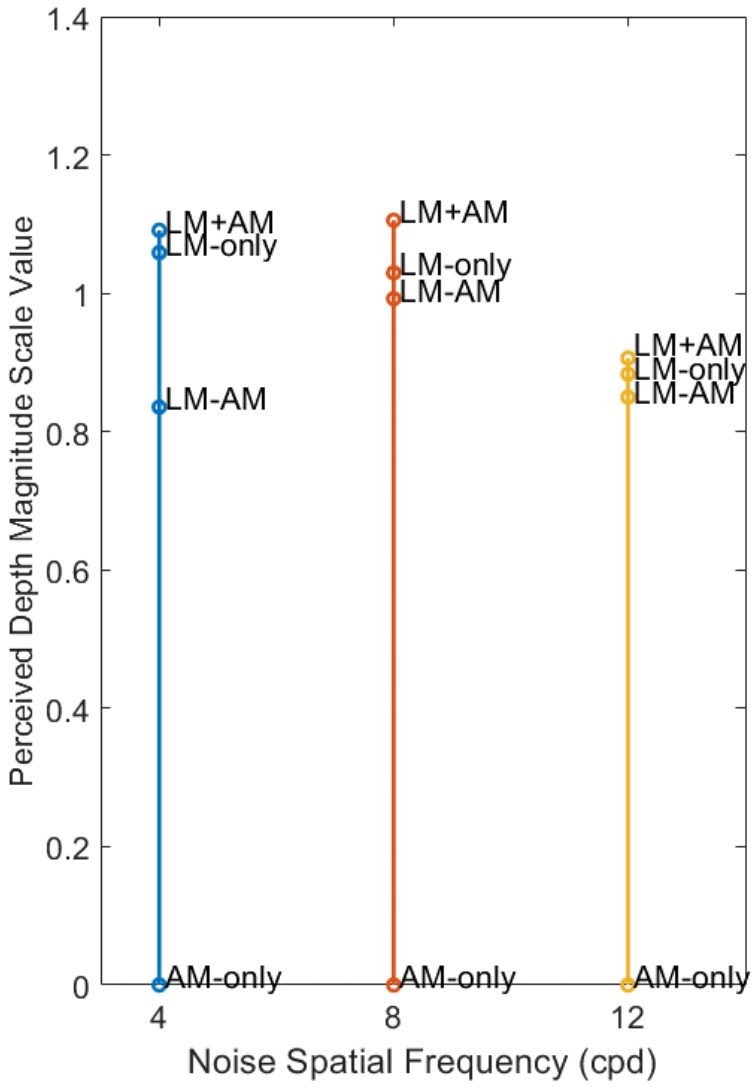

Figure 5-11. Scaling values for the perceived depth magnitude of stimuli with a high AM depth component (0.6) viewed by younger adults.

It was also observed in Figure 5-11 that PDM of each stimulus changed as spatial frequency changed. The difference in scale values for stimuli containing an LM component appear to diminish as spatial frequency increases, which is illustrated by the compression of plots correlating to LM+AM, LM-only and LM-AM gratings.

5.5 Discussion

In the present study, the perception of depth magnitude in different stimuli was examined. This was achieved by exploring the contributing factors to depth perception through shape-from-shading by examining LM and AM cues independently and how the perception of these cues may vary with age. Furthermore, the masking of shape-from-shading cues was further investigated through the interaction of spatial frequency and cue strength on PDM. To investigate this, gratings were displayed simultaneously but spatially independent. In this series of paired comparison tasks, the spatial frequency of the noise texture was manipulated, and the strength of the amplitude modulation (AM) cue was adjusted, specifically targeting younger adult participants. The effect of age on sensitivity of amplitude modulations and visual textures was also examined through a series of detection tasks where the spatial frequency of the noise texture was manipulated for both age groups to estimate their respective sensitivities.

5.5.1 LM+AM and LM-only shading cues possess greatest PDM, independent of age and spatial frequency

One key finding showed a consistent heightened perceived depth for LM+AM and LM-only shading cues, irrespective of carrier/texture spatial frequency. For older adults the LM-only stimulus was perceived to have more depth than an LM+AM grating, suggesting that older adults utilise LM cues to interpret depth more so than AM signals. This pattern of findings was also present for younger adults in the low AM condition. These findings contrast with previous research that determined LM+AM cues as possessing greater PDM than LM-only cues (Schofield et al., 2006). Furthermore, AM-only stimuli were reported to possess the lowest PDM across all conditions for both younger and older adults. This finding aligns with previous research which posits that an AM cue in isolation fails to generate a robust depth cue (Schofield et al., 2006). And lastly LM-AM gratings were consistently perceived to have lower PDM than LM+AM and LM-only stimuli, further corroborating observations from

real-world imagery that suggest an anti-phase relationship between LM and AM signals, are spatially coincident with a change in texture rather than depth (Schofield et al., 2006).

It was observed that as spatial frequency increased, the PDM for each stimulus changed, further affirming the link between carrier spatial frequency and perceived depth. Furthermore, as previously discussed, the percept of depth is usually conveyed through a change in local mean luminance, which is strengthened with spatially coinciding with a change in local mean amplitude in an image (Johnson & Baker, 2004; Kingdom, 2003; Sun & Schofield, 2011). The combination of two gratings spatially coincident was found to enhance PDM depth judgments and therefore would accentuate the PDM of an LM+AM oblique when juxtaposed with an LM-AM oblique (Schofield et al., 2006). In contrast, spatially independent gratings were reported to possess reduced discrepancies for PDM overall. As suggested in previous research, single obliques resulted in less distinction in PDM scale values between LM+AM and LM-only cues (Schofield et al., 2006). Therefore, it was concluded that these differing results could be attributed to the spatially independent presentation of the stimuli. This expands on the findings of Schofield et al. (2006) which suggested that when both LM+AM and LM-AM stimuli are presented at separate temporal intervals, the resulting perception of depth appears flatter compared to a single stimulus composed of two opposing gratings. In this investigation, we presented both LM+AM and LM-AM stimuli within the same temporal window but as distinct gratings and found that despite the same temporal presentation of these gratings, flattened perception persisted for both age groups, suggesting that the spatial coincidence plays more of a key role than temporal coincidence.

However, this fails to fully explain the changes in scale value order for PDM in the current dataset. When consulting Table 5-1, the scale values do not align with LM+AM/LM-only pairing proportions observed among older adults. Therefore, it was speculated that while these differences are apparent in the scaling plots, the visual differences in terms of

PDM were negligible and therefore differences in scale values between LM+AM and LM-only shape-from-shading cues were likely attributed to high variances for older adults.

5.5.2 Modulation of visual textures facilitate and mask depth cues for younger adults

Increased PDM was observed for LM+AM and LM cues when presented with a carrier at 8 cpd for younger adults. This increase could be substantiated when examining the contrast sensitivity function as discussed in Chapter 1. It was posited that peak performance for adults usually lies around 3-5 cpd, where sensitivity begins to attenuate beyond 10 cpd. This is supported by the threshold estimates from the contrast sensitivity detection task in the study, where sensitivity for younger adults remained steady with a marginal, non-significant reduction in sensitivity as noise spatial frequency increased, suggesting peak sensitivity. This pattern is mirrored in the younger adult dataset for high AM stimuli where increased PDM was observed at 8 cpd, while at 12 cpd, there is a reduction in PDM, as reflected in their scale values. This reduction underscores the notion that noises textures facilitate depth perception, as opposed to masking. These findings align with research that examines the use of noise textures in enhancing perception as discussed in Section 3.1.2 where additive noise enhanced sensitivity of depth cues for LM stimuli (Schofield & Georgeson, 1999). Although additive noise reduced sensitivity thresholds, when spatial frequencies contained within the carrier fell within 0.5 octaves of the modulation frequency, this could in turn mask the cue (Legge & Foley, 1980). The observed masking effect might elucidate the unexpected pattern of results for younger adults which reported lower PDM values at 4 cpd than higher spatial frequencies, despite falling within the hypothesised peak sensitivity range. If a masking effect was present in the 4 cpd condition, it could be attributed to some similarities between the signal frequency (1 cpd), and a noise central spatial frequency of 4 cpd (full-width half-height). Although the spatial frequencies of the noise and texture do not coincide to the extent of 0.5 octaves, it is plausible that some form of

interaction could occur between the noise and the texture, resulting in masking of the depth cue.

5.5.3 Does ageing affect shape-from-shading perception?

Upon examination of the scaling plots for older observers, minimal differences are noticeable in the 12 cpd condition between gratings containing an LM cue. Additionally, contrasting findings were observed between young and old adults in the two detection tasks. Specifically, a significant difference in threshold estimates was reported in the 12 cpd condition between age groups, indicating a significant reduction in contrast sensitivity for older adults at high spatial frequencies. Furthermore, sensitivities to amplitude modulations identified a significant difference between groups for thresholds in the 8 and 12 cpd conditions. This observation led to the conclusion that first-order sensitivities impact second-order modulations in amplitude.

When the sensitivity of the carrier is diminished, it results in diminished amplitude modulation perception, consequently leading to poorer judgments of PDM. This implies a reliance on the LM cue, notwithstanding the capability to use other depth cues when the carrier frequency is within the peak sensitivity range for older adults. This observation is in support of previous research suggesting that amplitude modulation affects the perceived depth magnitude of stimuli (Schofield et al., 2006). This furthers our understanding of age-related differences in depth perception, underscoring the interaction between first- and second-order sensitivities and the subsequent implications these relationships may have on the perception of depth.

5.5.4 When modulation depth is increased, there is reduced preference between LM+AM and LM-only stimuli

When examining scaling values for younger adults in the high AM depth condition, a distinct pattern of results was noted where the PDM of stimuli was reduced in comparison to scaling plots in the low AM condition. Furthermore, the dispersion of scaling values was

reduced in the high AM condition. This pattern of results was likely a result of interference from the high AM signal in shape-from-shading perception. Research by Schofield and Georgeson (1999) posits that for the AM signal to contribute to realistic depth perception, it must be near sensitivity threshold. Insights into amplitude modulation sensitivity in the present study suggest that thresholds for younger adults ranged from 0.161-0.135, in the high AM condition an AM intensity of 0.6 was used, a marked elevation from sensitivity threshold. Therefore, this finding strengthens the notion that only stimuli with AM signals near threshold provide accurate depth perception using shape-from-shading. This was the case for both older adults and younger adults in the low AM condition.

5.5.5 Considerations

In the case of the older adult dataset, one potential consideration could be that the threshold estimates for AM sensitivity had high variability across all conditions, and the AM depth employed for the paired comparisons task was not sufficiently close to sensitivity thresholds for many participants. Mean sensitivity thresholds ranged from 0.181 and 0.442 whereas an AM intensity of 0.6 was implemented in the paired comparisons task. Initially, the AM intensity was intended to be slightly elevated from threshold, however a large variance in AM threshold values across spatial frequencies for older adults meant AM intensity was most likely not optimal for the shape-from-shading judgements task. Therefore, the paired comparisons task should employ a lower AM intensity for older adults in future research. Moreover, reconsidering a constant AM intensity across conditions could be beneficial, where instead, adjusting the AM signal strength tailored to each observer's AM sensitivity thresholds could provide deeper insights into how visual textures interact with the noise.

Employing a stimulus containing an AM cue significantly elevated from sensitivity thresholds is thought to interfere with a depth cue, giving rise to visual scuffing which could manifest as irregular or degraded perception of the stimulus. It could be that interference or distortion of depth perception occurred for some older adults due the strong AM cue,

resulting in a perceived roughness or "scuffing" of the stimulus in the paired comparisons task. This was evidenced in our younger adult group, where the PDM was heightened when the AM depth cue was low. However, high AM depth cues resulted in lower PDM, and less discrepancy between stimuli, suggesting an interference with shape-from-shading depth cues. It remains uncertain if this was also the case for the older adults, but it is a potential consideration in understanding why the scaling values were constrained despite the visibility of the carrier and amplitude modulations.

5.5.6 Conclusions

In conclusion, the present study contributes to a more nuanced understanding of the interaction between first- and second-order sensitivity, and how these factors may influence depth perception. It was concluded that first-order sensitivities directly impact second-order modulations in amplitude, further supporting the interaction of these two processing channels. Moreover, these sensitivities shed light on the age-related differences in depth perception, highlighting that the visibility of an AM signal alone does not directly influence sensitivity of shape-from-shading. Instead, the combination of first- and second-order signals appears to be crucial for depth perception. This suggests that additional cognitive processes beyond detection are likely to be a factor. The findings indicated that while an AM cue alone might not be strong enough to produce a potent depth cue, a combination of in-phase LM and AM signals in a grating enhanced depth perception in both younger and older adults, whereas anti-phase LM and AM signals did not. This enhancement, however, was susceptible to degradation when AM signal intensity was markedly suprathreshold, interfering with depth perception.

In summary, further exploration into mechanisms underlying depth perception is required, particularly on how first- and second-order vision interact. Moreover, the role cognition plays in depth perception required further interrogation. By doing so, we can gain further insight, not only into the processes involved in depth perception through shape-from-shading, but also how the natural ageing process influences these mechanisms. This

understanding is critical in creating more effective interventions and solutions for age-related visual impairments.

6 The effects of age-related changes on shape-from-shading depth perception

In this chapter, the effects of age on second-order vision were investigated, specifically, how the loss of first-order and coarse-scale second-order sensitivity can affect how we perceive shape-from-shading. To investigate this, observers completed an orientation discrimination task along with tasks assessing luminance (carrier) and amplitude modulation sensitivity across a range of spatial frequencies. These tasks were employed to assess sensitivities to stimuli that compose a shape-from-shading cue and how they might influence depth perception. Performance in the carrier sensitivity and amplitude modulation task did not predict performance in the shape-from-shading orientation discrimination task. This implies that shape-from-shading perception is not necessarily a direct consequence of detection thresholds of luminance and amplitude modulations, suggesting that other factors may pay a crucial role in how we perceive shape-from-shading.

6.1 Introduction

Thus far, it has been discussed how shape-from-shading can be created artificially by modulations in luminance, amplitude, or luminance and amplitude together (Schofield et al., 2006). Furthermore, chapter 5 demonstrated that by manipulating noise textures, low frequency modulations can be introduced to an object, simulating changes in shape or texture (Schofield et al., 2017). Previous studies investigating the statistical properties of images discovered a strong relationship between changes in illumination and changes in local luminance and amplitude of a surface (Kingdom, 2008).

In Chapter 5, it was concluded that single grating stimuli with LM+AM and LM-only cues were perceived as having the greatest depth. It was also observed that older adults rely more on LM cues than AM cues, potentially due to reduced sensitivity of AM cues with

intermediate and high spatial frequencies. Chapter 6 builds on this by using sinusoidal plaids in an orientation discrimination task. This allows for a more detailed examination of AM depth modulation and enables the measurement of sensitivity of shape-from-shading stimuli and correlate contributing visual factors. Overall, these chapters aim to provide a comprehensive understanding of shape-from-shading perception using first- and second-order signals, and how these sensitivities change with age.

6.1.1 Sinusoidal plaids as an investigative measure of depth perception

Sinusoidal plaid patterns are used in psychophysical studies to determine whether impaired second-order vision also reduces depth perception via shape-from-shading (refer to Figure 6-1). Observers' sensitivity of shape-from-shading was assessed using an in-phase LM and AM modulated grating, which was paired with opposing anti-phase relationship on the oblique. The presence of two obliques in a single configuration strengthens the signal of each oblique so that it is possible for the viewer to discriminate between changes in shape and material changes, wherein an in-phase grating will appear to have greater depth when paired, in a plaid, with an anti-phase grating (Schofield et al., 2006).

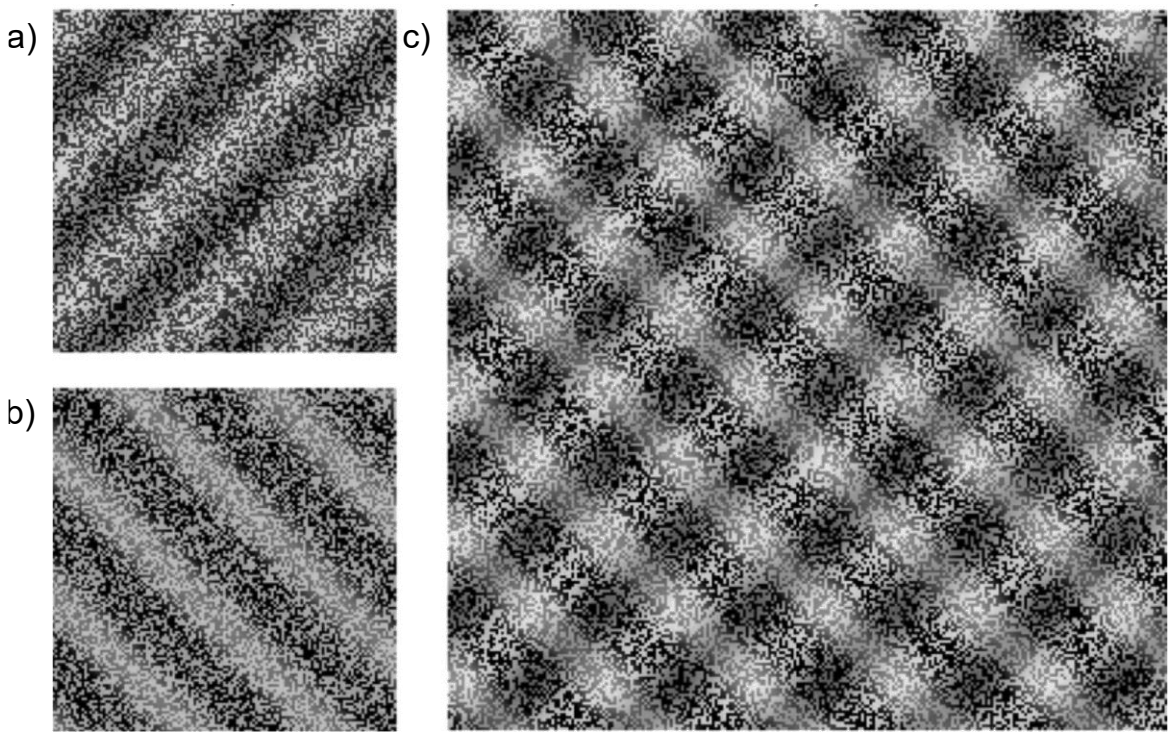

Figure 6-1**.** The spatial correlation between LM and AM components used to create a sinusoidal plaid. (a) depicts an in-phase, positively correlated grating of LM and AM (LM+AM). (b) demonstrates a negative correlation for these two components (LM-AM). (c) shows a plaid arrangement involving both LM + AM on the right oblique, and LM – AM on the left. Note. Reprinted from "What is second-order vision for? Discriminating illumination versus material changes" by Schofield, A. J., Rock, P. B., Sun, P., Jiang, X., and Georgeson, M., 2010, Journal of Vision, 10(9), p.6.

Figure 6-1 depicts the modulation of a broadband noise carrier which was employed in a stimulus to create two gratings arranged in a plaid. As a result, discrimination tasks provide a means to measure sensitivity of shape-from-shading while controlling potential artefacts stemming from localised feature detection (Schofield et al., 2010). Judgements on the PDM of highlighted locations within each stimulus revealed that when combined with LM + AM in a plaid format, LM - AM appears flat, but it appears corrugated when shown separately. At low AM modulation depths, the PDM for both LM - AM and LM + AM were similar. Plaid stimuli with little or no AM signal display an ‘egg box’ appearance, which led to

a reduced PDM average, therefore supporting the notion that an AM modulation enhances the percept of depth and enables the discrimination of shape and material changes.

These findings support the notion of separate processing streams for visual cues where LM and AM signals are independently detected at sensitivity threshold. However, Schofield et al. (2010) postulate a shading channel model where summation occurs at the stage after detection to disambiguate luminance cues. The model additively combines LM and AM responses within a particular orientation or frequency band. These pooled responses are then coordinated across different orientations. The outcome is a shading signal which is strengthened when AM is in-phase with LM. However, the shading signal weakened significantly when an anti-phase combination of LM and AM is presented in a plaid configuration alongside an LM + AM component.

6.1.2 Introduction to the study

The effects of ageing on vision are a complex interplay of factors. A decline in sensitivity of carrier signals, a reduction in the sensitivity of second-order vision, or a combination of both could contribute to these effects, particularly in complex tasks. As second-order stimuli inherently possess greater complexity, they demand further processing, potentially making them more susceptible to age-related impairments (Owsley, 2011)

Concurrent to the aims of chapter 5, this study sets out to explore whether a decline in carrier visibility is a consequence of age-related sensitivity loss, and how this decline impacts shape-from-shading perception. It was hypothesised that as the carrier frequency increases, older adults will exhibit greater impairments in carrier visibility, and similar impairments will manifest for second-order visibility. The study aimed to corroborate the idea that sensitivities in discerning shape-from-shading are tied to the visibility of carrier signals, the visibility of course-scale second-order components, and the subsequent effects of task complexity.

6.2 Methods

6.2.1 Stimuli

Isotropic noise was presented with three central spatial frequencies, 4 cpd, 8 cpd and 12 cpd. The frequency bandwidth of the noise was set to 1 octave (full width, half-height), and the overall rms contrast was 0.4. The spatial frequency of the sinusoidal modulations was set to 0.5 cycles per degree, equating to 5 cycles per stimulus size. The noise was modulated by LM, AM, and combinations of both. As stated in the General methods section 2.1.2, LM results in additive noise, while AM applies multiplicative noise.

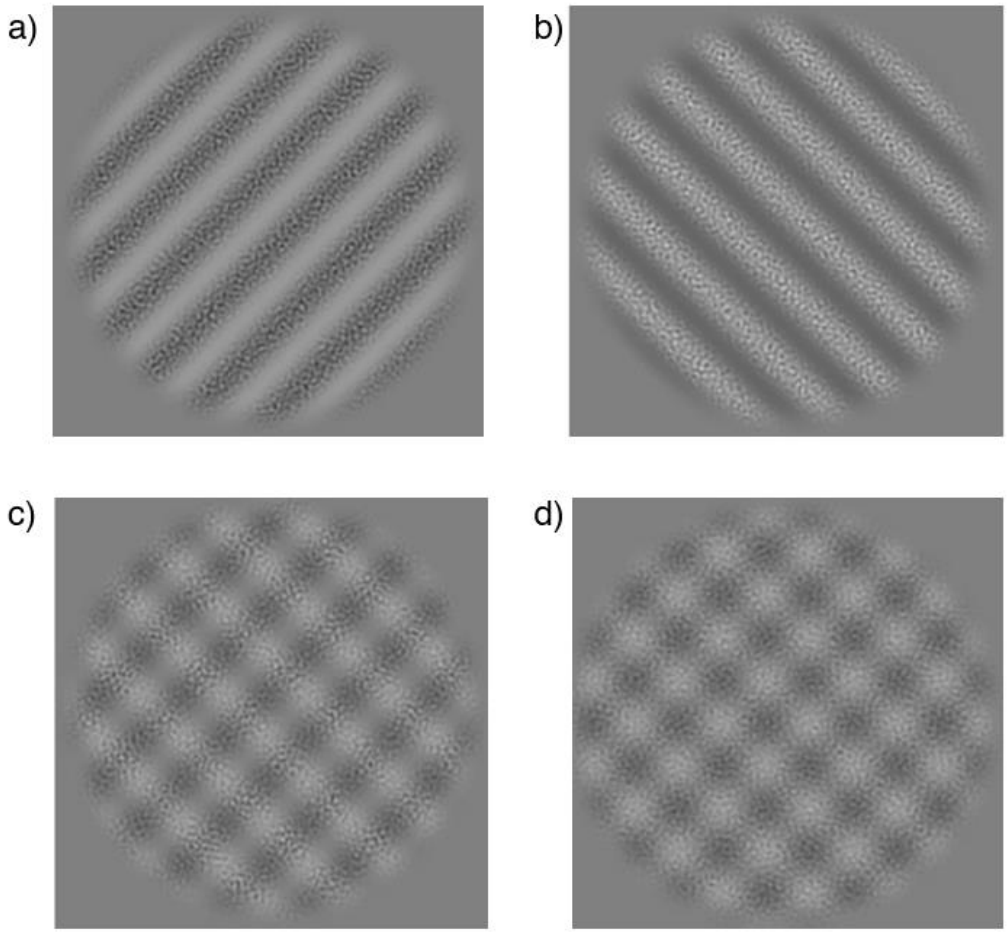

Figure 6-2. Stimulus components used to create the sinusoidal plaid with an isotropic noise carrier a) an anti-phase sinusoidal grating (LM-AM), b) an in-phase sinusoidal grating (LM+AM); a combination of in-phase and anti-phase grating components to form a sinusoidal plaid, with an in-phase grating at a 45° orientation and an anti-phase grating at a 135° orientation; c) an instance of high AM modulation depth (1.0), and d) an instance of low LM modulation depth (0.1).

The plaid orientation discrimination task used a sinusoidal plaid which consisted of two perpendicular, compound gratings, each presented on the oblique angle (Schofield et al., 2006). The average luminance of the noise pattern was modulated to create a luminance modulated grating (LM). The amplitude of the noise components was modulated such that the contrast of the elements varied between low contrast and high contrast to create an amplitude-modulated grating (AM) (see Figure 6-2). One grating consisted of in-phase (LM+AM) sinusoidal wave modulations of LM and AM, where a high amplitude measure

occurred simultaneously with a high luminance measure to simulate reflectance of the visual texture's surface.

The second grating component was composed of anti-phase (LM-AM) sinusoidal modulations (see Figure 6-2). This anti-phase component was constructed so that the high amplitude modulation of the noise pattern coincided with the location in the grating where the luminance was low, i.e., out of synchrony or phase by 0.5 of a cycle. The in-phase and anti-phase components were presented at 45° and 315°, randomly assigned for each trial. The absolute phase for each oblique was randomised to prevent participants from detecting the in-phase component by determining the wave phase at the edge of the window.

The noise component in the contrast- and amplitude modulation sensitivity task had an overall diameter of 5° multiplied with a raised cosine window. In the AM sensitivity task one noise carrier was multiplied by an amplitude-modulated sinusoidal grating orientated at 15° with a modulation frequency of 0.6 cpd, completing roughly 3 cycles in the stimulus size. Similarly, the rms contrast was set at 0.4, and the central spatial frequencies and bandwidth were kept the same.

6.2.2 Design/Procedure

This study utilised a mixed-design approach to probe how changes in stimulus carrier influence an observer's capability to detect modulations in texture amplitude. The experimental structure comprised three distinct tasks: a plaid orientation discrimination task, a noise detection task, and an amplitude modulation detection task. Sensitivity of shading discrimination was explored employing a sinusoidal plaid. In this context, observers were asked to discern the orientation of the coarse undulations, using a two-alternative forced-choice method (for further details see (Schofield et al., 2017). The visual texture used as a carrier was presented at three spatial frequencies. The experimental design has been summarised in Figure 6-3.

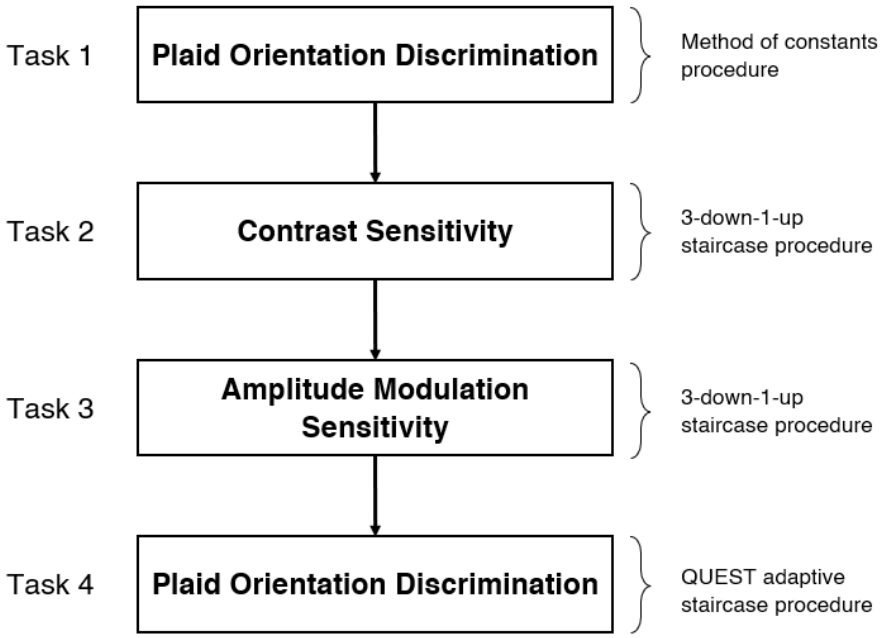

Figure 6-3. The sequence of tasks that participants undertook, starting with a plaid orientation discrimination task (utilising a method of constants design) which served as a practice and an approximate threshold measure to be input as the starting value for the later iteration of the plaid orientation task (using QUEST procedure), followed by a contrast sensitivity task, then an amplitude modulation sensitivity task (both utilising a 3-down-1-up staircase procedure), and concluding with the final plaid orientation discrimination task.

Observers viewed the screen binocularly and fixated on a central target in each trial. In the plaid orientation discrimination task, each plaid orientation discrimination trial was composed of a sinusoidal plaid with an isotropic texture displayed for 1000ms (75 frames). In each trial, the orientation of the in-phase and anti-phase grating was randomised, and observers indicated the orientation of the in-phase sinusoidal grating by indicating the orientation of perceived undulations. Participants could only make a response after the stimulus presentation period to ensure all participants had the same time viewing the stimulus. A coarse-scale isotropic noise with a central spatial frequency of 0.5 cpd was presented after each trial so that after-images of the luminance or contrast gratings did not affect the following trial.

The plaid orientation discrimination task utilised a method of constants design with five amplitude modulation levels from 0.2 to 0.9 at intervals of *2(sqrt(2)) with ten repetitions each. A psychometric function was then fitted to the data obtained from the method of constants experiment in order to provide an estimated threshold for a QUEST adaptive staircase threshold measurement method (Watson & Pelli, 1983). The staircase contained a total of 100 trials which estimated a 75% threshold for participants. Sensitivities to shading discrimination were investigated with a sinusoidal plaid on which observers were required to discriminate the orientation of the coarse undulations in a two-alternative forced-choice method (see (Schofield et al., 2017).

The contrast sensitivity task used a spatial two-alternative forced-choice method. During the first interval, isotropic noise was randomly presented for 1000 ms to the left or right of the fixation point (p=0.5). The stimuli were presented through a raised cosine window of diameter 5°. The central spatial frequencies were 4, 8 and 12 cpd, and the frequency bandwidth was set to 1 octave. The noise carrier and amplitude modulation detection tasks were designed with two consecutive staircases of 12 reversals each, where a 79.4% threshold was estimated from the final 8 reversals of the second staircase. The reversal intensities were specified at 4, 2, 2 and 1 dB, and a 1 up 3 down staircase was used. During the noise detection task, the contrast of noise was varied in the staircase and participants were prompted to indicate with a keypress the location of the isotropic noise (left or right).

The amplitude modulation detection task also used a two-interval forced-choice method. During the first interval, a noise stimulus was displayed for 1000 ms to one side of the fixation (left or right). The second interval presented an isotropic noise component modulated by an AM component oriented at ±45°, for 1000 ms on the opposite side of the fixation point. During each block, the strength of the amplitude modulations (modulation depth) was manipulated to measure the minimum intensity required for the observer to detect the changes in stimulus shading.

6.2.2.1 Equipment.

Stimuli were generated using Psychopy © (Peirce, 2007) and run on a Mac OS X El Capitan v10.11 (Apple Inc) operating system. Stimuli were presented using a Bits++ (Cambridge Research Systems) stimulus processor on a CRT monitor (Viewsonic P225f, display screen width 39cm, 1280 x 1024 pixels, pixel width = 0.0178° x .0178° at a 160cm viewing distance) with an overall screen refresh rate of 75Hz. The voltage to luminance function of the monitor was linearised via Psychopy (Peirce, 2007), and measurements of luminance were recorded with a Minolta LS-110 photometer. Participants were placed into a modified chinrest with an adjustable optical trial lens frame at a distance of 160cm from the monitor. Young observers viewed the stimuli through two lenses, +.12 and -.12, to create an aperture but no correction. Older observers viewed the stimuli through two lenses, +.12 and + .5, making a total power of +.67 to correct for presbyopia. Responses were made using a keyboard, and the study took place in a light-controlled room.

6.2.2.2 Participants

The study's participant recruitment and data acquisition process started with the recruitment of 45 participants, 23 older and 22 younger. After the initial data collection, the data were examined, and participants with thresholds exceeding a maximum threshold estimate (1.0) for each condition of the plaid orientation experiment were omitted from further analysis. Consequently, the final data set used for analysis included information from 40 participants who met the analysis criteria. The group of older adults consisted of 20 participants, with an equal gender split (10 males, 10 females), ranging in age from 61 to 79, mean = 69.4 (± 5.286). The younger adult group also contained 20 participants, 8 males and 12 females, aged between 18 and 26, mean = 21.45 (±3.38).

All participants had corrected-to-normal vision and were asked to wear their normal prescribed lenses for the distance throughout the experiment if required, and observers with bi- or varifocal lenses used the distance part of their lens. Participants underwent a short

period of training to help familiarise themselves with the stimuli and different tasks before completing the experiment.

6.2.3 Analysis

In this empirical chapter, the primary aim was to investigate the factors influencing shape-from-shading perception and to understand the effects of aging on this process. To achieve this, several ANOVA tests were conducted to explore age-related differences in key areas: contrast sensitivity, amplitude modulation sensitivity, and sensitivity to shape-from-shading cues.

To address the research question of whether perception of shape-from-shading is solely a sensory-based ability or if it's influenced by other factors, a multiple regression analysis was performed. This analysis was designed to examine the predictive relationship between contrast sensitivity thresholds, amplitude modulation thresholds, and age, and how these variables collectively impact performance in the shape-from-shading task. This approach allowed for a more detailed understanding of the interaction between sensory capabilities and ageing in depth perception from shading cues.

6.3 Results

6.3.1 Contrast sensitivity thresholds

In the analysis of contrast sensitivity thresholds, we observed a pattern where thresholds tend to increase as spatial frequency increases, as illustrated in Figure 6-4. For younger adults, these increases in threshold are relatively marginal across the range of spatial frequencies tested. However, for the older adult group, a more pronounced pattern emerged. Specifically, a significant increase in threshold moving from 4 to 8 cpd, followed by an even larger increase at 12 cpd. Additionally, the difference in thresholds between the younger and older adult groups becomes more pronounced as spatial frequency increases. This trend indicates that older adults experience a more substantial decline in contrast sensitivity at higher spatial frequencies compared to younger adults.

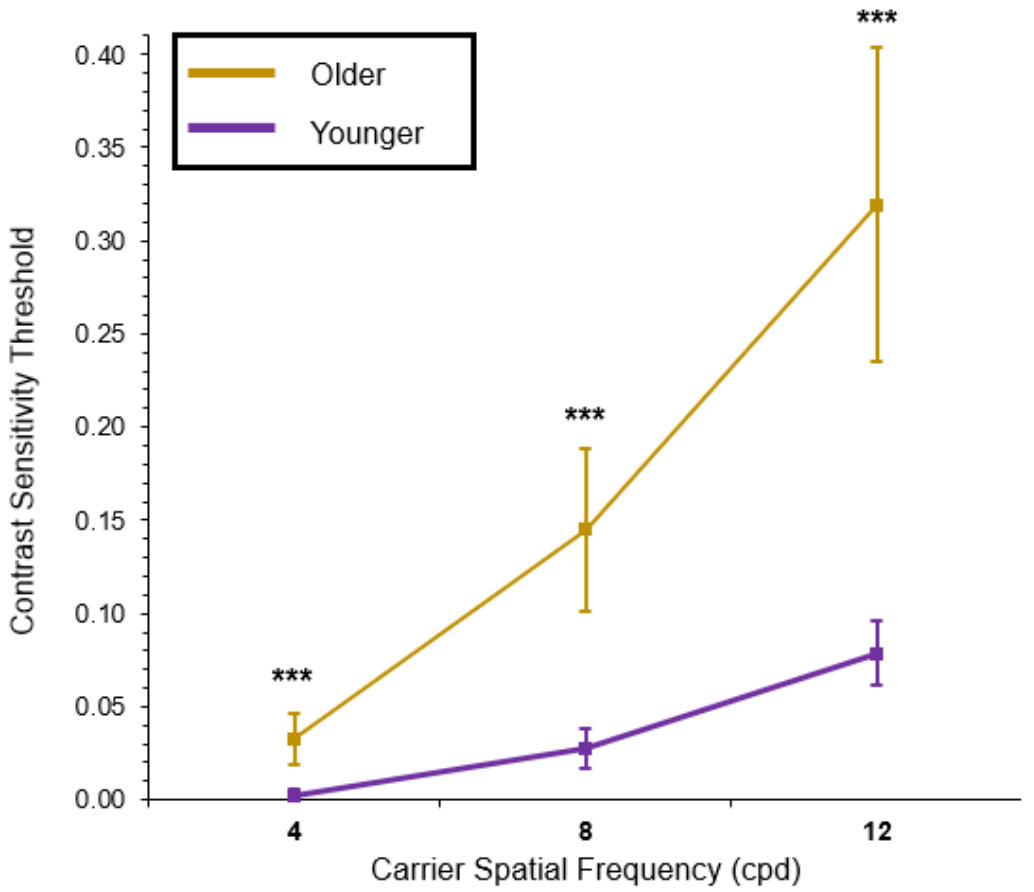

Figure 6-4. Contrast sensitivity thresholds for younger and older adults, the yellow plots illustrate older adult thresholds, whereas the purple line demonstrates younger adult contrast sensitivity thresholds. Note. Error bars represent 95% confidence intervals. *** highlights a significant difference between group means ($p < 0.001$)

There was a significant interaction between age group and spatial frequency[2], $F(1.272, 19.073) = 26.57$, $p < .001$, partial $\eta^2 = 0.7$. In the model, both factors were identified to significantly influence contrast sensitivity, with spatial frequency demonstrating a larger

[2] Before conducting a 3x2 mixed ANOVA, the assumption of sphericity was violated, as assessed by Mauchly's test of sphericity, $\chi^2(2) = 30.82$, $p < .001$. Therefore, a Greenhouse-Geisser correction was applied ($\varepsilon = .64$).

effect size, F(1.28, 48.56) = 70.12, p < .001, partial η^2 = 0.65. Furthermore, age group was found to affect contrast sensitivity thresholds, though the effect size was considerably smaller, F(1,38) = 32.44, p < 0.001, partial η^2 = 0.46.

Bonferroni post-hoc analyses revealed a significant difference in thresholds between younger adults (0.003 ± 0.005) and older adults (0.033 ± 0.005) at 4 cpd (p < 0.001). A significant difference was also found between younger adults (0.028 ± 0.016) and older adults (0.145 ± 0.016), at 8 cpd (p < 0.001). Furthermore, a significant difference was reported at 12 cpd between younger (0.079 ± 0.031) and older adults (0.319 ± 0.031) for contrast sensitivity thresholds (p < 0.001).

6.3.2 Amplitude modulation sensitivity

An interaction between age group and spatial frequency was also found in for amplitude modulation sensitivity thresholds[3], F(1.272, 48.57) = 20.1, p < .001, partial η2 = 0.35. Upon further analysis, it was determined that both spatial frequency, F(1.28, 48.57) = 14.00, p < 0.001, partial η^2 = 0.27, and age group, F(1,38)=18.22, p < 0.001, partial η^2 = 0.32, had similar effect sizes within the model.

[3] Before conducting a 3x2 mixed ANOVA, the assumption of sphericity was violated, as assessed by Mauchly's test of sphericity, $\chi^2(2) = 30.77$, p < .001. Therefore a Greenhouse-Geisser correction was applied (ε = .64).

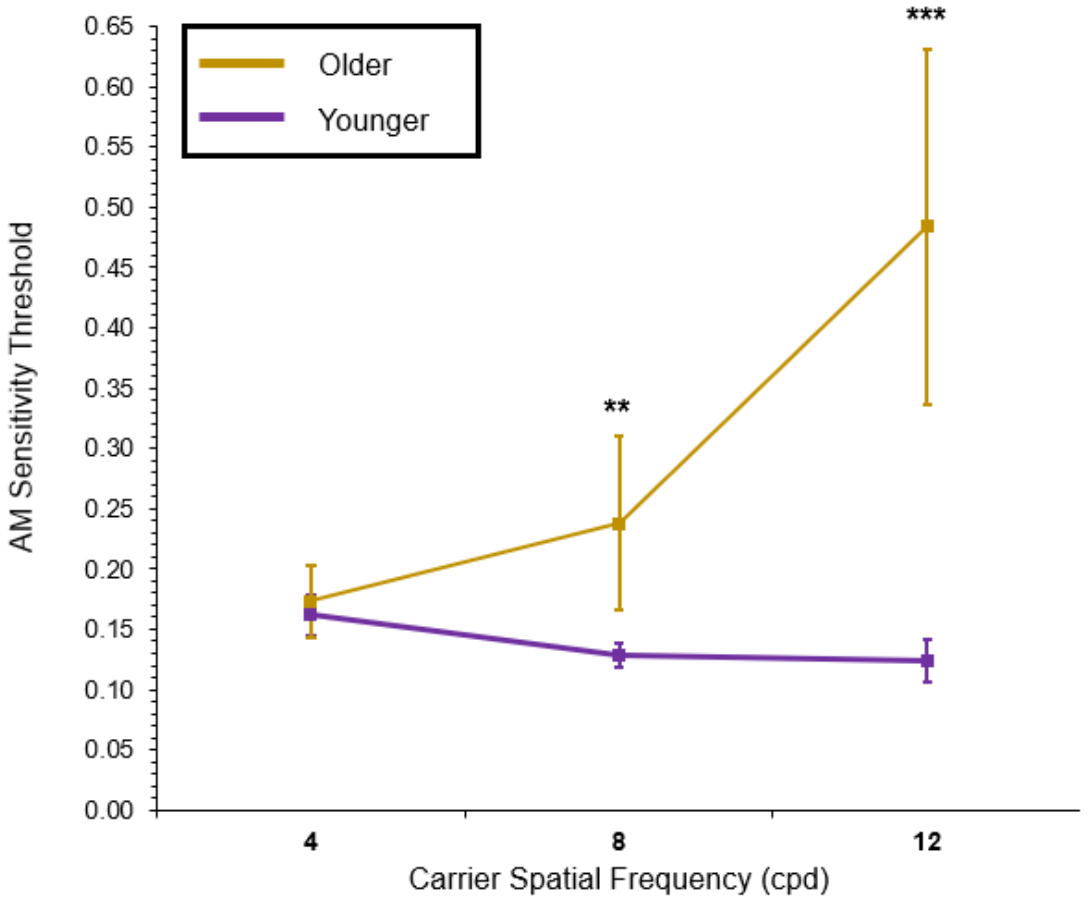

Figure 6-5. Threshold estimates by age group in the amplitude modulation sensitivity task. In this figure the yellow line signifies older adults, and purple line younger adults. Note. Error bars illustrate 95% confidence intervals. Significant differences between group means are highlighted by; ** $p < 0.01$, and *** $p < 0.001$.

Post hoc analyses further explored this interaction where group mean thresholds (±SE) were significantly different for younger (0.24 ± 0.03) and older adults (0.13 ± 0.05) at 8 cpd, $p < 0.01$, and also within 12 cpd for younger (0.13 ± 0.05) and older adults (0.48 ± 0.05), $p < 0.001$. However mean thresholds did not significantly differ at 4 cpd for younger (0.16 ± 0.01) and older adults (0.17 ± 0.01), n.s., $p > 0.05$. Moreover, sensitivity thresholds

varied significantly with spatial frequency in the older adult group[4], whereas younger adult thresholds remained stable (n.s., p > 0.05).

6.3.3 Contrast sensitivity predicted sensitivity of amplitude modulations

A multiple regression analysis showed that contrast sensitivity thresholds predicted performance in the amplitude modulation sensitivity task, along with age group and spatial frequency, $F(3, 119) = 100.35$, $p < 0.001$, $R^2_{Adjusted} = 0.72$).

$$x = 0.2 + \left(1.37(\sigma)\right) - \left(0.01(\gamma)\right) - \left(0.02(\delta)\right)$$

Equation 6-1

The regression model is characterised in Equation 6-1 whereby x denotes amplitude modulation sensitivity threshold, σ characterises the contrast sensitivity thresholds, γ spatial frequency, and δ represents age group. During the analysis, the dichotomous age group variable was adopted due to an unequal distribution of ages. The contributions towards amplitude modulation sensitivity demonstrate that contrast sensitivity thresholds, $\beta = 1.37$, $t(119) = 14.11$, $p < 0.001$, carrier spatial frequency, $\beta = -0.01$, $t(119) = -3.79$, $p < 0.001$, and age group, $\beta = -0.02$, $t(119) = -0.77$, $p < .001$, reported significant effects on the regression model.

6.3.4 Plaid orientation discrimination

It was previously discussed that participants were excluded from the analysis if a threshold of 1.0 (or 100% signal intensity) was estimated for all three conditions in the plaid orientation discrimination task. This was because accurate threshold measurements greater than 100%

[4] Significant differences for older adult AM sensitivity thresholds between 4 and 8 cpd, $p<.05$, and between 8 and 12 cpd, $p < 0.001$.

signal intensity were impossible. As illustrated in the frequency plot below (Figure 6-6), younger adults had thresholds in all three conditions. For older adults, 19 participants had a threshold less than 100% intensity at 4 cpd, 9 participants at 8 cpd, and at 12 cpd only two participants had thresholds below 100%. This finding indicates that older adults found the task very difficult at 12 cpd.

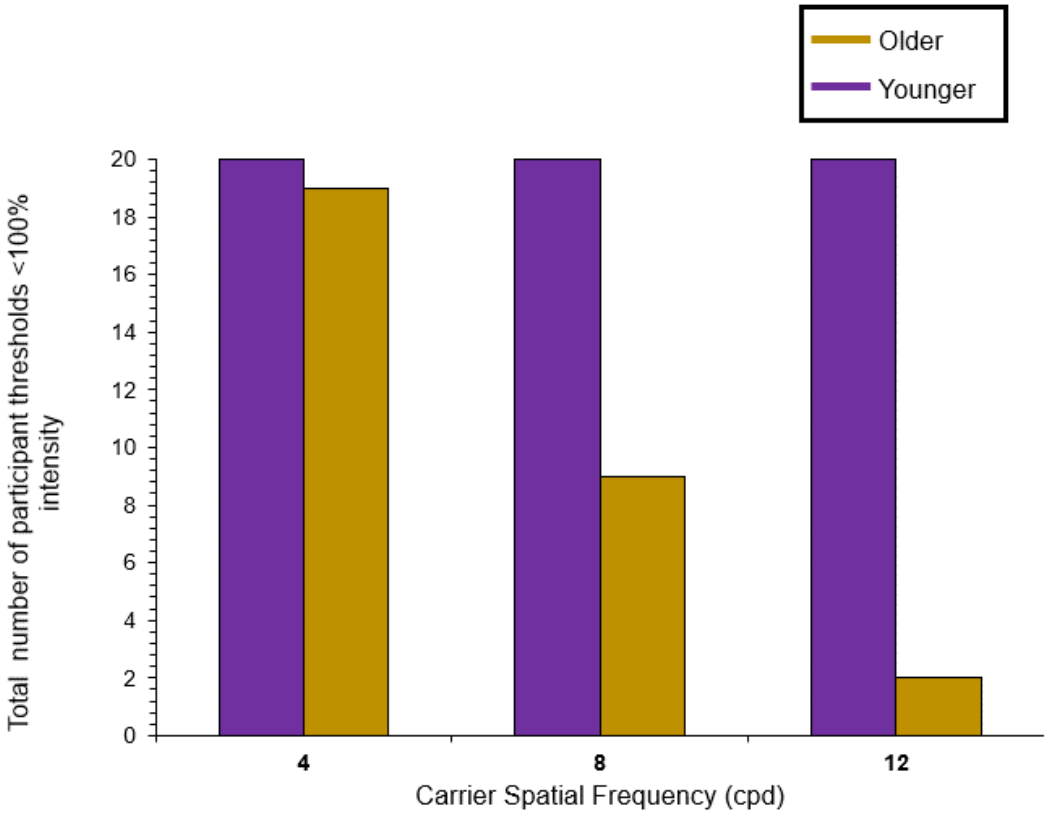

Figure 6-6. Frequency plot for total number of thresholds less than 100% AM signal intensity, whereby the yellow bar denotes older adults, and purple bar total count of younger adults.

Therefore the following analysis was conducted on threshold data from the 4 and 8 cpd conditions[5] which found that both spatial frequency and age group had a significant effect on sensitivity thresholds in the plaid orientation discrimination task, $F(1,26)=10.26$, $p < 0.005$, partial $\eta^2 = 0.28$.

[5] N = 28; 20 Younger, 8 Older.

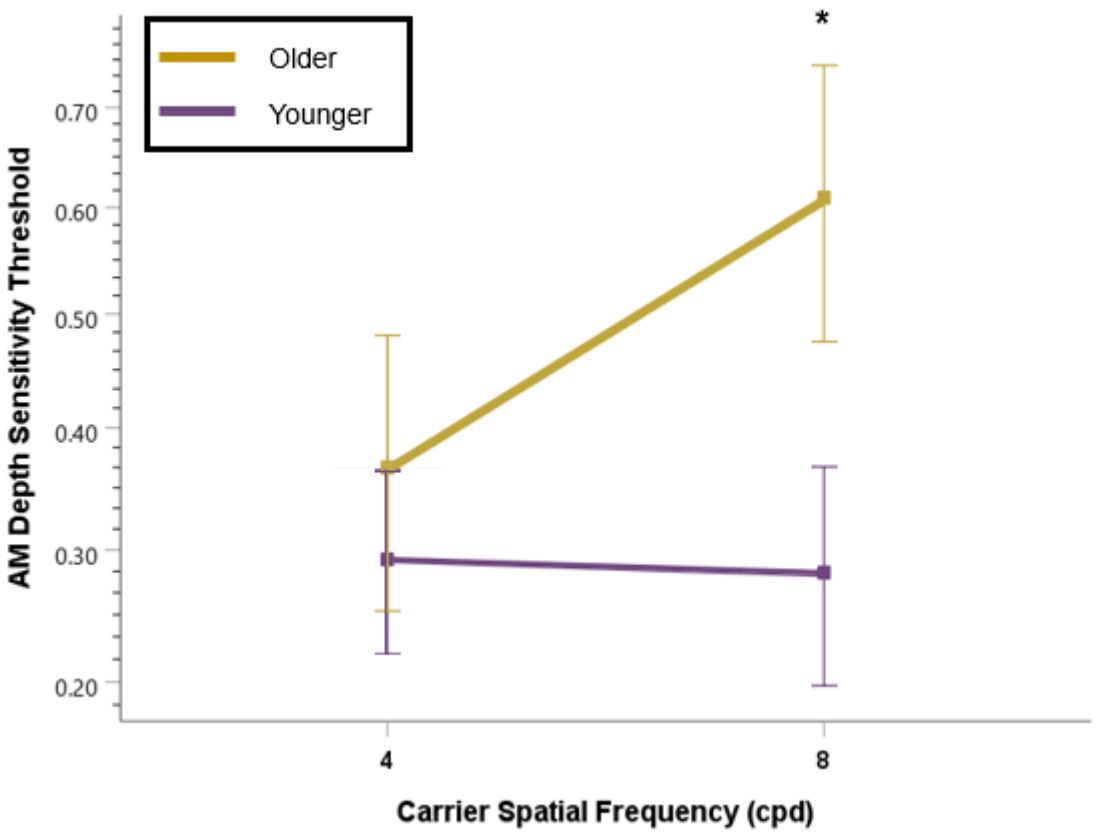

Figure 6-7. Amplitude modulation depth thresholds are illustrated as group means for the plaid orientation discrimination task. Note. Error bars depict 95% confidence intervals, yellow plots denote older adult threshold data and purple for younger adults.

Thresholds (±SE) were significantly different for younger (0.28 ± 0.04) and older adults (0.61 ± 0.07) at 8 cpd, $p < 0.05$, mean thresholds did not significantly differ at 4 cpd for younger (0.3 ± 0.04) and older adults (0.37 ± 0.06), n.s., $p > 0.05$. Older adults also differed in sensitivity between conditions ($p < 0.001$), whereas younger adult thresholds did not.

6.3.5 Relationship between shape-from-shading, contrast and amplitude sensitivity

By employing a multiple linear regression to look at significant predictors of plaid orientation discrimination thresholds within the 4 and 8 cpd conditions[6], contrast sensitivity and amplitude modulation sensitivity thresholds predicted plaid orientation thresholds, $F(2,89) = 8.11$, $p < 0.05$, $R^2_{Adjusted} = 0.14$.

$$x = 0.17 + \left(1.32(\sigma)\right) + \left(0.94(\gamma)\right)$$

Equation 6-2

The regression model is characterised in Equation 6-2 whereby x denotes plaid orientation discrimination sensitivity threshold, σ contrast sensitivity thresholds, γ amplitude modulation sensitivity. The coefficients in this model indicate a significant predictive relationship, showing how contrast sensitivity thresholds influence plaid thresholds, $\beta = 1.32$, $t(89) = 0.306$, $p < 0.005$, amplitude modulation sensitivity, $\beta = 0.94$, $t(89) = 2.3$, $p < 0.05$, reported significant coefficients in the regression model. Age group and spatial frequency were not significant predictors in the regression model.

A further binomial logistic regression was performed for all spatial frequencies, thereby replacing the existing dependent variable of plaid orientation threshold with a new dichotomous variable measuring whether a threshold below 100% signal intensity was reached, i.e. the psychometric function for the dataset reaches asymptote within the given range of stimulus intensities. The overall model predicting asymptotes within the stimulus intensity range was significant, $\chi^2(3) = 90.17$, $p < 0.001$, whereby contrast sensitivity thresholds were significant coefficients, $\beta = -18.44$, $p < 0.005$. In this model, amplitude

[6] Thresholds that were estimate to be less than 100% signal intensity (N = 30, 20 younger, 10 older).

modulation sensitivity and age group were not (n.s., $p > 0.05$). The model correctly classified 90.8% of the cases and explained 78.2% of the variance (Nagelkerke R^2). The non-significance of amplitude modulations as a predictive variable manifest only in models where contrast sensitivity thresholds possess greater predictive power. When contrast sensitivity thresholds are excluded, AM thresholds emerge as a significant predictive variable in the regression model, $\beta = -11.54$, $p < 0.05$, however age group remains non-significant, $\chi^2(2) = 60.69$, $p < 0.001$, $R^2 = 68.3$. It should be noted that this analysis is subject to the caveat that the dependent variable is binomial. Consequently, even a model devoid of predictive variables still accounts for 52.73% of the variance ($p < 0.001$).

6.4 Discussion

The present study explored the impact of age on shape-from-shading cues. Changes in sensitivity of first-order and coarse-scale second-order visual stimuli influence shape-from-shading perception. This was investigated by assessing sensitivity of first-order luminance and second-order amplitude properties, and lastly, how visual sensitivity of these cues affected sensitivity of shape-from-shading perception in an orientation discrimination task. The subsequent findings, which highlighted the significant roles of age and spatial frequency in visual sensitivity, are discussed in detail below.

6.4.1 Age-related differences in sensitivity of first-order stimuli

It was observed that first-order contrast sensitivity was significantly reduced for older adults. As noise texture spatial frequency increased, sensitivity of the noise carrier dropped for both age groups. However, older adults exhibited substantial reductions in sensitivity, particularly at higher spatial frequencies. This result, consistent with existing literature, underscores that age-related perceptual decline is not an overall loss, but specifically relates to high spatial frequencies (Elliott, 1987; Faubert, 2002; Owsley, 2011; Owsley et al., 1983; Pardhan, 2004). Although not particularly novel, it reinforces established understanding. This exacerbation of sensitivity reduction at higher spatial frequencies might stem from age-induced changes in eye physiology or changes in neural processing in the visual system, such as decreased neural efficiency or increased internal noise (Dakin & Mareschal, 2000; Derefeldt et al., 1979; Owsley, 2011; Owsley et al., 1983; Pardhan, 2004). The pattern of findings supports the CSF, where a peak in sensitivity around 4 cpd is observed for adults, and sensitivity declines for lower and higher spatial frequencies (Robson, 1966).

6.4.2 Is there a relationship between first-order and second-order sensitivity?

Similarly, older adults exhibited poorer amplitude modulation sensitivity, supported by a significant relationship between increased carrier spatial frequency and age group presented in Section 6.3.2. Older adults demonstrated a pattern like contrast sensitivity

thresholds, revealing a significant threshold elevation with each increment in carrier spatial frequency. Conversely, younger adults exhibited stable sensitivity across all conditions. This pattern contradicts previous studies that evaluated AM thresholds as a function of spatial frequency (Dakin & Mareschal, 2000). Previous research suggests that sensitivity improves with larger carrier-to-envelope spatial frequency ratios and that AM detection typically exhibits scale invariance. The current study used ratios of 1:8, 1:16, and 1:24. Despite these ratios; younger adults maintained consistent thresholds while older adults showed decreasing sensitivity with an increase in the ratio. The visual processing characteristics associated with ageing could introduce unique patterns that differ from those seen in younger populations. This suggests that scale invariance in amplitude modulation sensitivity may not apply to older age cohorts.

Contrast sensitivity thresholds, age group and spatial frequency were reported to predict amplitude modulation thresholds significantly. The interaction between LM texture and AM modulations lends support to the filter-rectify-filter model of visual processing where in the initial stages of visual processing, first-order information is detected and attached to a local region, meaning that sensitivity of second-order information is impacted by first-order channels (Landy & Bergen, 1991). In the present study, thresholds of older adults at higher spatial frequencies could reflect changes in early or late pooling. With ageing, there could be a reduced sensitivity at the level of these early detectors, particularly for high spatial frequency information. This reduced sensitivity could lead to increased thresholds for detecting amplitude modulations, as these modulations rely on the successful detection of the underlying luminance-defined features. Pooling could also account for the pattern of results for younger adults. If pooling is efficient, the successful detection of LM features can aid in AM sensitivity, as the pooled information provides a detailed carrier on which these AM features are conveyed. Therefore, if a decrease in sensitivity occurs at the pooling stage, for instance, due to ageing or increased spatial frequency, it can affect the perception of both LM and AM features, leading to an increased overall threshold for visual detection tasks.

6.4.3 Is there a relationship between shape-from-shading perception and first- and second-order vision?

In the plaid orientation discrimination task, older adults were observed to have significantly higher threshold estimates in the 8 cpd condition, whereas thresholds did not significantly differ at 4 cpd between age groups. The study's findings showed that performance in perceiving shape-from-shading was strongly predicted by sensitivities to both carrier and amplitude modulations. These outcomes offer further evidence for age-related changes in visual perception, where a specific decline in sensitivity of high spatial frequency information plays a significant role rather than a generalized loss of sensitivity across all spatial frequencies. Age-related declines at high spatial frequencies also support the pronounced drop-off in sensitivity observed at 12 cpd for older adults. It was predicted that as spatial frequency increased, sensitivity of shape-from-shading would decrease. However, perceptual difficulty reported by older participants in the 12 cpd condition was not predicted, although unsurprising given a marked reduction in first-order contrast (noise) and second-order AM sensitivity.

At 12 cpd, only two older participants had recorded thresholds beneath the maximum stimulus intensity range of 100%. This pattern of results strongly suggests that individuals aged 60 and above faced significant perceptual challenges in discerning depth at this carrier frequency, leading to their inability to perform the task successfully. Further analysis revealed that contrast sensitivity and sensitivity of amplitude modulations were significant predictors of completing the plaid orientation discrimination task. However, these predictive factors do not fully explain the variance in these regression models, which points to the possibility of an additional factor contributing to the decline in depth perception. One potential factor might be related to the cognitive load and complexity of the task. Tasks assessing carrier and amplitude detection were procedurally and perceptually easier to complete. However, the plaid orientation discrimination task added further complexity to complete. Beyond detecting, processing, and pooling first- and second-order cues, the task

procedure required participants to interpret which oblique displayed in-phase modulations evoked by the perception of depth or shape. These increases in perceptual and procedural requirements could therefore require more cognitive resources which influenced task performance more so than sensitivity of the carrier.

6.4.4 Constraints

A possible limitation could be the employment of different staircase procedures across tasks, which may have influenced the emergence of thresholds greater than 100% in the plaid orientation discrimination task. Adopting a QUEST adaptive staircase may have resulted in more perceptually challenging stimuli during the first portion of the staircase, meaning perceptual learning was not achieved. Although this is a possibility, participants underwent extensive training during the method of constants task, where they were exposed to the entire stimulus intensity range. The remaining dataset aligned with previous research investigating shape-from-shading at high-frequency carrier conditions (Schofield et al., 2017).

Furthermore, it was demonstrated that novice observers could successfully perform the task at high spatial frequencies, contrary to the present study. This divergence may be due to the use of an isotropic carrier in this study, compared to the Gabor noise carrier deployed in previous research. Therefore, the observed results are more attributable to inherent task and stimulus difficulty rather than the specific staircase method implemented for threshold estimation.

7 General Discussion

The thesis aimed to investigate how ageing affected shape-from-shading depth perception and whether a decline in visual acuity was solely responsible for reduced sensitivity of high spatial frequencies. To achieve this, the study isolated first- and second-order components of a shape-from-shading stimulus to quantify sensitivity and effect on depth perception. This chapter identifies common themes across chapters, referring to the research questions presented in Chapter 1, and highlights contributions to existing literature. Furthermore, limitations and potential future directions are discussed.

7.1 Objectives of the thesis

The primary objective of this thesis was to explore the sensitivity of the perception of shape-from-shading. Concurrently, age-related perceptual and cognitive function were also investigated to determine how these changes contribute to shape-from-shading sensitivity. The challenge of isolating their contributions and their potential to interact in ways that magnify age-related visual impairments has been central to the discourse. This research has highlighted themes of ageing, visual processing, and depth perception through shape-from-shading, which will be addressed in the following chapter. The following research questions have been addressed through the course of this thesis:

- How does ageing affect sensitivity of shape-from-shading?
- Does the perception of depth through shape-from-shading rely solely on the perception of its components?

These were addressed by isolating first- and second-order components in a shape-from-shading cue to determine their contribution to depth perception sensitivity and to examine whether age-related changes are a consequence of visual deficits. This final

chapter reflects on contributions made by this research to the existing literature in response to the above questions.

7.2 Summary of Findings

7.2.1 Chapter 3. Perceptual and cognitive load on shape-from-shading of textured surfaces

This study investigated the impact of perceptual and cognitive load on the shape-from-shading of textured surfaces alongside the interaction of age and cognition in shape-from-shading. Key findings include:

- Broadband noise masks low spatial frequency luminance modulated shape-from-shading cues. This underscores that environmental conditions, like broadband noise, can substantially influence the perception of shape-from-shading cues.
- Significant differences were found in the perception of shape-from-shading under narrowband and broadband noise conditions. This finding highlights that varying types of noise can differentially impact our ability to perceive shape in textured surfaces.
- The interaction between age and cognition in shape-from-shading suggests that cognitive ability and age significantly impact the perception of shape-from-shading cues.

7.2.2 Chapter 4: Piloting and methodology refinement for psychophysical studies

In this chapter advancements were made in refining the methodology for investigating first- and second-order contributions to shape-from-shading perception. These improvements set the stage for more in-depth empirical investigations in subsequent chapters. The main findings from this chapter include:

- While the differences in sensitivity to shape-from-shading cues were not statistically significant, there was an observable trend in decreasing sensitivity as spatial frequency increased. This finding warranted further investigation and was explored in Chapter 6, with a study that is sufficiently powered to detect these changes in sensitivity.
- The adoption of the QUEST staircase method for threshold estimates in later chapters was hypothesised to be more effective than method of constants and traditional n-up n-down staircase methods. Using QUEST hoped to result in more reliable thresholds and reduce participation time, as the staircase adapts to participants' performance.

7.2.3 Chapter 5. Perceived depth magnitude of luminance and contrast-modulated noise textures

This chapter explored the perceived depth magnitude of first- and second-order modulations of noise textures by using paired comparisons in a depth judgement task. The main findings include:

- Both LM+AM and LM-only shading cues exhibit the highest perceived depth magnitude (PDM), regardless of age and spatial frequency. This suggests a general resilience of these cues to these variables, indicating their fundamental role in depth perception.
- Modulations of visual textures can aid and obscure depth cues for younger adults. This emphasises the nuanced role that texture plays in shaping depth perception.
- There is an increased reliance on LM cues for depth perception when carrier visibility declines with age. This shift in perceptual strategy could be a compensatory response to decreased visibility.

- When AM modulation depth was presented much higher than threshold, a scuffing effect occurred, where preference between LM+AM and LM-only stimuli diminished for younger adults.

7.2.4 Chapter 6. The effects of age-related changes on shape-from-shading depth perception

This chapter expands upon the findings of Chapter 5 by expanding to plaid configurations composed of first- and second-order cues. The findings were as follows:

- Age and higher spatial frequencies have a significant impact on contrast sensitivity. As individuals age or when visual stimuli are presented at high spatial frequencies, contrast sensitivity decreases.
- A relationship between first- and second-order sensitivities found that the visibility of first-order carriers supports visibility of second-order modulations, which lends support to interaction models.
- The findings support the shading channels model, where older adults display reduced sensitivity of differences at high carrier spatial frequencies. These frequencies are unperceivable to this demographic, leading to the two inputs into the gain control stage being identical, where a lack of differentiation further influences their visual processing of amplitude modulation, reinforcing the age-related changes observed in sensitivity patterns.

The following sections summarise the conclusions from each empirical chapter. For each empirical chapter, data was collected from two distinct age groups to ascertain whether differences in visual sensitivity significantly influenced the sensitivity of shape-from-shading. By exploring these various factors, the objective was to comprehensively understand how ageing impacts perception of shape-from-shading.

7.3 Does ageing affect shape-from-shading perception?

Across the four empirical chapters, the objective was to explore interactions between ageing, sensory load, and cognitive demand. The conclusions regarding sensory load suggest that older adults had more perceptual difficulty perceiving high spatial frequencies than younger adults, which is amplified when detecting shape-from-shading. When considering the cognitive demand of participants, chapter 3 concluded that as cognitive load increased, performance for younger and older adults declined, as indicated by decreased accuracy and longer response times. Furthermore, an interaction between age group and cognitive load was noted, implying that the effect of cognitive load was more pronounced among older adults, leading to diminished performance. In Chapter 5, it was observed that older adults struggled to perceive shape-from-shading when comparing pairs of stimuli at high carrier frequency conditions. Initial conclusions attributed this to the visibility of the carrier. However, when assessing the contributions to shape-from-shading in Chapter 6, it emerged that visual sensitivity, although essential, does not entirely explain the deficit.

As illustrated in Chapter 3, an increase in cognitive load presents more significant challenges for older adults in processing information efficiently and effectively. The cognitive load theory proposes a trade-off between cognitive load and visual perception, suggesting that an increase in cognitive load diminishes visual perception in older adults (S. Li et al., 2001; Lindenberger & Baltes, 1994). This decline in older adults' performance is more pronounced due to the decreased cognitive resources inherent with age.

This theory, therefore, supports a relationship between cognitive load and visual sensitivity where increased cognitive demands result in a proportional reduction in performance. If this relationship is present, then age-related declines may not be attributable solely to visual deterioration but could also involve compensatory mechanisms where the degree of facilitative cognitive scaffolding is proportional to the degree of physiological depletion (Park & Reuter-Lorenz, 2009). Lifelong cognitive demands and resource utilisation

can either enhance or deplete neural resources, thus affecting overall cognitive performance.

It might be oversimplistic to attribute the decline in depth perception solely to visual deterioration that comes with age, and compensatory mechanisms are employed to deal with the perceptual deterioration of a stimulus. Suppose younger and older adults were matched in sensitivity for a shape-from-shading cue. In that case, the differences in threshold caused by ageing may diminish as older adults have developed compensatory mechanisms that younger adults have not yet acquired.

7.4 Age-related differences in sensitivity of first- and second-order stimuli

The thesis findings suggest that age-related differences in contrast sensitivity are more prominent at high spatial frequencies. The findings presented in chapters 5 and 6 found a significant drop off in contrast sensitivity for older adults at 12 cpd but some preservation at lower frequencies. In contrast, younger adults showed minimal variation in sensitivity. These findings are consistent with the contrast sensitivity function, which indicates that younger adults maintain consistent sensitivity at 12 cpd while older adults have a more pronounced reduction in sensitivity at this frequency (Owsley, 2011; Robson, 1966; Weale, 1975, 1982). The extent of this deficit shows considerable variation within the older age group, hypothesised to be due to large variability in lens density in older adult populations that lead to heightened light scattering. Similarly, older adults were observed to have sensitivity deficits to amplitude modulations of visual textures, especially using carriers with high spatial frequencies, compared to their younger counterparts in empirical chapters 5 and 6. This observation is consistent with previous studies that reported similar deficiencies in older adults, whereas younger adults show minimal sensitivity changes.

The findings from both datasets showed a consistent relationship between luminance and amplitude sensitivities among younger and older adults. Diminished sensitivity of the first-order carrier manifested as reduced sensitivity of second-order amplitude modulations.

Conversely, high sensitivity of the carrier resulted in heightened sensitivity of the amplitude modulations. This relationship sheds light on the processes employed in identifying second-order modulations. The filter-rectify-filter model is thought to rely on a two-stage filtering process (Wilson et al., 1992). This initial stage is sensitive to fine details, whereas the following stage is sensitive to contrast modulations at lower frequencies (Dakin & Mareschal, 2000; Schofield, 2000; Sutter et al., 1995). Therefore, an impairment in the first-stage filters, specifically those attuned to higher frequencies, could further deteriorate signal strength during the proposed rectification stage that serves to demodulate the signal.

7.5 How do first- and second-order signals combine to create a shape-from-shading cue?

A relationship was identified between contrast sensitivity and depth perception through shape-from-shading. This trend emerged when examining sensitivity of carrier and amplitude modulations, specifically when consulting the scaling plots for older adults, as discussed in empirical chapter 5. For older adults at 12 cpd, sensitivity of the carrier resulted in a decrease in amplitude modulation sensitivity. This reduced the ability to distinguish between in-phase and anti-phase shape-from-shading stimuli, reflected in the scaling plots. In contrast, this distinction was apparent at lower carrier frequencies for younger adults in the low AM contrast condition, where an in-phase stimulus was perceived as having more depth than an anti-phase.

Chapter 6 demonstrated that carrier and amplitude modulation thresholds significantly predicted a reduction in sensitivity of shape-from-shading, whereas age did not. Therefore, greater sensitivity of carrier and amplitude modulations resulted in preserved depth perception through shape-from-shading.

Younger adults did not have this pattern of decline in shape-from-shading perception as carrier spatial frequency increased. This aligns with prior research, indicating minimal

changes in shape-from-shade sensitivity at 12 cpd (Schofield et al., 2017). However, most older adults could not accurately discriminate shape-from-shading material changes at 12 cpd, which points to the diminished carrier visibility observed in the binomial logistic regression. This observed relationship aligns with previous research where a decline in sensitivity of shape-from-shading resulted from increased spatial frequency (Schofield et al., 2017).

The decline in shape-from-shading perception for older adults at 12 cpd was unprecedented. Previous research reported a threshold of approximately 40% AM depth intensity at 12 cpd, whereas in our current dataset, many older participants exhibited threshold estimates exceeding 100% AM depth intensity (Schofield et al., 2017). Furthermore, the deterioration of perceived depth magnitude within the scaling plots for older in empirical chapter 5 was also not anticipated. This deterioration of sensitivity of shape-from-shading could be attributed to a larger sample size in the present datasets, leading to a broader variation in sensitivity among older adults. In the prior study, participants were screened and had a contrast sensitivity within the normal range. Hence, the present dataset likely displayed more variation, including poorer contrast sensitivity than previous datasets, resulting in worse performance in shape-from-shading discrimination. This variation might be due to differences in lens density, which is known to reduce contrast sensitivity due to lens scattering (Xu et al., 1997).

The findings across these chapters lend support to the shading channel model, where deterioration of sensitivity of high spatial frequency carriers made the second-order components of stimuli harder to see, thus removing the additive and subtractive signals that would typically drive differences between components in the shading channel model (Schofield et al., 2010). In this model, presented in Chapter 1, the final filter stage extracts information about shading from the rectified signal, which is then subject to gain control, enabling the generation of shading maps. Therefore, similar to the filter-rectify-filter model, if

there is deterioration in the first-stage filters, rectification and contrast gain control could magnify these deficits when integrated into a shading profile.

7.6 Contributions to the existing literature made by this thesis

The research presented in this thesis contributes to our understanding of the interaction between age-related factors and shape-from-shading in depth perception – specifically about second-order processing. While previous studies have highlighted the role of age in sensitivity of shape-from-shading and examined the impact of varying visual textures on perception, an extensive investigation has not previously been conducted into what contributes to the deterioration of shape-from-shading. Therefore, the presented research aids further understanding of the relationship between ageing-related deficits in first- and second-order mechanisms and shape-from-shading.

Disparities between younger and older adults' sensitivity of fine-grained visual textures in shape-from-shading tasks have previously been researched. However, the scope of these findings is limited to the extremes of the contrast sensitivity function. Chapter 5 suggests that an intermediary spatial frequency could provide further insight into patterns of change in sensitivity of shape-from-shading when evaluating age-related differences. It was concluded that in-phase luminance and amplitude-modulated and luminance-only stimuli conveyed greater depth magnitude than anti-phase and amplitude-only stimuli, which deteriorated with increased spatial frequency for older adults but was preserved in younger adults. In Chapter 5, older adults made depth judgements based on the luminance cues alone at high spatial frequencies, attributed to their lack of sensitivity of the carrier. This finding was consistent with Chapter 6 when using plaid stimuli in orientation discrimination tasks, concluding that carrier sensitivity significantly predicted performance. If this were the case, it is conceivable that older adults misjudge depth due to sole reliance on low-frequency luminance modulations when the supporting texture is fine-grained. This, in turn, could support why the prevalence of trips and falls in elderly populations are much higher than in younger age groups.

Furthermore, by exploring sensitivity of shape-from-shading at an intermediary carrier spatial frequency, further comparisons could be made to the contrast sensitivity function to disambiguate further the relationship between sensitivity of shape-from-shading and contrast sensitivity. Whilst minimal changes in sensitivity were observed for younger adults, a decline in sensitivity was observed for the older group, suggesting that the dependence of sensitivity of shape-from-shading is not solely reliant on carrier visibility or amplitude modulations.

Before this thesis, studies investigating the effects of ageing on shape-from-shading suggest a decline in sensitivity due to a decrease in visual acuity. The potential impact of cognitive ageing on depth perception has not been thoroughly explored. Chapter 3 examined the interaction between visual and cognitive factors, establishing that cognition plays a significant role in depth perception with first-order depth cues. The findings suggest that the interplay between cognitive load and stimulus difficulty impacts shape-from-shading perception. Moreover, findings from Chapter 6 indicate that the sensitivity to shape-from-shading is only partially explained by the visibility of modulations. This supports the thesis that a visual decline does not solely explain the sensitivity of shape-from-shading when the test stimulus is perceptually challenging. Therefore, this thesis posits that perceptual and task difficulty might aggravate deficits in shape-from-shading for older adults.

7.7 Limitations and Future Directions

The selection of isotropic noise is a significant factor in interpreting these results. We chose isotropic noise as the carrier to avoid interference with the grating's orientation. Although binary noise was dismissed due to its lack of control over spatial frequency, Gabor noise was also considered, as it has been previously touted as a suitable carrier for amplitude modulations, and its orientation can be altered to include all orientations.

This might have contributed to the high thresholds reported in Chapter 6, where older adults struggled with the plaid orientation task, yielding thresholds greater than 100%. In comparison, Schofield's 2016 paper shows that using high spatial frequency Gabor noise in

a similar study produced thresholds of roughly 40%. Making direct comparisons between thresholds is impossible due to different experimental setups and monitor specifications. Still, in Chapter 6, it is significant that older adults could not attain a threshold at maximum modulation depth, suggesting they could not reliably discern shape-from-shading in this condition. Although Gabor noise might have resulted in measurable thresholds, it was deemed unsuitable for these experimental studies, primarily due to worries about potential interference between the grating and noise orientations when their spatial frequencies have overlapping bandwidth. This is particularly pertinent to Chapters 5 and 6, which explored a range of spatial frequencies from 4 to 12 cpd, where potential interaction might exist in low spatial frequency conditions. This raises the question of whether there is a facilitatory interaction between the carrier and grating orientations when detecting shape-from-shading.

It is likely that sensitivity to depth cues from shape-from-shading were affected by viewing conditions, particularly in terms of whether the stimuli were observed using one eye (monocular viewing) or both eyes (binocular viewing). In this thesis all conditions were presented under binocular viewing conditions which introduces stereopsis. This is where the brain creates a 3D representation by integrating the two different images from each eye, enhancing depth perception. Therefore, it is possible that stereopsis cues could interfere with the shape-from-shading cues presented in the experiments. This interference occurs because stereopsis cues indicate that all stimuli are displayed on a flat screen, which then conflicts with the shape-from-shading depth cues. Despite the viewing distance being set to minimise the impact of stereoscopic cues, it would likely influence the perception of depth. Therefore, a replication under monocular viewing conditions may lead to a greater sensitivity to shape-from-shading depth cues, as the conflicting stereoscopic cues would be absent. In the older adult group, there were significant variations in sensitivity of the stimuli. These age groups are defined and supported by previous literature, where a decline in visual sensitivity at 60 years and over. The variation within this age group could be related to age, where an observer aged 60-65 performed to similar levels as younger adults. In contrast, an observer

aged 80+ typically has much more significant losses to fine-grained information (Owsley et al., 1983). Further constriction on age group, or perhaps a regression analysis of age and sensitivity in the older age group, could have further explained this distinction. The pattern of age differences between young and older adults shed light on the research questions. It is concluded that both visual and cognitive factors play a role in depth perception, but further investigation into quantifying the impact of cognitive deficits and their interaction with visual deficits would provide additional insights into the progression of sensitivity of shape-from-shading in the elderly. Therefore, future research into shape-from shading and cognitive load would provide further insight into theories of ageing.

Extraneous factors such as computer use and experience were not controlled for in the studies, which may confound results, particularly regarding reaction times. Although visual deficits were controlled for in observers, control within the older age group could be useful for follow-up research, and further controlling of mitigating factors such as computer usage and mild cognitive impairment could be recorded, especially if a relationship between sensitivity of shape-from-shading and cognitive decline were to be established. Future work would need to account for this to explore the effect of cognitive load on sensitivity of shape-from-shading.

The surrounding environment is typically chromatic, meaning the human visual system is responsive to light intensity and wavelength variations. These colour-luminance relationships are also utilised as shape-from-shading depth cues, and patterns of suppression and facilitation of depth perception can occur when a luminance grating is paired with a chromatic grating (Kingdom, 2003). Furthermore, if this relationship is fundamental to the human visual system, it could develop over time, serving as a compensatory mechanism in older adults as spatial visual acuity diminishes. Therefore, incorporating chromatic gratings with first- and second-order depth cues could provide further insight into how the human visual system perceives shape-from-shading in the real world.

7.8 Conclusions

This thesis sought to investigate the influence of ageing on shape-from-shading, examining whether age differences could be ascribed to a decline in visual perception. It was determined that both first- and second-order sensitivity contribute to depth perception and that a loss of sensitivity of high spatial frequencies disrupted shape-from-shading in older adults. A potential compensatory mechanism may involve older adults increasingly depending on luminance-modulated signals to overcome deficits in perceiving noise carriers and amplitude-modulated cues. However, these elements could not be entirely accounted for by perceptual difficulty alone, and an unexplored interaction might exist between task or stimulus difficulty and shape-from-shading, resulting in a magnified cognitive load with greater complexity, further exacerbating depleted resources for older adults.

8 References

Adelson, E. H., & Pentland, A. P. (1996). The perception of shading and reflectance. In Perception as Bayesian Inference (Vol. 1, pp. 409–424). Cambridge University Press. https://doi.org/10.1017/CBO9780511984037.014

Allard, R., & Faubert, J. (2006). Same calculation efficiency but different internal noise for luminance- and contrast-modulated stimuli detection. Journal of Vision, 6(4), 322–334. https://doi.org/10.1167/6.4.3

Anobile, G., Cicchini, G. M., & Burr, D. C. (2014). Separate Mechanisms for Perception of Numerosity and Density. Psychological Science, 25(1), 265–270. https://doi.org/10.1177/0956797613501520

Appelle, S. (1972). Perception and discrimination as a function of stimulus orientation: The 'oblique effect' in man and animals. Psychological Bulletin, 78(4), 266–278. https://doi.org/10.1037/h0033117

Arena, A., Hutchinson, C. V., Shimozaki, S. S., & Long, M. D. (2013). Visual discrimination in noise: Behavioural correlates of age-related cortical decline. Behavioural Brain Research, 243(1), 102–108. https://doi.org/10.1016/j.bbr.2012.12.039

Artal, P., Berrio, E., Guirao, A., & Piers, P. (2002). Contribution of the cornea and internal surfaces to the change of ocular aberrations with age.

Baker, C. L., & Mareschal, I. (2001). Processing of second-order stimuli in the visual cortex. Progress in Brain Research, 134, 171–191. https://doi.org/10.1016/S0079-6123(01)34013-X

Barbot, A., Landy, M. S., & Carrasco, M. (2012). Differential effects of exogenous and endogenous attention on second-order texture contrast sensitivity. Journal of Vision, 12(8), 1–15. https://doi.org/10.1167/12.8.6

Barrow, H. G., & Tanenbaum, J. M. (1978). Recovering Intrinsic Scene Characteristics from Images. Academic Press, 3–26.

Bennett, P. J., Sekuler, R., & Sekuler, A. B. (2007). The effects of aging on motion detection and direction identification. Vision Research, 47(6), 799–809. https://doi.org/10.1016/j.visres.2007.01.001

Blakemore, C., & Campbell, F. W. (1969). On the existence of neurones in the human visual system selectively sensitive to the orientation and size of retinal images. The Journal of Physiology, 203(1), 237–260. https://doi.org/10.1113/jphysiol.1969.sp008862

Blakemore, C., Muncey, J. P. J., & Ridley, R. M. (1973). Stimulus specificity in the human visual system. Vision Research, 13(10), 1915–1931. https://doi.org/10.1016/0042-6989(73)90063-1

Braddick, O., Campbell, F. W., & Atkinson, J. (1978). Channels in Vision: Basic Aspects. In Perception (pp. 3–38). Springer Berlin Heidelberg. https://doi.org/10.1007/978-3-642-46354-9_1

Braunstein, M. L., Andersen, G. J., & Riefer, D. M. (1982). The use of occlusion to resolve ambiguity in parallel proj ections. In Perception & Psychophysics (Vol. 31, Issue 3).

Brooks, M. J., & Horn, B. K. (1985). Shape and source from shading.

Burton, K. ! B., Owsley, C., & Sloane, M. E. (1993). Aging and Neural Spatial Contrast Sensitivity: Photopic Vision. In Vision Res (Vol. 33, Issue 7). https://doi.org/https://doi.org/10.1016/0042-6989(93)90077-A

Campbell, F. W., & Robson, J. G. (1968). Application of fourier analysis to the visibility of gratings. The Journal of Physiology, 197(3), 551–566. https://doi.org/10.1113/jphysiol.1968.sp008574

Carter, B. E., & Henning, G. B. (1971). The detection of gratings in narrow-band visual noise*. The Journal of Physiology, 219(2), 355–365. https://doi.org/10.1113/jphysiol.1971.sp009666

Cavanagh, P., & Mather, G. (1989). Motion: the long and short of it. Spatial Vision, 4(2–3), 103–129. https://doi.org/10.1163/156856889X00077

Cavonius, C. R., & Robbins, D. O. (1973). Relationships between luminance and visual acuity in the rhesus monkey. The Journal of Physiology, 232(2), 239–246. https://doi.org/10.1113/jphysiol.1973.sp010267

Charman, W. N. (2008). The eye in focus: Accommodation and presbyopia. In Clinical and Experimental Optometry (Vol. 91, Issue 3, pp. 207–225). https://doi.org/10.1111/j.1444-0938.2008.00256.x

Chaudhuri, A., & Albright, T. D. (1997). Neuronal responses to edges defined by luminance vs. temporal texture in macaque area V1. In Visual Neuroscience (Vol. 14, Issue 5, pp. 949–962). https://doi.org/10.1017/S0952523800011664

Chaudhuri, S., & Rajagopalan, A. N. (1999). Depth from defocus: a real aperture imaging approach. Springer Science & Business Media.

Christou, C. G., & Koenderink, J. J. (1997). Light source dependence in shape from shading. Vision Research, 37(11), 1441–1449. https://doi.org/10.1016/S0042-6989(96)00282-9

Chubb, C., & Sperling, G. (1988). Drift-balanced random stimuli: a general basis for studying non-Fourier motion perception. Journal of the Optical Society of America A, 5(11), 1986. https://doi.org/10.1364/josaa.5.001986

Cornsweet, T. N. (1962). The staircrase-method in psychophysics. The American Journal of Psychology, 75(3), 485–491. https://doi.org/10.2307/1419876

Dakin, S. C., & Bex, P. J. (2003). *Natural image statistics mediate brightness ' filling in '*. April, 2341–2348. https://doi.org/10.1098/rspb.2003.2528

Dakin, S. C., & Mareschal, I. (2000). Sensitivity to contrast modulation depends on carrier spatial frequency and orientation. Vision Research, 40(3), 311–329. https://doi.org/10.1016/S0042-6989(99)00179-0

De Valois, R. L., William Yund, E., & Hepler, N. (1982). The orientation and direction selectivity of cells in macaque visual cortex. Vision Research, 22(5), 531–544. https://doi.org/10.1016/0042-6989(82)90112-2

De Weerd, P., Desimone, R., & Ungerleider, L. G. (1996). Cue-dependent deficits in grating orientation discrimination after V4 lesions in macaques. Visual Neuroscience, 13(3), 529–538. https://doi.org/10.1017/S0952523800008208

Derefeldt, G., Lennerstrand, G., & Lundh, B. (1979). Age Variations in Normal Human. Acta Ophthalmologica, 57(Arden 1978), 679–690.

Derrington, A. M., & Ukkonen, O. I. (1999). Second-order motion discrimination by feature-tracking. Vision Research, 39(8), 1465–1475. https://doi.org/10.1016/S0042-6989(98)00227-2

Doerschner, K., Fleming, R. W., Yilmaz, O., Schrater, P. R., Hartung, B., & Kersten, D. (2016). Report Visual Motion and the Perception of Surface Material. Current Biology, 21(23), 2010–2016. https://doi.org/10.1016/j.cub.2011.10.036

Dövencioğlu, D. N., Welchman, A. E., & Schofield, A. J. (2013). Perceptual learning of second order cues for layer decomposition. Vision Research, 77, 1–9. https://doi.org/10.1016/j.visres.2012.11.005

Elliott, D. B. (1987). Contrast Sensitivity Decline With Ageing: a Neural or Optical Phenomenon? Ophthalmic and Physiological Optics, 7(4), 415–419. https://doi.org/10.1111/j.1475-1313.1987.tb00771.x

Enroth-Cugell, C., & Robson, J. G. (1966). The contrast sensitivity of retinal ganglion cells of the cat. The Journal of Physiology, 187(3), 517–552. https://doi.org/10.1113/jphysiol.1966.sp008107

Faubert, J. (2002). Visual perception and aging. Canadian Journal of Experimental Psychology, 56(3), 164–176. https://doi.org/10.1037/h0087394

Felipe, A., Buades, M. J., & Artigas, J. M. (1993). Influence of the contrast sensitivity function on the reaction time. Vision Research, 33(17), 2461–2466. https://doi.org/10.1016/0042-6989(93)90126-H

Field, A. (2013). Discovering Statistics Using SPSS.

Foley, J. M., & Legge, G. E. (1981). Contrast detection and near-threshold discrimination in human vision. Vision Research, 21(7), 1041–1053. https://doi.org/10.1016/0042-6989(81)90009-2

Fox, J. (2016). Applied Regression Analysis and Generalized Linear Models (Vol. 3). Sage Publications.

Georgeson, M. A., & Schofield, A. J. (2003). Shading and texture: Separate information channels with a common adaptation mechanism? Spatial Vision, 16(1), 59–76. https://doi.org/10.1163/15685680260433913

Georgeson, M. A., Yates, T. A., & Schofield, A. J. (2009). Depth propagation and surface construction in 3-D vision. Vision Research, 49(1), 84–95. https://doi.org/10.1016/j.visres.2008.09.030

Gillam, B. (1995). The Perception of Spatial Layout from Static Optical Information.

Glasser, A., & Campbell, M. C. W. (1998). Presbyopia and the optical changes in the human crystalline lens with age. Vision Research, 38(2), 209–229. https://doi.org/10.1016/S0042-6989(97)00102-8

Glasser, A., Croft, M. A., & Kaufman, P. L. (2001). Aging of the Human Crystalline Lens and Presbyopia. International Ophthalmology Clinics, 41(2), 1–15. https://doi.org/10.1097/00004397-200104000-00003

Graham, N., & Sutter, A. (1998). Spatial summation in simple (fourier) and complex (non-fourier) texture channels. Vision Research, 38(2), 231–257. https://doi.org/10.1016/S0042-6989(97)00154-5

Habak, C., & Faubert, J. (2000). Larger effect of aging on the perception of higher-order stimuli. Vision Research, 40(8), 943–950. https://doi.org/10.1016/S0042-6989(99)00235-7

Hall, J. L. (1981). Hybrid adaptive procedure for estimation of psychometric functions. The Journal of the Acoustical Society of America, 69(6), 1763–1769. https://doi.org/10.1121/1.385912

He, S., & MacLeod, D. I. A. (1998). Contrast-modulation flicker: Dynamics and spatial resolution of the light adaptation process. VISION RESEARCH, 38(7), 985–1000. https://doi.org/10.1016/S0042-6989(97)00290-3

Held, R. T., Cooper, E. A., & Banks, M. S. (2012). Blur and disparity are complementary cues to depth. Current Biology, 22(5), 426–431. https://doi.org/10.1016/j.cub.2012.01.033

Hennelly, M. L., Barbur, J. L., Edgar, D. F., & Woodward, E. G. (1998). The effect of age on the light scattering characteristics of the eye. Ophthalmic and Physiological Optics, 18(2), 197–203. https://doi.org/10.1046/j.1475-1313.1998.00333.x

Horn, B. K. (1970). Shape from Shading: A Method for Obtaining the Shape of a Smooth Opaque Object from One View. MIT.

Horn, B. K. (1989). Obtaining Shape from Shading Information. In Shape from Shading (pp. 123–171). MIT Press.

Hubel, D. H., & Wiesel, T. N. (1962). Receptive fields, binocular interaction and functional architecture in the cat’s visual cortex. The Journal of Physiology, 160(1), 106–154. https://doi.org/10.1113/jphysiol.1962.sp006837

Humphrey, G. K., Goodale, M. A., Bowen, C. V., Gati, J. S., Vilis, T., Rutt, B. K., & Menon, R. S. (1997). Differences in perceived shape from shading correlate with activity in early visual areas. Current Biology, 7(2), 144–147. https://doi.org/10.1016/S0960-9822(06)00058-3

Hutchinson, C. V., Ledgeway, T., & Baker, C. L. (2016). Phase-dependent interactions in visual cortex to combinations of first- and second-order stimuli. Journal of Neuroscience, 36(49), 12328–12337. https://doi.org/10.1523/JNEUROSCI.1350-16.2016

Ikeuchi, K., & Horn, B. K. (1981). Numerical Shape from Shading and Occluding Boundaries. Artificial Intelligence, 17(1–3), 141–184.

Jamar, J. H. T., & Koenderink, J. J. (1985). Contrast detection and detection of contrast modulation for noise gratings. Vision Research, 25(4), 511–521. https://doi.org/10.1016/0042-6989(85)90154-3

Johnson, A. P., & Baker, C. L. (2004). First- and second-order information in natural images: a filter-based approach to image statistics. Journal of the Optical Society of America A, 21(6), 913. https://doi.org/10.1364/JOSAA.21.000913

Johnson, A. P., Kingdom, F. A. A., & Baker, C. L. (2005). Spatiochromatic statistics of natural scenes: first- and second-order information and their correlational structure. Journal of the Optical Society of America A, 22(10), 2050–2059. https://doi.org/10.1364/JOSAA.22.002050

Johnson, A. P., Prins, N., Kingdom, F. A. A., & Baker, C. L. (2007). Ecologically valid combinations of first- and second-order surface markings facilitate texture discrimination. Vision Research, 47(17), 2281–2290. https://doi.org/10.1016/j.visres.2007.05.003

Kastner, S., De Weerd, P., & Ungerleider, L. G. (2000). Texture Segregation in the Human Visual Cortex: A Functional MRI Study. Journal of Neurophysiology, 83(4), 2453–2457. https://doi.org/10.1152/jn.2000.83.4.2453

Kaufman, L., Bacon, J., & Barroso, F. (1973). Stereopsis without image segregation. Vision Research, 13(1), 137-IN1. https://doi.org/10.1016/0042-6989(73)90169-7

Kingdom, F. A. A. (2003). Color brings relief to human vision. Nature Neuroscience, 6(6), 641–644. https://doi.org/10.1038/nn1060

Kingdom, F. A. A. (2008). Perceiving light versus material. Vision Research, 48(20), 2090–2105. https://doi.org/10.1016/j.visres.2008.03.020

Kingdom, F. A. A., Keeble, D., & Moulden, B. (1995). Sensitivity to orientation modulation in micropattern-based textures. Vision Research, 35(1), 79–91. https://doi.org/10.1016/0042-6989(94)E0079-Z

Kingdom, F. A. A., & Prins, N. (2016). *Psychophysics : A Practical Introduction* (2nd ed.). Elsevier Academic Press.

Kingdom, F. A. A., Prins, N., & Hayes, A. (2003). Mechanism independence for texture-modulation detection is consistent with a filter-rectify-filter mechanism. Visual Neuroscience, 20(1), 65–76. https://doi.org/10.1017/S0952523803201073

Kleffner, D. A., & Ramachandran, V. S. (1992). On the perception of shape from shading. Perception & Psychophysics, 52(1), 18–36. https://doi.org/10.3758/BF03206757

Klein, S. A., Hu, Q. J., & Carney, T. (1996). The adjacent pixel nonlinearity: Problems and solutions. Vision Research, 36(19), 3167–3181. https://doi.org/10.1016/0042-6989(96)00051-X

Kontsevich, L. L., & Tyler, C. W. (1999). Nonlinearities of near-threshold contrast transduction. Vision Research, 39(10), 1869–1880. https://doi.org/10.1016/S0042-6989(98)00286-7

Krotkov, E. (1988). Focusing. International Journal of Computer Vision, 1(3), 223–237. https://doi.org/10.1007/BF00127822

Landy, M. S., & Bergen, J. R. (1991). Texture segregation and orientation gradient. Vision Research, 31(4), 679–691. https://doi.org/10.1016/0042-6989(91)90009-T

Landy, M. S., & Oruç, I. (2002). Properties of second-order spatial frequency channels. Vision Research, 42(19), 2311–2329. https://doi.org/10.1016/S0042-6989(02)00193-1

Langley, K., Fleet, D. J., & Hibbard, P. B. (1996). Linear filtering precedes nonlinear processing in early vision. Current Biology, 6(7), 891–896. https://doi.org/10.1016/S0960-9822(02)00613-9

Larsson, J., Landy, M. S., & Heeger, D. J. (2006). Orientation-selective adaptation to first- and second-order patterns in human visual cortex. Journal of Neurophysiology, 95(2), 862–881. https://doi.org/10.1152/jn.00668.2005

Ledgeway, T., & Hutchinson, C. V. (2005). The influence of spatial and temporal noise on the detection of first-order and second-order orientation and motion direction. Vision Research, 45(16), 2081–2094. https://doi.org/10.1016/j.visres.2005.02.005

Ledgeway, T., & Smith, A. T. (1994). Evidence for separate motion-detecting mechanisms for first- and second-order motion in human vision. Vision Research, 34(20), 2727–2740. https://doi.org/10.1016/0042-6989(94)90229-1

Ledgeway, T., Zhan, C., Johnson, A. P., Song, Y., & Baker, C. L. (2005). The direction-selective contrast response of area 18 neurons is different for first- and second-order motion. Visual Neuroscience, 22(1), 87–99. https://doi.org/10.1017/S0952523805221120

Legge, G. E., & Foley, J. M. (1980). Contrast masking in human vision. Journal of the Optical Society of America, 70(12), 1458–1471. https://doi.org/10.1364/JOSA.70.001458

Leventhal, A. G., Wang, Y., Schmolesky, M. T., & Zhou, Y. (1998). Neural correlates of boundary perception. Visual Neuroscience, 15(6), 1107–1118. https://doi.org/10.1017/s0952523898156110

Levi, D. M., & Carney, T. (2011). The effect of flankers on three tasks in central, peripheral, and amblyopic vision. Journal of Vision, 11(1), 10–10. https://doi.org/10.1167/11.1.10

Li, A., & Zaidi, Q. (2003). Observer strategies in perception of 3-D shape from isotropic textures: Developable surfaces. Vision Research, 43(26), 2741–2758. https://doi.org/10.1016/j.visres.2003.07.001

Li, G., Yao, Z., Wang, Z., Yuan, N., Talebi, V., Tan, J., Wang, Y., Zhou, Y., & Baker, C. L. (2014). Form-cue invariant second-order neuronal responses to contrast modulation in primate area V2. Journal of Neuroscience, 34(36), 12081–12092. https://doi.org/10.1523/JNEUROSCI.0211-14.2014

Li, S., Lindenberger, U., & Sikström, S. (2001). Aging cognition: from neuromodulation to representation. Trends in Cognitive Sciences, 5(11), 479–486. https://doi.org/10.1016/S1364-6613(00)01769-1

Lindenberger, U., & Baltes, P. B. (1994). Sensory functioning and intelligence in old age: A strong connection. In Psychology and Aging (Vol. 9, Issue 3, pp. 339–355). https://doi.org/10.1037//0882-7974.9.3.339

Lindenberger, U., Scherer, H., & Baltes, P. B. (2001). The strong connection between sensory and cognitive performance in old age: Not due to sensory acuity reductions operating during cognitive assessment. Psychology and Aging, 16(2), 196–205. https://doi.org/10.1037/0882-7974.16.2.196

Liu, B., & Todd, J. T. (2004). Perceptual biases in the interpretation of 3D shape from shading. Vision Research, 44(18), 2135–2145. https://doi.org/10.1016/j.visres.2004.03.024

Lu, Z. L., & Sperling, G. (1995). The functional architecture of human visual motion perception. Vision Research, 35(19), 2697–2722. https://doi.org/10.1016/0042-6989(95)00025-U

Manahilov, V., Calvert, J., & Simpson, W. A. (2003). Temporal properties of the visual responses to luminance and contrast modulated noise. Vision Research, 43(17), 1855–1867. https://doi.org/10.1016/S0042-6989(03)00275-X

Manahilov, V., Simpson, W. A., & Calvert, J. (2005). Why is second-order vision less efficient than first-order vision? Vision Research, 45(21), 2759–2772. https://doi.org/10.1016/j.visres.2005.06.004

Mareschal, I., & Baker, C. L. (1998). A cortical locus for the processing of contrast-defined contours. Nature Neuroscience, 1(2), 150–154. https://doi.org/10.1038/401

MathWorks, I. (2012). MATLAB and Statistics Toolbox Release. Natick, MA: The MathWorks.

McGrath, C., & Morrison, J. D. (1981). The Effects of Age on Spatial Frequency Perception in Human Subjects. Quarterly Journal of Experimental Physiology, 66(3), 253–261. https://doi.org/10.1113/expphysiol.1981.sp002554

McIntosh, R. D., & Lashley, G. (2008). Matching boxes: Familiar size influences action programming. Neuropsychologia, 46(9), 2441–2444. https://doi.org/10.1016/j.neuropsychologia.2008.03.003

Merigan, W., Nealey, T., & Maunsell, J. (1993). Visual effects of lesions of cortical area V2 in macaques. The Journal of Neuroscience, 13(7), 3180–3191. https://doi.org/10.1523/JNEUROSCI.13-07-03180.1993

Morgan, M. W. (1944). The Clinical Aspects of Accommodation and Convergence. Optometry and Vision Science, 21(8), 301–313. https://doi.org/10.1097/00006324-194408000-00001

Movshon, J. A., & Lennie, P. (1979). Pattern-selective adaptation in visual cortical neurones. Nature, 278(5707), 850–852. https://doi.org/10.1038/278850a0

Muller, C. M. P., Brenner, E., & Smeets, J. B. J. (2009). Maybe they are all circles: Clues and cues. Journal of Vision, 9(9). https://doi.org/10.1167/9.9.10

Nishida, S., Edwards, M., & Sato, T. (1997). Simultaneous motion contrast across space: Involvement of second-order motion? Vision Research, 37(2), 199–214. https://doi.org/10.1016/S0042-6989(96)00112-5

Norman, J. F., Bartholomew, A. N., & Burton, C. L. (2008). Aging preserves the ability to perceive 3D object shape from static but not deforming boundary contours. Acta Psychologica, 129(1), 198–207. https://doi.org/10.1016/j.actpsy.2008.06.002

Norman, J. F., Cheeseman, J. R., Adkins, O. C., Cox, A. G., Rogers, C. E., Dowell, C. J., Baxter, M. W., Norman, H. F., & Reyes, C. M. (2015). Aging and solid shape recognition: Vision and haptics. Vision Research, 115, 113–118. https://doi.org/10.1016/j.visres.2015.09.001

Norman, J. F., & Wiesemann, E. Y. (2007). Aging and the perception of local surface orientation from optical patterns of shading and specular highlights. Perception and Psychophysics, 69(1), 23–31. https://doi.org/10.3758/BF03194450

Ooi, T. L., Wu, B., & He, Z. J. (2001). Distance determined by the angular declination below the horizon. Nature, 414(6860), 197–200. https://doi.org/10.1038/35102562

O'Shea, R. P., Govan, D. G., & Sekuler, R. (1997). Blur and Contrast as Pictorial Depth Cues. Perception, 26(5), 599–612. https://doi.org/10.1068/p260599

Owsley, C. (2011). Aging and vision. Vision Research, 51(13), 1610–1622. https://doi.org/10.1016/j.visres.2010.10.020

Owsley, C., Sekuler, R., & Siemsen, D. (1983). Contrast Sensitivity Throughout Adulthood. Vision Research, 23f(7), 689–699. https://doi.org/10.1016/0042-6989(83)90210-9

Pantle, A., & Sekuler, R. (1968). Size-Detecting Mechanisms in Human Vision. Science, 162(3858), 1146–1148. https://doi.org/10.1126/science.162.3858.1146.b

Pardhan, S. (2004). Contrast sensitivity loss with aging: sampling efficiency and equivalent noise at different spatial frequencies. Journal of the Optical Society of America. A, Optics, Image Science, and Vision, 21(2), 169–175. https://doi.org/10.1364/JOSAA.21.000169

Peirce, J. W. (2007). PsychoPy-Psychophysics software in Python. Journal of Neuroscience Methods, 162(1–2), 8–13. https://doi.org/10.1016/j.jneumeth.2006.11.017

Pelli, D. G., & Blakemore, C. (1990). The quantum efficiency of vision. Vision: Coding and Efficiency, 3–24.

Pelli, D. G., & Zhang, L. (1991). Accurate control of contrast on microcomputer displays. Vision Research, 31(7–8), 1337–1350. https://doi.org/10.1016/0042-6989(91)90055-A

Pentland, A. P. (1984). Local Shading Analysis. IEEE Transactions on Pattern Analysis and Machine Intelligence, PAMI-6(2), 170–187. https://doi.org/10.1109/TPAMI.1984.4767501

Pentland, A. P. (1988). Shape information from shading: a theory about human perception. [1988 Proceedings] Second International Conference on Computer Vision, 404–413.

Pichora-Fuller, M. K., Schneider, B. A., & Daneman, M. (1995). How young and old adults listen to and remember speech in noise. The Journal of the Acoustical Society of America, 97(1), 593–608. https://doi.org/10.1121/1.412282

Prins, N., & Kingdom, F. A. A. (2006). Direct evidence for the existence of energy-based texture mechanisms. Perception, 35(8), 1035–1046. https://doi.org/10.1068/p5546

Prins, N., & Kingdom, F. A. A. (2009). Palamedes: Matlab routines for analyzing psychophysical data. http://www.palamedestoolbox.org

Raghuram, A., Lakshminarayanan, V., & Khanna, R. (2005). Psychophysical estimation of speed discrimination II Aging effects. Journal of the Optical Society of America A, 22(10), 2269. https://doi.org/10.1364/josaa.22.002269

Ramachandran, V. S. (1988). Perception of shape from shading. Nature, 331(6152), 446. https://doi.org/10.1038/331163a0

Rapp, P. R., & Gallagher, M. (1996). Preserved neuron number in the hippocampus of aged rats with spatial learning deficits. Proceedings of the National Academy of Sciences of the United States of America, 93(18), 9926–9930. https://doi.org/10.1073/pnas.93.18.9926

Reynaud, A., Tang, Y., Zhou, Y., & Hess, R. F. (2014). A normative framework for the study of second-order sensitivity in vision. Journal of Vision, 14(9), 1–16. https://doi.org/10.1167/14.9.3

Robson, J. G. (1966). Spatial and Temporal Contrast-Sensitivity Functions of the Visual System. Journal of the Optical Society of America, 56(8), 1141. https://doi.org/10.1364/josa.56.001141

Rosenberg, A., & Issa, N. P. (2011). The Y Cell Visual Pathway Implements a Demodulating Nonlinearity. Neuron, 71(2), 348–361. https://doi.org/10.1016/j.neuron.2011.05.044

Roudaia, E., Farber, L. E., Bennett, P. J., & Sekuler, A. B. (2011). The effects of aging on contour discrimination in clutter. Vision Research, 51(9), 1022–1032. https://doi.org/10.1016/j.visres.2011.02.015

Salthouse, T. A. (1996). The Processing-Speed Theory of Adult Age Differences in Cognition. Psychological Review, 103(3), 403–428. https://doi.org/10.1037/0033-295X.103.3.403

Schneider, B. A., & Pichora-Fuller, M. K. (2000). Implications of Perceptual Deterioration for Cognitioc Aging Research. The Handbook of Aging and Cognition, 155–219.

Schofield, A. J. (2000). What does second-order vision see in an image? Perception, 29(9), 1071–1086. https://doi.org/10.1068/p2913

Schofield, A. J., Curzon-Jones, B., & Hollands, M. A. (2017). Reduced sensitivity for visual textures affects judgments of shape-from-shading and step-climbing behaviour in older adults. Experimental Brain Research, 235(2), 573–583. https://doi.org/10.1007/s00221-016-4816-0

Schofield, A. J., & Georgeson, M. A. (1999). Sensitivity to modulations of luminance and contrast in visual white noise: Separate mechanisms with similar behaviour. Vision Research, 39(16), 2697–2716. https://doi.org/10.1016/S0042-6989(98)00284-3

Schofield, A. J., & Georgeson, M. A. (2000). The temporal properties of first- and second-order vision. Vision Research, 40(18), 2475–2487. https://doi.org/10.1016/S0042-6989(00)00111-5

Schofield, A. J., & Georgeson, M. A. (2003). Sensitivity to contrast modulation: The spatial frequency dependence of second-order vision. Vision Research, 43(3), 243–259. https://doi.org/10.1016/S0042-6989(02)00542-4

Schofield, A. J., Hesse, G., Rock, P. B., & Georgeson, M. A. (2006). Local luminance amplitude modulates the interpretation of shape-from-shading in textured surfaces. Vision Research, 46(20), 3462–3482. https://doi.org/10.1016/j.visres.2006.03.014

Schofield, A. J., Rock, P. B., & Georgeson, M. A. (2011). Sun and sky: Does human vision assume a mixture of point and diffuse illumination when interpreting shape-from-shading? Vision Research, 51(21–22), 2317–2330. https://doi.org/10.1016/j.visres.2011.09.004

Schofield, A. J., Rock, P. B., Sun, P., Jiang, X., & Georgeson, M. A. (2010). What is second-order vision for? Discriminating illumination versus material changes. Journal of Vision, 10(9), 1–18. https://doi.org/10.1167/10.9.2

Scott-Samuel, N. E., & Georgeson, M. A. (1999). Does early non-linearity account for second-order motion? Vision Research, 39(17), 2853–2865. https://doi.org/10.1016/S0042-6989(98)00316-2

Seddon, J., Fong, D., West, S. K., & Valmadrid, C. T. (1995). Epidemiology of risk factors for age-related cataract. Survey of Ophthalmology, 39(4), 323–334. https://doi.org/10.1016/S0039-6257(05)80110-9

Skalka, H. W. (1980). Grating Acuity. 11, 21–23.

Sloane, M. E., Owsley, C., & Jackson, C. A. (1988). Aging and luminance-adaptation effects on spatial contrast sensitivity. Journal of the Optical Society of America A, 5(12), 2181. https://doi.org/10.1364/josaa.5.002181

Smith, A. T., Greenlee, M. W., Singh, K. D., Kraemer, F. M., & Hennig, J. (1998). The processing of first- and second-order motion in human visual cortex assessed by functional magnetic resonance imaging (fMRI). J Neurosci, 18(10), 3816–3830. http://www.ncbi.nlm.nih.gov/pubmed/9570811

Smith, A. T., & Ledgeway, T. (1997). Separate detection of moving luminance and contrast modulations: Fact or artifact? Vision Research, 37(1), 45–62. https://doi.org/10.1016/S0042-6989(96)00147-2

Smith, A. T., & Ledgeway, T. (1998). Sensitivity to second-order motion as a function of temporal frequency and eccentricity. Vision Research, 38(3), 403–410. https://doi.org/10.1016/S0042-6989(97)00134-X

Solomon, J. A. (2000). Channel selection with non-white-noise masks. Journal of the Optical Society of America A, 17(6), 986. https://doi.org/10.1364/josaa.17.000986

Speranza, F., Daneman, M., & Schneider, B. A. (2000). How aging affects the reading of words in noisy backgrounds. Psychology and Aging, 15(2), 253–258. https://doi.org/10.1037/0882-7974.15.2.253

Stevens, K. A. (1981). The information content of texture gradients. Biological Cybernetics, 42(2), 95–105. https://doi.org/10.1007/BF00336727

Stevens, K. A., & Brookes, A. (1988). Integrating stereopsis with monocular interpretations of planar surfaces. Vision Research, 28(3), 371–386. https://doi.org/10.1016/0042-6989(88)90180-0

Sun, P., & Schofield, A. J. (2011). The efficacy of local luminance amplitude in disambiguating the origin of luminance signals depends on carrier frequency: Further evidence for the active role of second-order vision in layer decomposition. Vision Research, 51(5), 496–507. https://doi.org/10.1016/j.visres.2011.01.008

Sutter, A., & Graham, N. (1995). Investigating simple and complex mechanisms in texture segregation using the speed-accuracy tradeoff method. Vision Research, 35(20), 2825–2843. https://doi.org/10.1016/0042-6989(95)00045-2

Sutter, A., Sperling, G., & Chubb, C. (1995). Measuring the spatial frequency selectivity of second-order texture mechanisms. Vision Research, 35(7), 915–924. https://doi.org/10.1016/0042-6989(94)00196-S

Tang, Y., & Zhou, Y. (2009). Age-related decline of contrast sensitivity for second-order stimuli: Earlier onset, but slower progression, than for first-order stimuli. Journal of Vision, 9(7), 1–15. https://doi.org/10.1167/9.7.18

Thurstone, L. L. (1929). Theory of attitude measurement. Psychological Review, 36(3), 222.

Thurstone, L. L. (1932). Stimulus dispersions in the method of constant stimuli. Journal of Experimental Psychology, 15(3), 284–297.

Thurstone, L. L. (1959). The measurement of values. Psychological Review, 61(1), 47.

Von Der Heydt, R., & Peterhans, E. (1989). Mechanisms of contour perception in monkey visual cortex. I. Lines of pattern discontinuity. Journal of Neuroscience, 9(5), 1731–1748.

Wallach, H., & Norris, C. M. (1963). Accommodation as a Distance-Cue. The American Journal of Psychology, 76(4), 659. https://doi.org/10.2307/1419717

Warren, P. A., & Mamassian, P. (2010). Recovery of surface pose from texture orientation statistics under perspective projection. Biological Cybernetics, 103(3), 199–212. https://doi.org/10.1007/s00422-010-0389-3

Watson, A. B., & Pelli, D. G. (1983). Quest: A Bayesian adaptive psychometric method. Perception & Psychophysics, 33(2), 113–120. https://doi.org/10.3758/BF03202828

Weale, R. A. (1975). Senile changes in visual acuity. Transactions of the Ophthalmological Societies of the United Kingdom, 95(1), 36–38.

Weale, R. A. (1982). Retinal Senescence. Progressive Ophthalmology\nYoung RW\nThe Bowman Lecture, 1986, 53–73.

Weinstein, B., & Grether, W. F. (1940). A comparison of visual acuity in the rhesus monkey and man. Journal of Comparative Psychology, 30(2), 187–195. https://doi.org/10.1037/h0061507

Westrick, Z. M., & Landy, M. S. (2013). Pooling of first-order inputs in second-order vision. Vision Research, 91(858), 108–117. https://doi.org/10.1016/j.visres.2013.08.005

Wilson, H. R., Ferrera, V. P., & Yo, C. (1992). A psychophysically motivated model for two-dimensional motion perception. Visual Neuroscience, 9(1), 79–97. https://doi.org/10.1017/S0952523800006386

Xu, J., Pokorny, J., & Smith, V. C. (1997). Optical density of the human lens. Journal of the Optical Society of America A, 14(5), 953. https://doi.org/10.1364/JOSAA.14.000953

Yan, F. F., Hou, F., Lu, H., Yang, J., Chen, L., Wu, Y., Chen, G., & Huang, C. B. (2020). Aging affects gain and internal noise in the visual system. Scientific Reports, 10(1), 1–10. https://doi.org/10.1038/s41598-020-63053-0

Zhou, Y., & Baker, C. L. (1993). A processing stream in mammalian visual cortex neurons for non-fourier responses. Science, 261(5117), 98–101. https://doi.org/10.1126/science.8316862

Zhou, Y., & Baker, C. L. (1996). Spatial Properties of Envelope-Responsive Cells in Area 17 and 18 Neurons of the Cat. In JOURNALOF NEUROPHYSIOLOGY (Vol. 75, Issue 3).